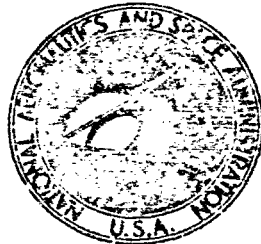


NASA
TN
D
7090
c.1

NASA TECHNICAL NOTE



NASA TN D-7090

c.1

NASA TN D-7090

LOAN COPY: RETURN
AF 1 TECHNICAL LIB
KIRTLAND AFB, N.M.



TECH LIBRARY KAFB, NM

(NASA-TN-D-7090) A TECHNIQUE FOR
DESIGNING ACTIVE CONTROL SYSTEMS FOR
ASTRONOMICAL TELESCOPE MIRRORS W.E.
Howell, et al (NASA) Jan. 1973 98 p

CSCL 131 H1/10

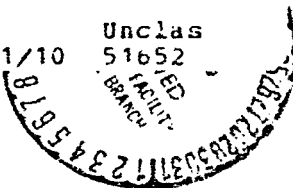
873-14247

Unclass

51652

ED

BRANCH



A TECHNIQUE FOR DESIGNING
ACTIVE CONTROL SYSTEMS FOR
ASTRONOMICAL-TELESCOPE MIRRORS

by W. E. Howell and J. F. Creedon

Langley Research Center
Hampton, Va. 23365

NATIONAL AERONAUTICS AND SPACE ADMINISTRATION • WASHINGTON, D. C. • JANUARY 1973



0133525

1. Report No. NASA TN D-7090	2. Government Accession No.	3. Recipient's Catalog No.	
4. Title and Subtitle A TECHNIQUE FOR DESIGNING ACTIVE CONTROL SYSTEMS FOR ASTRONOMICAL-TELESCOPE MIRRORS		5. Report Date January 1973	
		6. Performing Organization Code	
7. Author(s) W. E. Howell and J. F. Creedon		8. Performing Organization Report No. L-8557	
		10. Work Unit No 188-78-57-07	
9. Performing Organization Name and Address NASA Langley Research Center Hampton, Va. 23365		11. Contract or Grant No.	
		13. Type of Report and Period Covered Technical Note	
12. Sponsoring Agency Name and Address National Aeronautics and Space Administration Washington, D.C. 20546		14. Sponsoring Agency Code	
15. Supplementary Notes			
16. Abstract: This paper considers the problem of designing a control system to achieve and maintain the required surface accuracy of the primary mirror of a large space telescope. Control over the mirror surface is obtained through the application of a corrective force distribution by actuators located on the rear surface of the mirror. The design procedure is an extension of a modal control technique developed for distributed parameter plants with known eigenfunctions to include plants whose eigenfunctions must be approximated by numerical techniques. Instructions are given for constructing the mathematical model of the system, and a design procedure is developed for use with typical numerical data in selecting the number and location of the actuators. Examples of actuator patterns and their effect on various errors are given.			
17. Key Words (Suggested by Author(s)) Active optics Diffraction Diffraction limited Space telescopes		18. Distribution Statement Unclassified - Unlimited	
19. Security Classif. (of this report) Unclassified	20. Security Classif. (of this page) Unclassified	21. No. of Pages 97	22. Price* \$3.00

CONTENTS

	Page
SUMMARY	1
INTRODUCTION	2
SYMBOLS	3
CONTROL SYSTEM DESCRIPTION	6
The Modal Control Concept	6
System Configuration	7
Modal Representation of Figure Error	10
Evaluation of Steady-State Errors	12
Determination of Pad Effects	15
PERFORMANCE EVALUATION	18
Calculation of the Performance Index	18
Treatment of Initial Errors or Disturbances	20
DESIGN PROCEDURE	22
Numerical and Physical Data	22
Control System Design Evaluation	24
Results for Deterministic Errors	29
Results for Uncorrelated Errors	31
Comparison of Modal Control and Optimal Control Laws	35
Design Examples	36
CONCLUDING REMARKS	38
APPENDIX A - COMPUTER PROGRAM DESCRIPTION, LISTING, AND PRINTOUT	40
APPENDIX B - EIGENVECTORS OF THE MIRROR	60
APPENDIX C - EIGENVECTOR DIAGRAMS	66
APPENDIX D - EIGENVALUES AND MASS MATRIX FOR THE MIRROR	72
APPENDIX E - BEST ACTUATOR LOCATIONS - DETERMINISTIC CASE	74
APPENDIX F - BEST ACTUATOR LOCATIONS - UNCORRELATED ERRORS	87
REFERENCES	93
TABLES	94

**A TECHNIQUE FOR DESIGNING ACTIVE CONTROL SYSTEMS
FOR ASTRONOMICAL-TELESCOPE MIRRORS**

By W. E. Howell and J. F. Creedon
Langley Research Center

SUMMARY

This paper considers the problem of designing a control system to achieve and maintain the required surface accuracy of the primary mirror of a large space telescope. Control over the mirror surface is obtained through the application of a corrective force distribution by actuators located on the rear surface of the mirror. The design procedure is an extension of a modal control technique developed for distributed parameter plants with known eigenfunctions to include plants whose eigenfunctions must be approximated by numerical techniques. Instructions are given for constructing the mathematical model of the system, and a design procedure is developed for use with typical numerical data in selecting the number and location of the actuators.

Two techniques for treating disturbances to the plant are discussed. These two techniques, which treat the errors as deterministic and uncorrelated, respectively, are examined from the standpoints of sensitivity to various mirror errors, determining the number of actuators required, and means of finding the best locations. For the deterministic case it was found that the "best" actuator locations (those locations which will minimize the steady-state error) are very sensitive to the error distribution. In addition, these locations can presently be found only by exhaustive searches of all possible actuator locations, and the number of actuators required for a specific mirror and specific error can only be estimated after much computer time is used. In practice the error distribution over the mirror surface would be expected to change with the telescope attitude relative to the sun. Also, the exact nature of the mirror errors will be time varying and will not, in any case, be known very precisely. For these reasons it is not recommended that the errors be treated deterministically. In addition, when the errors at any particular time are treated as uncorrelated random variables, the actuator locations are much less sensitive to specific variations in error distribution, an estimate of the number of actuators required to produce a desired reduction in figure error can easily be made, and locations which will yield results near the estimated figure accuracy can be found in a reasonable manner. Thus, at present this technique is preferred even though it requires more actuators than the deterministic method for a specific assumed error.

Several numerical examples are presented for a 76-cm-diameter (30-inch), thin spherical mirror and the computer program to implement the design procedure is given in an appendix. The results include a comparison of the modal control law and an optimal (least-squares) control law. The results of this comparison indicate that not much performance is to be gained by the added complexity of this optimum control law.

INTRODUCTION

One of the most fundamental problems associated with orbiting a large, diffraction-limited telescope of the size and type discussed in reference 1 is that of manufacturing, figuring, and maintaining the figure of the large primary mirror. Many factors such as initial figuring errors, the change from 1g to 0g, and changing temperature gradients on the mirror while in orbit make conventional techniques of figuring and supporting telescope mirrors unsuitable. An alternate approach has been developed in which the mirror is actively controlled by first sensing figure errors on the primary mirror and then nulling them by properly deforming the mirror. This technique (ref. 2) has been successfully applied to a 76-cm-diameter (30-inch), 1.27-cm-thick ($\frac{1}{2}$ -inch) mirror with an initial error of 1/2 wavelength rms ($\lambda = 0.6328 \mu\text{m}$). By using 58 actuators, the mirror was controlled to a figure accuracy of better than $\lambda/50$.

Since the time of the investigation reported in reference 2, consideration has been given to the application of a modal control technique to a class of mirrors. The modal control technique represents the plant to be controlled in terms of the eigenvalues and eigenfunctions of the linear differential operator which describes the behavior of the plant. In reference 3, this technique was applied to distributed parameter plants whose eigenvalues and eigenfunctions could be obtained in closed form. In many practical examples, however, the required eigenfunctions are not available. For the mirror, for example, the restrictions of practical mounts (boundary conditions) and the existence of holes in the center of the primary mirror used in Cassegrain telescopes preclude obtaining the required eigenfunctions in closed form. Estimates of these functions must be obtained via numerical approximation techniques. The purpose of this paper is to set forth for such a system a design procedure based on the use of the modal control law described in reference 3. First, the modal control concept is explained, the control system described, and the analysis procedure set forth. Certain specific details, such as accounting for the pad effects and the treatment of initial or expected error, are then covered. Numerical data for the 76-cm-diameter (30-inch) mirror are given and examples are presented. Appendix A contains a listing of the computer program; appendixes B, C, and D, eigenvector listings and diagrams and eigenvalue listings for the mirror; appendixes E and F, several examples of actuator placement and resultant mirror errors.

SYMBOLS

Values in the body of the paper are given both in SI Units and U.S. Customary Units. The measurements and calculations were made in the U.S. Customary Units. The values in the appendixes are in U.S. Customary Units and are consistent with the program in appendix A.

A	area of mirror
a_i	i th modal coefficient which expands P in terms of the mode shapes (see eq. (35))
a^N	$N \times 1$ vector of coefficients of the force distribution in the modal domain which corresponds to the controlled modes
a^R	$R \times 1$ vector of coefficients of the force distribution on the mirror; these coefficients arise from the action of the N actuators
C	$M \times 1$ vector which is the sum of the control system displacements and the disturbances in the modal domain; C is partitioned into C^N and C^R
C_M	figure sensor estimate of C
C^N	$N \times 1$ vector which contains the elements of C which are being controlled
\hat{C}^N	figure sensor estimate of the N modal coefficients corresponding to the controlled modes
C_{ss}^N	steady-state or final value of C^N
C^R	$R \times 1$ vector which contains the remaining elements of C
C_{ss}^R	steady-state or final value of C^R
D^N	$N \times N$ diagonal matrix which contains the control system compensation (also referred to as the diagonal controller)
E	performance index under the assumption of uncorrelated errors

E_N	E for a particular set of N actuators
f	frequency
H	$M \times N$ matrix which converts the actuator forces to modal coefficients retaining the dimensions of force; H is partitioned into H^N and H^R
H^N	$N \times N$ matrix which contains the rows of the H matrix corresponding to the N modes being controlled
H^R	$R \times N$ matrix containing the remaining elements of the H matrix
h_{ij}	ijth element of the H matrix
J, J^*, J_1	performance indices
K	gain constant
M	total number of modes (eigenvectors) used to model the mirror
m	diagonal matrix of elemental masses Δm_i
m_t	total mass of mirror
Δm_i	mass of i th element of the structural model
N	number of actuators or number of controlled modes
P	total force distribution on the mirror from N actuators
q	vector of disturbance coefficients in the modal domain
q_i	modal error coefficient of the i th mode
q^M	the $M \times 1$ vector q
q^N	$N \times 1$ vector of disturbances in the modal domain which correspond to the controlled modes

q^R	$R \times 1$ vector of disturbances which remain after q is partitioned into q^N and q^R
R	remaining modes, $R = M - N$
s	Laplace operator
U	$M \times M$ matrix of eigenvectors
W	$M \times 1$ vector of mirror errors at the grid points
w_i	figure error of the mirror at the i th grid point
x,y,t	x,y coordinates on mirror at time t
Z	coordinate axis directed (positive) along the optical axis
α^N	$N \times 1$ vector of forces applied to the mirror surface ($\alpha = \alpha^N$)
β_j	force distribution over the pad area of the j th actuator
Γ	area over which the pads act
ϵ_i	structural damping of the i th mode
Λ	$M \times 1$ vector of eigenvalues
λ	wavelength of light
ξ^M	figure sensor error in determining C^M
ρ	density of the mirror expressed in terms of its area
$\sigma_{q_i}^2$	variance of the i th modal error
τ, τ', τ''	time constants
ϕ_i^2	defined by equation (59); under the assumption of uncorrelated errors, this quantity gives the fraction of the i th modal error which appears in the final error

ϕ_{1N}^2 ϕ_i^2 for a particular set of N actuators

ψ $R \times N$ matrix $\Lambda^{R_H R} [\Lambda^{N_H N}]^{-1}$

ω natural frequency

Subscripts:

i general term of a vector

i,j general element of a matrix

M last calculated mode

N last mode or actuator under consideration

n nth term of a set

Superscripts:

\sim estimate

T transpose of a matrix

CONTROL SYSTEM DESCRIPTION

The Modal Control Concept

The modal control concept, as applied to mirrors for use in orbiting telescopes, is treated in detail in reference 3, and design examples for flat plates are presented. For purposes of analysis in the present study, the mirror is considered to be a structure tied to a set of supports or mounts that prevent rigid-body motions. The elasticity of the mounts themselves may or may not be considered, depending upon the degree of sophistication of the analysis. (The analysis used throughout this paper considers the mounts to be rigid.) The modes of vibration of the mirror, subject to the constraints of the supports, are the modes used in the analysis. The mode shapes are referred to as eigenvectors of the mirror and the frequencies are the eigenvalues.

Generally the mode shapes and frequencies must be obtained by numerical methods since the solution of the governing partial differential equation is not available. The eigenvectors and eigenvalues of the structure that are used in this paper were obtained from a

numerical program (SAMIS, ref. 4) and have been checked by NASTRAN (ref. 5). These results have been verified experimentally (ref. 6). The eigenvectors obtained from the numerical program are tabulated in the U matrix (see appendix B), with column 1 denoting the first, or lowest frequency, eigenvector and each succeeding column denoting higher order mode shapes. The vector of eigenvalues Λ (see appendix D) is ordered with the lowest frequency first.

The finite-element model that was used in SAMIS is given in reference 7. This model was used to extract the first 58 eigenvectors and eigenvalues of the mirror. (See appendix D.) This set of eigenvectors and eigenvalues has been used throughout the analysis.

One motivation for using the modal control law was to allow the designer to decouple the dynamic behavior of the control system; another and more important aspect of this control law is that the mode shapes provide a hierarchy of errors that are likely to occur in practice. That is, the modes may be ordered in such a way that mode 1, or the fundamental mode shape, is more likely to occur than mode 2. Also, a measure of the relative amplitude is available by examining the eigenvalues of the two modes. That is, if the eigenvalues of modes 1 and 2 differ by a factor of n , the second mode will require about n times the input force disturbance to produce the same displacement error. This is just another way of saying that the mirror (plant) acts as a filter to high-order modes. The one exception to this is that careless initial polishing and figuring of the mirror could generate considerable error (as displacements) in the high-order modes. Conversely, this knowledge of the mirror should be used to avoid fabrication errors which will be particularly difficult to correct.

System Configuration

For the purposes of designing a control system for a mirror, the designer obtains a transformation from mirror surface deflections (or errors) to modal coefficients, which can be viewed as a coordinate transformation. That is,

$$q = [U]^{-1} w \quad (1)$$

represents a transformation from the error at a set of points w over the surface of the mirror to a set of modal coordinates q . Figure 1 shows a block diagram of the mirror, figure error sensor, and actuators as they appear in a finite modal representation. The mirror itself is mathematically represented by the five blocks (matrices) labeled H^N and H^R , Λ^N and Λ^R , and U^M . The superscripts N and R have the relationship

$$N + R = M$$

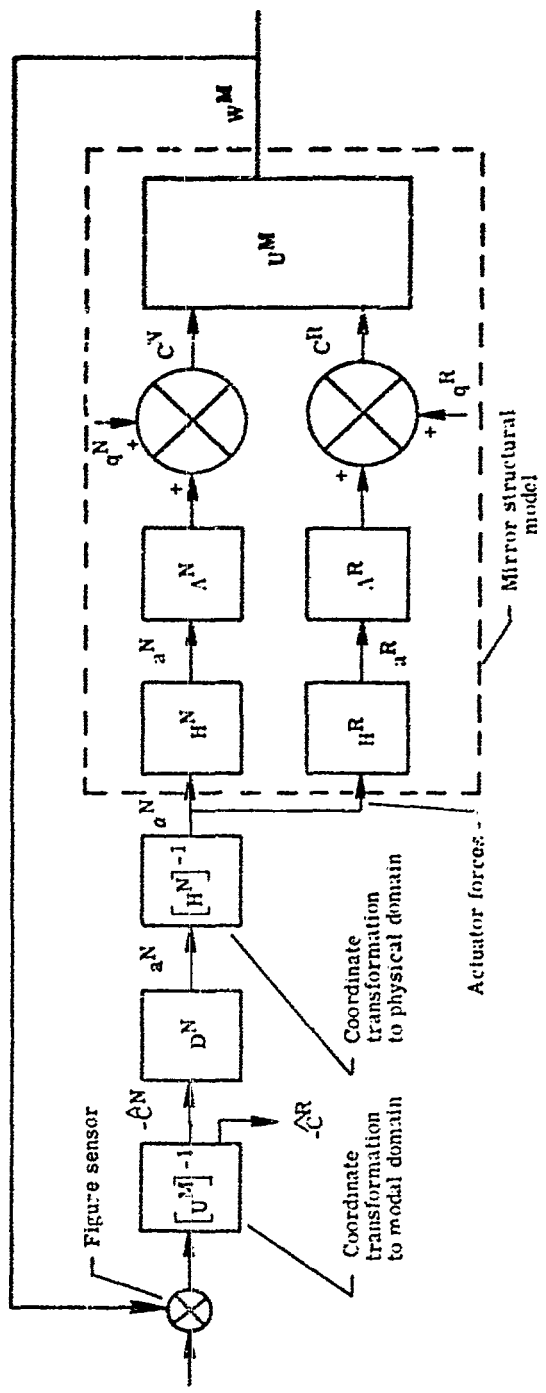


Figure 1.- Block diagram of mirror and control system.

where

- M number of modes used to model the mirror (although there are an infinite number of mirror modes, practical limitations require a finite number, and 58 will be used later for numerical evaluation)
- N number of actuators used (numerically equal to the number of controlled modes)
- R remaining modes

In the physical world the actuator forces α^N are translated directly into mirror figure displacements $W(x,y,t)$; in the mathematical model the N forces are transformed by the H^N and H^R matrices into a set of force coefficients a^N and a^R , respectively, in the modal domain. These forces are then transformed by the A matrices into the modal coefficients of displacement. These coefficients, generated by the control system, are summed with the coefficients representing the error in the modal domain that previously existed on the mirror, and the result (denoted by C^N and C^R) is transformed by $[U^M]$ into the final displacement $W(x,y,t)$ according to the relationship

$$[U^M] \begin{Bmatrix} C^N \\ \cdots \\ C^R \end{Bmatrix} = W^M \quad (2)$$

To combine this model into a control system requires a sensor to measure $W(x,y,t)$. The sensor output is then changed into the modal coordinate system by the proper transformation $[U^M]^{-1}$. Since N actuators can control only N modes, the subset of the N selected modes to be controlled is usually all that is generated. One would normally control only the first, or lowest, N modes.

The N selected modes are then fed through the dynamic compensation $D^N(s)$ in which the proper gains and compensation are applied to each mode independently. If a type I system is used, as will be specified in the section entitled "Evaluation of Steady-State Errors," then each diagonal element of D^N corresponding to one channel of the decoupled controller will contain an integration. The output of D^N , denoted a^N , is still in the modal domain. In fact, this output is a set of modal coefficients which describe the desired force patterns to be distributed on the mirror. To change these to discrete forces, which is the way they must be applied to the mirror, the values of a^N must be transformed by multiplying by $[H^N]^{-1}$. This matrix $[H^N]^{-1}$ also accounts for the effect

of the physical mechanism through which the actuator applies a load to the plant. This completes the description of the control system which will be analyzed in later sections. For a more complete and rigorous discussion, see reference 3.

Modal Representation of Figure Error

The modal control technique has been developed for mirrors whose modes, denoted by $U_i(x,y)$, are assumed to be members of a complete orthonormal set. Since this set of modes is complete, a modal expansion of any shape the mirror can take can be obtained by using the correct coefficient for each mode:

$$W(x,y,t) = \sum_{i=1}^{\infty} C_i(t) U_i(x,y) \quad (3)$$

Therefore, for any N points on the mirror, the following equation may be written symbolically in matrix format:

$$\begin{bmatrix} W(x_1, y_1, t) \\ \vdots \\ W(x_N, y_N, t) \end{bmatrix} = \begin{bmatrix} U_1(x_1, y_1) & \dots & U_N(x_1, y_1) \\ \vdots & \ddots & \vdots \\ U_1(x_N, y_N) & \dots & U_N(x_N, y_N) \end{bmatrix} \begin{bmatrix} C_1(t) \\ C_2(t) \\ \vdots \\ C_N(t) \end{bmatrix} + \begin{bmatrix} \sum_{i=N+1}^{\infty} C_i(t) U_i(x_1, y_1) \\ \vdots \\ \sum_{i=N+1}^{\infty} C_i(t) U_i(x_N, y_N) \end{bmatrix} \quad (4)$$

or

$$W^R = U^R C^R + U^{R,C^R} \quad (5)$$

where

$$U^{R,C^R} = \begin{bmatrix} U_{N+1}(x_1, y_1) & \dots & U_M(x_1, y_1) & \dots & [C_{N+1}(t) \\ \vdots & & \vdots & & \vdots \\ U_{N+1}(x_N, y_N) & \dots & U_M(x_N, y_N) & \dots & C_M(t) \end{bmatrix} \quad (6)$$

and U^R is an $N \times \infty$ matrix and C^R is an $\infty \times 1$ vector.

The second term in equation (5) causes an error when the mode amplitudes are determined since they are not available, and the amplitudes C^N are estimates denoted \hat{C}^N

$$\hat{C}^N = [U^N]^{-1} W^N = C^N + [U^N]^{-1} U^R C^R \quad (7)$$

The term $[U^N]^{-1} U^R C^R$ represents the error in the estimate of C . It is possible to take more measurements than the number of actuators used. If for example the number of measurements is selected to be M ($M > N$), then

$$\hat{C}^M = [U^M]^{-1} W^M = C^M + \xi^M \quad (8)$$

where

$$\xi^M = \begin{bmatrix} U_{M+1}(x_1, y_1) & \dots & \\ \vdots & & \vdots \\ U_{M+1}(x_N, y_N) & \dots & \end{bmatrix} \begin{bmatrix} C_{M+1}(t) \\ \vdots \\ \end{bmatrix} \quad (9)$$

If M is sufficiently large, then ξ^M will be negligible. Therefore, it will be assumed that

$$\xi^M = 0$$

From figure 1, the following equation may be written (with the x, y, t notation dropped):

$$C^N = q^N + A^N H^N \alpha^N \quad (10)$$

Since

$$\alpha^N = [H^N]^{-1} D^N \hat{C}^N \quad (11)$$

and it is assumed that

$$C^N = \hat{C}^N \quad (12)$$

substituting equations (11) and (12) into equation (10) gives

$$C^N = q^N - \Lambda^N H^N [H^N]^{-1} D^N C^N \quad (13)$$

or

$$C^N = [I + \Lambda^N D^N]^{-1} q^N \quad (14)$$

From the other path in the system model in figure 1,

$$C^R = \Lambda^R H^R \alpha^N + q^R \quad (15)$$

Substituting equations (11) and (12) into equation (15) yields

$$C^R = -\Lambda^R H^R [H^N]^{-1} D^N C^N + q^R \quad (16)$$

Substituting equation (14) into equation (16) to eliminate C^N gives

$$C^R = -\Lambda^R H^R [H^N]^{-1} D^N [I + \Lambda^N D^N]^{-1} q^N + q^R \quad (17)$$

By inserting $[\Lambda^N]^{-1} \Lambda^N$ into equation (17), the following expression for C^R is obtained:

$$C^R = -\Lambda^R H^R [H^N]^{-1} [\Lambda^N]^{-1} \Lambda^N D^N [I + \Lambda^N D^N]^{-1} q^N + q^R \quad (18)$$

Equations (14) and (18) give the dynamic values of the modal coefficients of the error in the mirror surface. In the present application it is anticipated that the primary errors will be the initial figuring errors and thermal gradients that vary relatively slowly with time. Therefore it is reasonable to expect that the system will be generally at or near its steady state. The steady-state performance of the system is discussed in the following section.

Evaluation of Steady-State Errors

In determining the steady-state performance of the entire system, first equation (14) will be used to assess the resulting error in the controlled modes and then equation (18)

will be used to determine the error in the remaining modes. Taking the Laplace transform of equation (14) and considering the disturbance vector \mathbf{q} as a step input allows application of final-value theorem to determine the steady-state condition:

$$C_{ss}^N = \lim_{t \rightarrow \infty} C^N(t) = \lim_{s \rightarrow 0} sC^N(s) = \lim_{s \rightarrow 0} s[I + \Lambda^N D^N]^{-1} \text{col} \left\{ \frac{q_i}{s} \right\} \quad (i = 1, \dots, N) \quad (19)$$

The matrices Λ^N and D^N are both diagonal with

$$\Lambda^N = \text{diag} \left[\frac{1}{s^2 + \epsilon_i s + \omega_i^2} \right] \quad (i = 1, \dots, N; \epsilon > 0) \quad (20)$$

where equation (20) assumes some structural damping.

The diagonal matrix D^N can be formulated at the discretion of the designer; however, a type 1 system is assumed, so that the combination of Λ^N and D^N is of the form

$$\Lambda^N D^N = \text{diag} \left[\frac{K(\tau_1 s + 1) \dots (\tau_n s + 1)}{s(\tau_1' s + 1) \dots (\tau_n' s + 1)} \right] \quad (21)$$

and

$$[I + \Lambda^N D^N] = \text{diag} \left[\frac{s \prod_{i=1}^n (\tau_i' s + 1) + K \prod_{i=1}^n (\tau_i s + 1)}{s \prod_{i=1}^n (\tau_i' s + 1)} \right] \quad (22)$$

which can be simplified to the form

$$[I + \Lambda^N D^N] = \text{diag} \left[\frac{K \prod_{i=1}^{r+1} (\tau_i'' s + 1)}{s \prod_{i=1}^n (\tau_i' s + 1)} \right] \quad (23)$$

by properly combining the numerator of equation (22) and factoring. Putting equation (23) into equation (19) and taking account of the inverse yields

$$C_{ss}^N = \lim_{s \rightarrow 0} \left\{ s \operatorname{diag} \left[\frac{s \prod_{i=1}^n (\tau_i s + 1)}{K \prod_{i=1}^{n+1} (\tau_i s + 1)} \right] \operatorname{col} \left(\frac{q_i}{s} \right) \right\} = 0 \quad (i = 1, \dots, N) \quad (24)$$

This is the expected result that a type 1 system will drive the error in the controlled modes to zero.

In anticipation of evaluating the steady state of equation (18), equation (21) and the inverse of equation (23) are combined to get

$$\lim_{s \rightarrow 0} \Lambda^N D^N [I + \Lambda^N D^N]^{-1} = \lim_{s \rightarrow 0} \operatorname{diag} \left[\frac{K \prod_{i=1}^n (\tau_i s + 1) s \prod_{i=1}^n (\tau_i' s + 1)}{s \prod_{i=1}^n (\tau_i s + 1) K \prod_{i=1}^{n+1} (\tau_i' s + 1)} \right] = I \quad (25)$$

Furthermore, since

$$\lim_{s \rightarrow 0} \Lambda^R = \lim_{s \rightarrow 0} \operatorname{diag} \left[\frac{1}{s^2 + \epsilon_i s + \omega_i^2} \right] = \operatorname{diag} \left[\frac{1}{\omega_i^2} \right] \quad (26)$$

and

$$\lim_{s \rightarrow 0} [\Lambda^N]^{-1} = \lim_{s \rightarrow 0} \operatorname{diag} \left[\frac{1}{s^2 + \epsilon_i s + \omega_i^2} \right]^{-1} = \operatorname{diag} [\omega_i^2] \quad (27)$$

equation (25) can be used to determine the steady-state value of equation (18):

$$C_{ss}^R = \lim_{s \rightarrow 0} s C_{(s)}^R = -\Lambda^R H R [H^N]^{-1} [\Lambda^N]^{-1} q^N + q^R \quad (28)$$

or

$$C_{ss}^R = q^R - \Lambda^R H R [\Lambda^N H^N]^{-1} q^N \quad (29)$$

where equations (26) and (27) indicate the nature of A^R and $[A^N]^{-1}$. The nature of the H matrix and how to evaluate it is given in the next section. Equation (29) states that the final steady-state error consists of two parts. The first part (q^R) is that due to the original error in the $R = M - N$ modes which were not controlled. The second part of the error is that generated by the control system itself as it corrects the error in the first N modes.

A few notes on the dimensionality of the matrices in equation (29) are in order. The error vector q^N is the initial error in the N modes (not necessarily the first N) selected to be controlled and is $N \times 1$; q^R is the set of errors in the remaining modes and is $R \times 1$. Therefore,

$$\begin{bmatrix} q^L \\ \dots \\ q^R \end{bmatrix} = \begin{bmatrix} q^M \end{bmatrix} \quad (30)$$

The A^N matrix is an $N \times N$ diagonal matrix which consists of the natural frequencies of the modes being controlled; A^R is an $(M - N) \times (M - N)$ diagonal matrix of the frequencies of the remaining modes. The H^N and ψ^R matrices are $N \times N$ and $(M - N) \times N$, respectively. How these are obtained is given in the next section.

Determination of Pad Effects

The function of the H matrices (H^N and H^R) is to take the point loads of the actuators and transform them into modal coordinates. To determine the elements of the two H matrices, consider first the continuous case. Let the force distribution on the mirror $P(x,y,t)$ be denoted by P

$$P = \sum_{j=1}^N \alpha_j(t) \beta_j(x,y) \quad (31)$$

where $\alpha_j(t)$ is the time-varying coefficient of the j th actuator and $\beta_j(x,y)$ is the distribution of the force on the mirror because of the pad. A "pad" is the physical device that connects the actuator to the mirror. This force distribution may be expanded by using the complete orthonormal set of modes:

$$\beta_j = \sum_{i=1}^{\infty} h_{ij} U_i \quad (32)$$

where the (x, y, t) notation is understood. Because of the properties of this set, the coefficients may be determined immediately:

$$h_{ij} = \int_{\Gamma} U_i \beta_j d\Gamma \quad (33)$$

where Γ is the area over which the pad acts.

Substituting equation (32) into equation (31) gives

$$P = \sum_{j=1}^N \alpha_j \sum_{i=1}^{\infty} h_{ij} U_i = \sum_{i=1}^{\infty} \left(\sum_{j=1}^N h_{ij} \alpha_j \right) U_i \quad (34)$$

Another way of writing equation (31) is

$$P = \sum_{i=1}^{\infty} a_i U_i \quad (35)$$

which expresses P directly in terms of the eigenvectors. The implication of equations (35) and (34) is that

$$a_i = \sum_{j=1}^N h_{ij} \alpha_j \quad (36)$$

or

$$\begin{Bmatrix} a \\ a^N \\ a^R \end{Bmatrix} = \begin{Bmatrix} a \\ H^N \\ H^R \end{Bmatrix} \begin{Bmatrix} \alpha \\ \alpha^N \end{Bmatrix}$$

The elements of the H matrix are defined by equation (33). If small pads are assumed and it is further assumed that the load distribution is uniform, then

$$\beta_j = \frac{1}{\int_{\Gamma} dA} \quad (37)$$

The assumption of small pads leads to the conclusion that the mode shape is relatively constant over the area of one pad, and equation (33) becomes

$$h_{ij} = \int_{\Gamma} U_i \beta_j d\Gamma = \beta_j \int_{\Gamma} U_i d\Gamma = \frac{U_i(x_j, y_j) \int_{\Gamma} dA}{\int_{\Gamma} dA} \quad (38)$$

and

$$\lim_{\Gamma \rightarrow 0} H = \begin{bmatrix} U_1(x_1, y_1) & U_1(x_2, y_2) & \dots & U_1(x_N, y_N) \\ U_2(x_1, y_1) & U_2(x_2, y_2) & \dots & U_2(x_N, y_N) \\ \vdots & \vdots & & \vdots \\ U_M(x_1, y_1) & U_M(x_2, y_2) & \dots & U_M(x_N, y_N) \end{bmatrix} \quad (39)$$

When selecting the terms $U_i(x_j, y_j)$ in equation (39), the coordinates (x_j, y_j) are determined by the actuator locations since β_j is assumed zero everywhere except at the actuator location. Note that the H matrix is not square. There will be N columns corresponding to the N actuator locations used; however, all M rows will be present since each and every actuator will, in general, excite all M modes. For analysis purposes it is convenient to partition the H matrix into two parts:

$$H = \begin{bmatrix} H^N \\ \cdots \\ H^R \end{bmatrix} \quad (40)$$

The first matrix H^N consists of the N rows which correspond to the modes which have been selected to be controlled by the N actuators; H^N is therefore square. It is not necessary that the first N rows (N modes) be selected; however, this is usually desired. The reason for this will become clear in the examples. This arrangement will be assumed in future notation for the H^N matrix.

Since H^N , H^R , A^N , A^R , q^N , and q^R have now been obtained, the steady-state error from equation (29) may be calculated for a given choice of actuator locations and modes to be controlled. The only remaining consideration is the performance index.

PERFORMANCE EVALUATION

Calculation of the Performance Index

To obtain the best performance from an optical system, it is necessary to minimize the rms surface error of the elements (ref. 8). This error is defined as

$$J^* = \sqrt{\frac{1}{A} \int_A w^2(A) dA} \quad (41)$$

For analysis purposes it is usually easier to work with a slightly different quantity which provides an equally valid measure of relative performance:

$$J = J^{*2} \quad (42)$$

Using J as the performance index and changing to discrete notation because of the numerical nature of the mirror problem gives

$$J = \frac{1}{A} \sum_{i=1}^M w_i^2 \Delta A_i \quad (43)$$

or, in matrix notation,

$$J = \frac{1}{A} W^T [\Delta A] W \quad (44)$$

where

$$[\Delta A] = \text{diag } [\Delta A_i]$$

W $M \times 1$ vector of mirror displacements or errors

A total area

The first N modes will contribute no steady-state error to a step response in a type 1 system since it was assumed that $\hat{C}^N = C^N$. The final value of W is therefore given by

$$W = [U] \begin{bmatrix} 0 \\ C_{ss}^R \end{bmatrix} \quad (45)$$

where C_{ss}^R is the $(M - N) \times 1$ or $R \times 1$ vector of the final error in the uncontrolled model and is obtained from equation (29). If U , the matrix of eigenvectors, is obtained from a finite-element program — as was done herein — then the eigenvector matrix is orthogonal with respect to the mass matrix m (refs. 4 and 5):

$$U^T m U = I$$

For a homogeneous mirror of uniform thickness, m may be specified as an area associated with each grid point in the analysis times an area density constant ρ . Then m may be written as

$$m = \rho \operatorname{diag}[\Delta A_i] = \rho [\Delta A] \quad (46)$$

or

$$\frac{1}{\rho} [m] = [\Delta A] \quad (47)$$

Using equations (47) and (45) in equation (44) gives

$$J = \frac{1}{A} \left[C_{ss}^R \right]^T U^T \frac{1}{\rho} [m] U \left[C_{ss}^R \right] \quad (48)$$

$$J = \frac{1}{\rho A} \left[C_{ss}^R \right]^T U^T [m] U \left[C_{ss}^R \right] \quad (49)$$

$$J = \frac{1}{\rho A} \left[C_{ss}^R \right]^T \left[C_{ss}^R \right] \quad (50)$$

$$J = \frac{1}{m_t} \left[C_{ss}^R \right]^T C_{ss}^R = \frac{1}{A} W^T [\Delta A] W \quad (51)$$

where the total mass is

$$m_t = \sum_{i=1}^M \Delta m_i \quad (52)$$

The contribution to the mean-square error of any mode is seen from equation (51) to be given by C_i^2/m_t .

In any approach where the controller is designed by use of an alternate representation of the mirror, it is important to express the desired system performance within the framework of the alternate reference frame. The significance of equation (51) is that it expresses the figure of merit of the system performance — rms error — as a very simple function of the amplitudes of the higher order modes. Thus, minimum rms surface error on the mirror is obtained by minimizing the sum of the squares of the amplitudes of the higher order modes. If only a relative measure of one actuator arrangement over another is of interest, the term $1/m_t$ may also be dropped since it is constant for any given mirror. This gives

$$J_1 = \left[C_{S\bar{S}}^R \right]^T \left[C_{S\bar{S}}^R \right] \quad (53)$$

Treatment of Initial Errors or Disturbances

The q vector obtained from equation (1) assumes that the error at each grid point on the mirror surface is known. When this is used in equation (29), the resulting design represents a deterministic treatment of the errors. While such a treatment of the errors will lead to minimum final error, the result can also lead to overoptimism on the part of the designer. Consider the following case.

Given a set of initial errors, the designer determines that a specific actuator arrangement will reduce the final error to an acceptable value. When the mirror is placed in orbit, it is highly likely that the errors will be different from those anticipated. As a result, the second term in equation (29) — the error generated by the control system — will change, possibly significantly. Consequently, the total error as given by equation (29) may now be unacceptable. It is concluded, therefore, that the "best" actuator location, based on deterministic errors, is sensitive to initial error. The question is, of course, how sensitive? Usually very sensitive, because the actuator positions have been chosen to generate specific amounts of error in the uncontrolled modes (generally opposite and equal to what was originally there) when specific amounts of error are removed in the controlled modes. A slight change in the error in the controlled modes, therefore, could make a great deal of difference in the final error.

An alternate way to treat an error is in an uncorrelated fashion, as suggested in reference 3. In this approach the values of C_{SS}^R are still given by equation (29); however, the performance index is now the expected value of the mean-square error

$$E(J) = \frac{1}{A} E[W^T \Delta A W] \quad (54)$$

where E is the expectation operator. If the errors are uncorrelated, then

$$E(q_i q_j) = 0 \quad (i \neq j) \quad (55)$$

and the performance index becomes

$$E(J) = E\left(\left[q^R\right]^T q^R + \left[q^N\right]^T \psi^T \psi q^N\right) \quad (56)$$

For the assumed type 1 system, where

$$\psi = \Lambda^R H R \left[\Lambda^N H^T N \right]^{-1} \quad (57)$$

equation (56) may be rewritten as

$$E(J) = \sum_{i=N+1}^M c_{q_i}^2 + \sum_{j=1}^{M-N} \left(\sum_{i=1}^N \psi_{j,i}^2 \sigma_{q_i}^2 \right) \quad (58)$$

where the variance of the error, which is assumed to have zero mean, is given by $\sigma_{q_i}^2$. By reversing the order of summation in the second term of equation (58) and making the additional substitution

$$\phi_i^2 = \sum_{j=1}^{M-N} \psi_{j,i}^2 \quad (59)$$

equation (58) can be rewritten

$$E(J) = \sum_{i=N+1}^M \sigma_{q_i}^2 + \sum_{i=1}^N \phi_i^2 \sigma_{q_i}^2 \quad (60)$$

One notation addition is needed in equation (60), that is, to add the subscript N to E and to ϕ_i^2 to indicate the number of actuators being used. This will prevent confusion later. Equation (60) is then written

$$E_N = \sum_{i=N+1}^M \sigma_{q_i}^2 + \sum_{i=1}^N \phi_{iN}^2 \sigma_{q_i}^2 \quad (61)$$

It should be pointed out that equation (61) represents an expected error. Depending upon the inclination of a particular individual, he may choose J^* , J , or J_1 , given by the previous equations, as a measure of the performance. The only problem with these equations for the performance is that they require exact knowledge of the error vector and may be quite sensitive to changes in the error vector, while equation (61) requires only a knowledge of the variance of the error. It is more realistic to make an engineering estimate of this latter quantity than of the actual errors.

In equation (61) both parts of the error are seen to be positive. This means that the two error components will add directly. To influence the expected error, the designer may do two things. First, he should encourage the opticians to keep the error in the higher order modes as small as possible because he cannot do anything to reduce this error except possibly increase the value of N . Second, he should select actuator locations which would minimize the value of ϕ_{iN}^2 . In fact, if ϕ_{iN}^2 could be made zero for $i = 1, \dots, N$, then the expected error would be independent of the initial error in the controlled modes. Since most of the error will likely occur in the first N modes, choosing actuator locations to minimize ϕ_{iN}^2 will lead to locations which tend to produce performance indices virtually independent of changes in error.

In the following sections and the appendixes, various design examples will be given which are based upon the theory developed up to this point. Effects of initial errors, actuator placement, error treatment, and the number of actuators necessary for a particular case will be discussed.

DESIGN PROCEDURE

Numerical and Physical Data

The mirror which will be used in the analysis is shown in figure 2. It is a 1.27-cm-thick (1/2-inch), 76-cm-diameter (30-inch), F/3 spherical mirror which is supported on a kinematic (non-overconstrained) mount.

As mentioned in the Introduction, it is generally not possible to obtain closed-form expressions of the eigenfunctions of a practical mirror configuration such as that con-



Figure 2.- Photograph of 76-cm-diameter (30-inch) deformable mirror which was modeled for this report.

sidered here. Therefore, estimates of the eigenfunctions are sought through numerical techniques. An analysis of the mirror was made with the SAMIS structural analysis program (ref. 4) and the grid breakup shown in figure 3(a). This grid breakup was adopted to comply with the SAMIS recommendation for use of equilateral triangles for maximum accuracy. This pattern also insured the location of a grid point (where forces may be applied and displacements sensed) at each actuator and sensor location of the existing mirror shown in figure 2. The actuator and sensor locations are shown in figure 3(b), where the numbers refer to grid points. As reported in reference 7, this procedure provides a satisfactory discrete model of the mirror behavior.

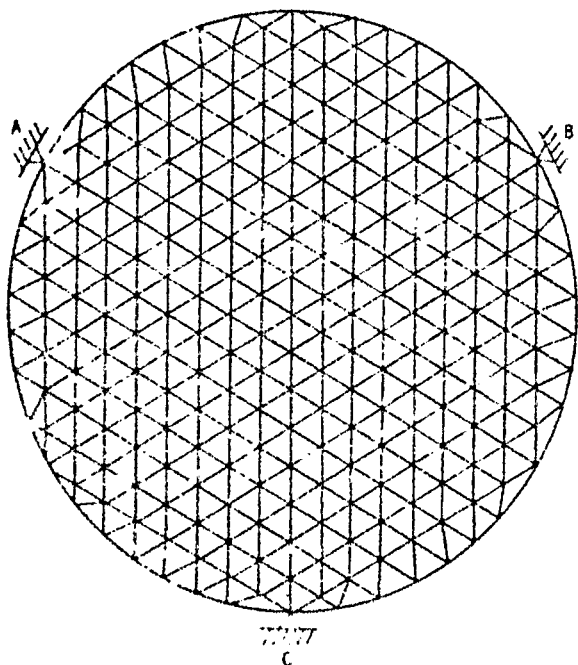
In the preceding sections, M has represented the finite number of modes used in lieu of the infinite number which would be required for an exact representation of the mirror. In performing a specific design it is desirable to select a value for M which is high enough to limit the error in the analysis and yet is not so high that it would require an excessive amount of calculation. Because of the inability to place a bound on the error incurred through the choice of a specific value of M , the choice is not subject to precise evaluation. In the present study the mirror shown in figure 2 was available for corroboration of theoretical results. This mirror has 58 displacement sensors, which similarly limit the maximum number of mode amplitudes that can be estimated. For this reason $M = 58$ was selected for the present study. It is believed that this number is more than adequate for the present application; however, an exhaustive study on this point was not performed and it is possible that a smaller value of M might also be satisfactory.

The matrix of eigenvectors determined from this model is given in appendix B, and appendix C contains plots of node lines for a selected set of modes. The numbers on these plots are the value of the eigenvectors at the grid points. Therefore, each figure represents one eigenvector. The orientation of the figures in appendix C is the same as that in figure 3(b) to allow grid point numbers and eigenvalues to be correlated. The eigenvalues of the mirror are given in appendix D and are plotted in figure 4. For completeness appendix D also contains a listing of the diagonal mass matrix.

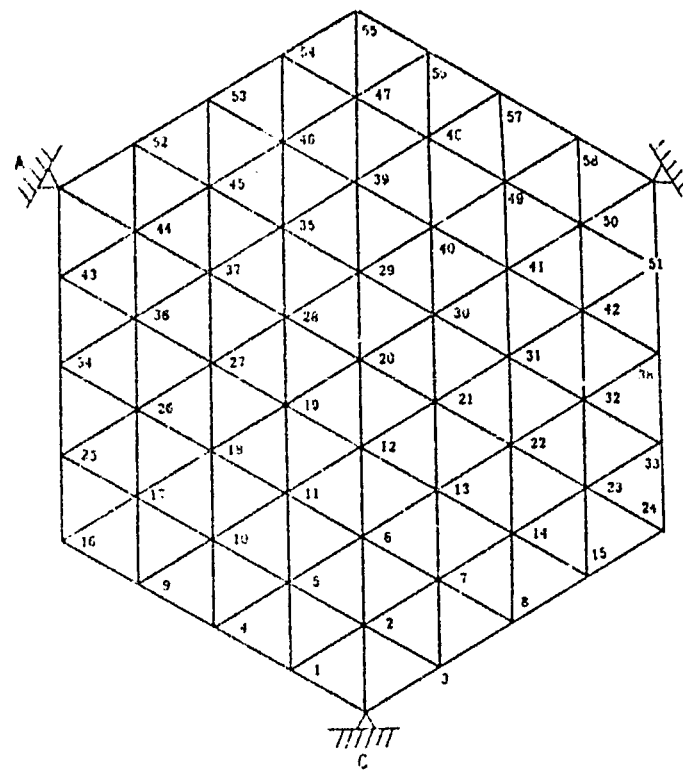
For design and analysis purposes three error vectors were assumed. The first error vector was obtained from reference 2 and is the error in figuring the mirror. The second and third were arbitrarily generated. The second was generated by assuming a set of four forces of 4.448 newtons (1 pound) located at grid points 16, 20, 21, and 40. The third example error was a parabolic error. The modal coefficients q_1 for these three error examples are listed in table I.

Control System Design Evaluation

The basic design procedure consists of setting up a trial design, evaluating C_{ss}^R from equation (29), calculating J_1 from equation (53), and comparing this value of J_1



(a) Grid arrangement used for analytical structural
program of the main mirror. Point A is
represented by a cross; point B, by a 'v'; point C,
by a dot.



(b) Grid arrangement and numbering used for control
system analysis.

Figure 1.4. Control system and grid arrangement for the analytical solution.

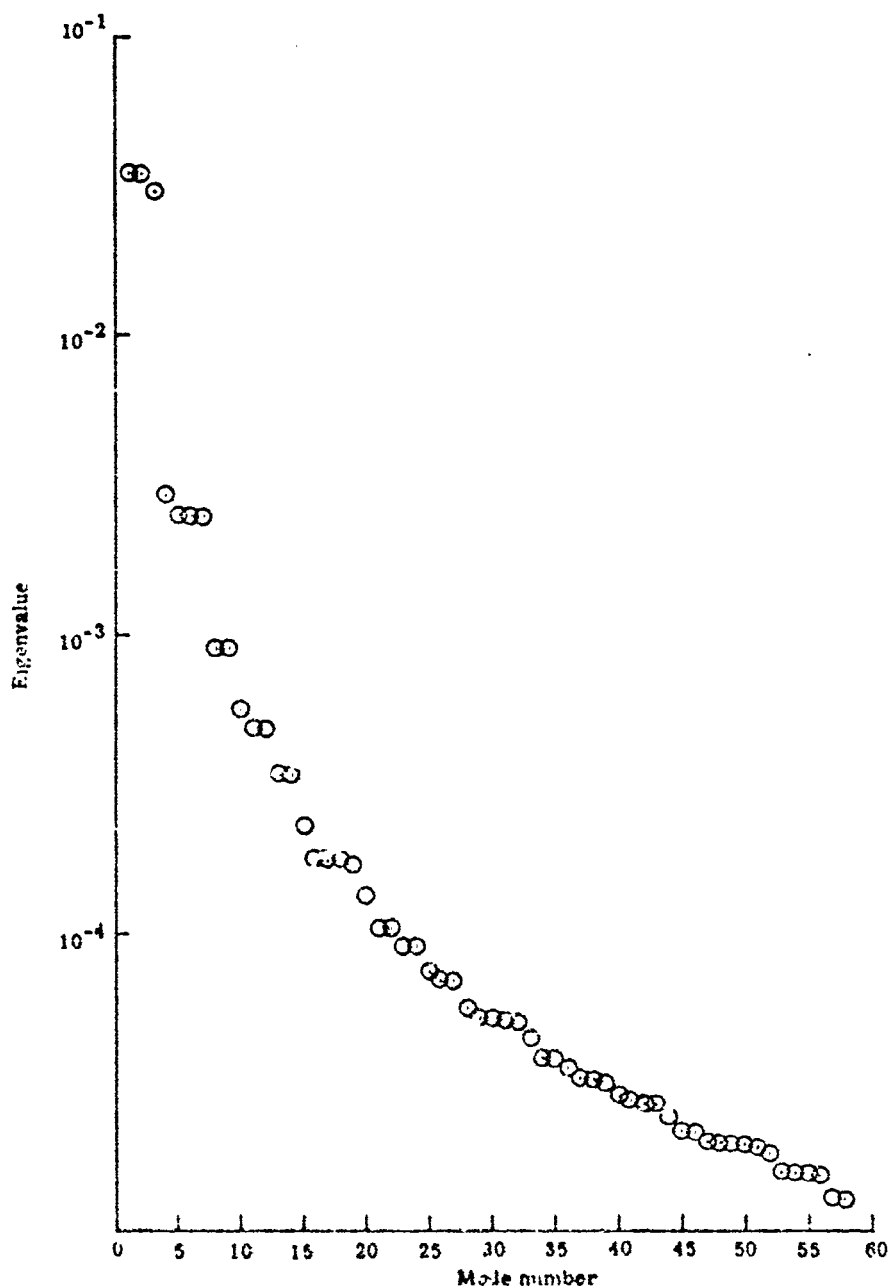


Figure 1 - Eigenvalues of thin mirror as determined by SAMIS. Lowest frequency is associated with mode 1. 'SAMIS eigenvalues are inversely proportional to frequency.'

with previous or desired results. If the results are not satisfactory, then a new design is tried. Since many trials will be necessary, the only practical approach is to perform the design with the aid of a computer. A program to build the various matrices and to evaluate C_{ss}^R and the performance index J_1 has been written in FORTRAN IV and is given in appendix A. The flow diagram for the program is given in figure 5, where the steps of the design procedure are set out in a straightforward manner.

As shown in figure 5, the program will first read in values of the eigenvector matrix, the eigenvalues, and the initial error, or disturbance, vector. The program must then be supplied with the number of actuators N to be used and the placement of these actuators. Actuator placement is specified by grid numbers. The selection of actuator location and number is the major degree of freedom that the control system designer has, and this selection more than any other will influence the value of J_1 . The program must then be supplied with the number of modes to be controlled (the number of controlled modes must equal the number of actuators) and these modes identified. Identification of modes is by mode number corresponding to the column numbers of the U matrix. With minor exceptions, these should always be the first N modes. From this point the program will sort the Λ , q , and H matrices and carry out the calculation of C_{ss}^R and J_1 . The program will also do one other task; namely, it will calculate the actuator forces and final error on the basis of making a least-squares fit of the errors to the desired shape. This allows a comparison of the modal control law to an optimal control law for the same actuator locations. One restriction on the program, and ultimately the designer's freedom, is that the choice of actuator placement must be restricted to grid points of the structural analysis model. This restriction has not been found to be serious in the present model, which has 58 grid points.

One particular word of caution is in order about this, or any other program, which is used to calculate the final error. For a given pad shape and size and a given set of modes to be controlled, selecting the actuator placement pattern fixes the H^N matrix. Since the inverse of H^N is part of the controller, the actuator locations must be chosen to insure that H^N is nonsingular. A singular (or ill-conditioned) H^N matrix indicates that the designer has placed actuators in such a manner that the amplitude of at least one controlled mode at these actuator locations is (or is nearly) a linear combination of the amplitudes of the other controlled modes. If H^N is singular, the actuators cannot independently control the given modes. If H^N is ill conditioned, the modes can be controlled but only at the expense of large applied control forces, which generate considerable error in the higher order modes. The designer obviously must avoid these cases; however, spotting a potentially singular matrix mainly on the basis of an actuator-placement pattern is almost impossible. The computer especially has trouble spotting this condition, since for reasons of numerical roundoff and the particular inversion procedure used, it will obtain "inverses" for very ill-conditioned or even singular matrices. The program given in

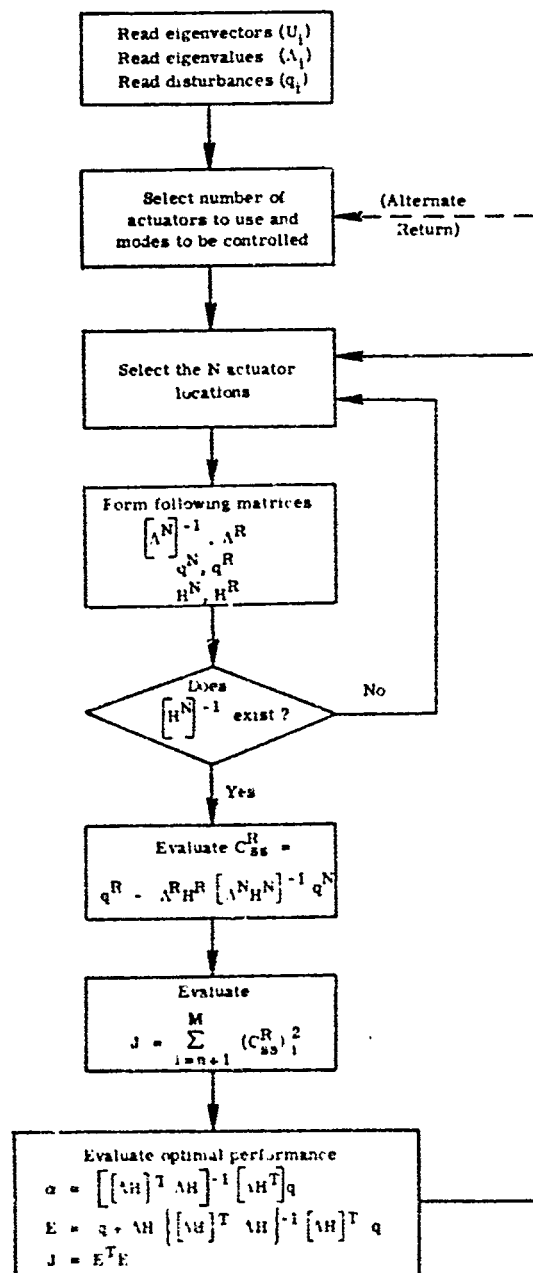


Figure 5.- Flow diagram of computer program in appendix A. This program evaluates the performance index for a given mirror and a given, or selected, set of actuator locations.

appendix A treats this problem by calculating and printing out the normalized determinant of H^N . If the normalized determinant is very small relative to 1.0, then H^N is said to be ill conditioned. (See ref. 9.) Usually an ill-conditioned H^N matrix will result in a large value of J_1 , which automatically excludes that actuator arrangement. This, however, is not always the case. (See, e.g., fig. E10 and associated discussion.)

Results for Deterministic Errors

From the first set of errors a series of design trials were run with various numbers of actuators. For the 58-node mirror model, all possible combinations of one, two, three, four, and five actuators were surveyed. Beyond five actuators, the number of possible combinations becomes too large to make exhaustive searches. Several design "rules of thumb" were tried to choose actuator locations; however, none of these provided values of J_1 that were considered to be near the minimum in light of the results from the exhaustive searches carried out for fewer actuators.

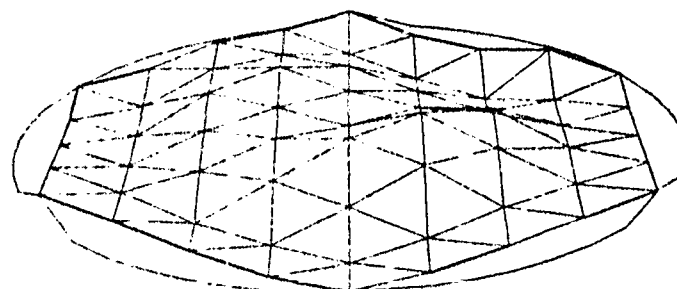
The technique that produced the best results was a gradient-type search which used the computer interactively. In this technique an initial actuator placement is chosen and the output of the computer is presented on a CRT. A perspective view of the mirror is also generated which shows the deformed state after control. A series of these perspective plots for five actuators is given in figure 6. On the basis of the tabulated data and the perspective plot, one actuator is moved one grid point and the program rerun to see whether a gradient can be set up on J_1 to improve the mirror performance. At most, six trials are required to exhaust the possible moves for one actuator. The most important single piece of information turned out to be the perspective plot — especially early in the search procedure. This plot allowed the grid point with the largest error to be easily spotted, and the actuator nearest this error was moved. The series in figure 6 took approximately 2 hours and improved the performance index J_1 from an initial value of 1136.6 to a value of 100, a factor of 10. Further effort beyond this point failed to provide improvement.

The results obtained from these gradient runs can be compared with the known minimum value $J_1 = 72$, obtained from an exhaustive search. The total number of runs that were required in the gradient-search process was 63. If the program were implemented so that the computer made all the choices of actuator placement, the gradient search would require about 30 seconds of computer time. The use of the computer in the interactive mode, however, allowed considerably more insight to be gained into what factors were affecting performance and what factors were not.

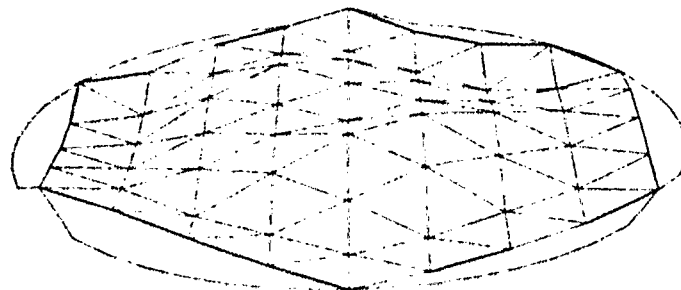
The results of the exhaustive searches for up to five actuators are given in appendix E. In each case the best 10 locations are shown. The initial performance index in all cases was $J_1 = 1136.6$ and two final errors are given. The first is the final error



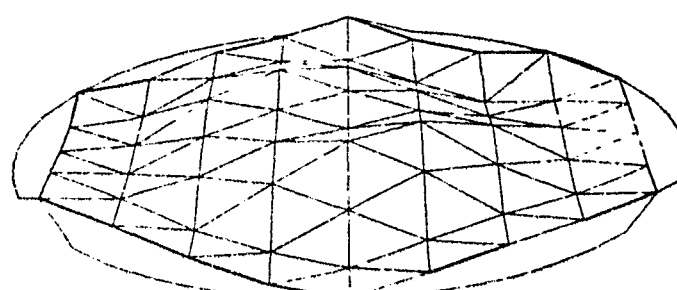
A
Initial figure error
 $\text{Error } U_1 = 1136.5$



B
Figure at first actuator trial
 $\text{Error } U_1 = 131$



C
Figure after 20 actuator moves
 $\text{Error } U_1 = 112$



D
Figure after 48 actuator moves
 $\text{Error } U_1 = 100$

Figure 6.- Perspective views of the mirror at various stages during the gradient search for best actuator location - five-actuator case. The final diagram D is a local minimum, i.e., moving any one actuator one grid point will not improve the figure. (Vertical scaling is variable for visibility purposes.)

obtained with the modal control law and the second is the result obtained when the actuator force is selected to minimize the rms error on the mirror. This is referred to herein as the optimal control law. A summary of these results is given in figure 7 for the modal control law. This figure shows the minimum error obtained plotted against the number of actuators used. The top curve is for the first error example and the lower curve is for the parabolic-error condition. Note that the vertical scale is logarithmic.

The plot in figure 7 suggests an empirical method of estimating the minimum number of actuators that a particular disturbance vector might require for a given mirror and performance index. That is, an exhaustive search over the model is made for a limited number of actuators and the results extrapolated to the desired performance. This would, of course, be equivalent to assuming an exponential decay of error with increasing number of actuators. The class of errors and plants for which such an assumption would hold is not known. Clearly, the error generated by the four loads of 4.448 newtons (1 pound) at the discrete grid points is not in this class since the final error is zero for four or more properly located actuators.

The problem with the deterministic approach is that first, there is presently no way to determine readily the best actuator placement, and second, the placement is very sensitive to initial error.

Results for Uncorrelated Errors

When the designer assumes uncorrelated errors, considerably more can be said about where actuators should be placed and how many actuators will be needed.

First, equation (61) is minimized instead of equation (29). Since the first term in equation (61) is constant for a particular number of actuators, the goal is to minimize the second term, which is the error generated in the uncontrolled modes by the control system. Instead of writing a program to do this, an alternative procedure which enabled the existing computer program to be used was adopted. This procedure yielded results that closely approximated those which would be obtained from equation (61). The alternate procedure consisted of a deterministic minimization of the second term in equation (29). This corresponds to the intent of the uncorrelated case in eliminating the possibility of a control-system-generated error canceling an existing error. If the values of ϕ_{iN}^2 are sufficiently small, there will only be a trivial difference in performance between the two procedures. Since the second term of equation (61) is to be assumed small, the final value of the expected error is the first term of equation (61). A plot of this portion of the equation is given in figure 8.

Since the actuator locations are less sensitive to initial error for this criterion, exhaustive searches were run for only the first error example. The results of these searches are given in appendix F for one, two, three, and four actuators. The values of

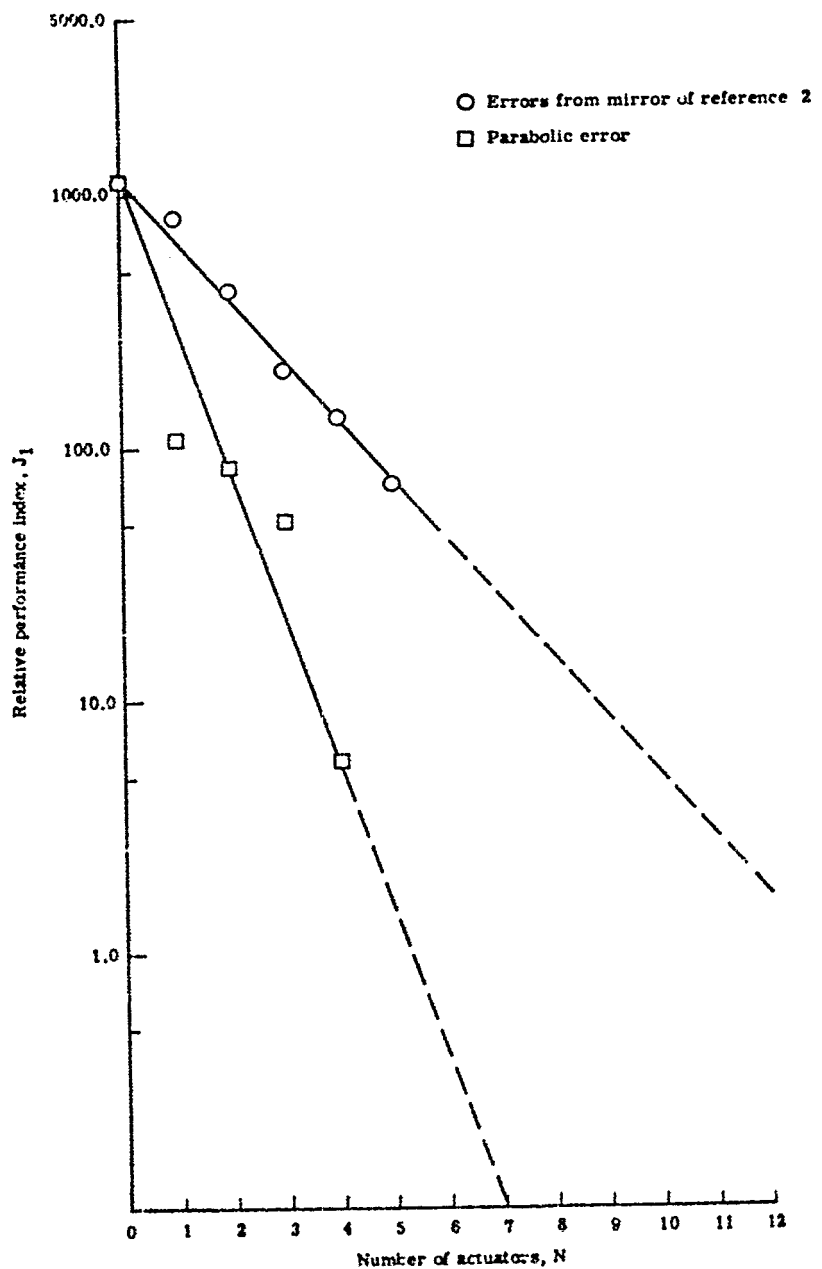


Figure 7.- Error decay as a function of number of actuators for deterministic errors.

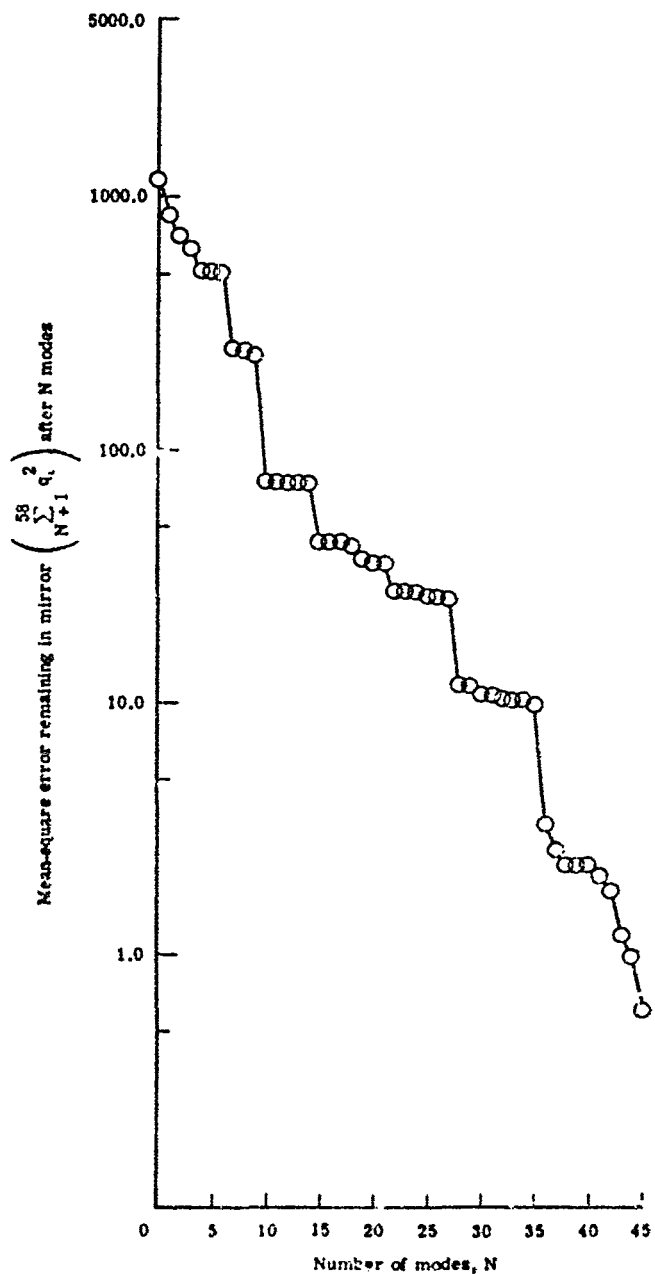


Figure 5.- Mean-square error $\sum_{i=N+1}^{58} q_i^2$ after N controlled modes. This plot indicates expected performance with N actuators, assuming uncorrelated errors. (Mode errors were taken from mirror of ref. 2.)

ϕ_{IN}^2 for the best run of each number of actuators are given in table II. Since the values of ϕ_{IN}^2 are relatively small, the expected error falls right on the predicted values of figure 8.

The choice of possible actuator locations can be considerably reduced when it is desired to minimize the generated error. A look at the actuator location for four actuators shows that each set lies very close to the node lines of mode 5 and several higher modes. As pointed out in reference 3, this means that these modes will not be excited to any great extent. The first mode that is excited to any great extent by this arrangement of four actuators is mode 11. The ratio of eigenvalues for mode 11 to mode 4 is

$$\frac{\Lambda_{11}}{\Lambda_4} = \frac{4.69 \times 10^{-4}}{2.95 \times 10^{-3}} = 0.166 \quad (62)$$

This means that the filtering action by the mirror is about 6 times as much for mode 11 as for mode 4, the last controlled mode.

To test the concept of placing actuators at, or near, nodes of higher order modes to minimize the generated error, the case for seven actuators was tried. The seven-actuator case was chosen because of two factors. First the eigenvalue plot of figure 4 shows a distinct jump between modes 7 and 8. This implies good filtering action by the mirror at this point. Second, the expected-error plot of figure 8 shows a jump between six and seven actuators. This implies that a considerable increase in performance can be obtained with seven actuators over six actuators. In selecting the actual grid locations the node lines for modes 8, 9, and 10 were overlaid and a set of grid points near the junction of these modes was selected. (See the last diagram of fig. F5 in appendix F.) This reduced set of grid points was searched for those locations which yielded minimum generated error. The results of this search are given in table II (ϕ_{17}^2) and in the last set of figures of appendix F (actuator locations). The expected performance index with the best arrangement of seven actuators, obtained by using the minimum generated-error criterion, was $J_1 = 274.9$. Had all the values of ϕ_{17}^2 been exactly zero, the performance index would have been $J_1 = 250.6$. The results, therefore, are very close to the predicted values of figure 8.

It should be noted that this result was obtained by searching only a relative few of the possible actuator locations, therefore, it cannot be said that the result represents the actual minimum. The important point is that a relatively short computer run was able to establish a set of actuator locations having a final error very close to the absolute minimum.

Comparison of Modal Control and Optimal Control Laws

As was stated earlier the computer program which was used to calculate the final errors also calculated the error that would have been obtained if an optimal control law (least-squares fit to best sphere) had been used. In the modal domain the error is given by merging equations (10) and (15) to get

$$\mathbf{C} = \begin{bmatrix} \mathbf{C}_N \\ \mathbf{C}_R \end{bmatrix} = \begin{bmatrix} \mathbf{q}_N \\ \mathbf{q}_R \end{bmatrix} + \begin{bmatrix} \Lambda_{NHN} \\ \Lambda_{RH\bar{R}} \end{bmatrix} \alpha_N$$

$$\mathbf{C} = \mathbf{q} + \Lambda H \alpha \quad (63)$$

It is desired to find the value of α which minimizes

$$J_1 = \mathbf{C}^T \mathbf{C} \quad (64)$$

Therefore,

$$\frac{\partial J_1}{\partial \alpha} = 2[\Lambda H]^T [\Lambda H] \alpha + 2[\Lambda H]^T \mathbf{q} \quad (65)$$

This yields

$$\alpha = -\left[[\Lambda H]^T [\Lambda H] \right]^{-1} [\Lambda H]^T \mathbf{q} \quad (66)$$

From equation (66) the value of the forces needed to minimize the value of J_1 is calculated. The vector \mathbf{C} is then calculated from equation (63), and J_1 is determined from equation (64). The computer program outputs the α vector and the value of J_1 . This can then be compared with the similar value of J_1 under the modal control law.

Numerical comparisons are given in appendixes E and F. Generally, given a set of actuator locations that were "good," there was little difference in the final result. The counterbalancing features of these two control laws are that the modal control law enables the dynamic behavior of the mirror to be considered while the optimal control law would never make the mirror worse than it was originally. To create more error than the original error would require a rather gross misplacement of actuators on the part of the control-system designer; however, it is possible.

For example, when the errors of example 2 in table I are treated deterministically, the conclusion is that the best actuator location is in the center of the mirror. If now the

error distribution changes so that the mode 1 error and the mode 3 error are interchanged, the final error will be much worse than the original.

The reason for this is that the actuator was placed on a node of mode 1 while instructed to control mode 1. This produces considerable force, which generates considerable error. In the original distribution it was desirable to generate a lot of extraneous mode 3 error, but in the modified error distribution it is not desirable to generate much mode 3 error. The optimal control law, faced with the same situation, would do almost nothing in the second case, resulting in almost no change of figure error. For either control law the actuator placement was bad.

It should be recognized that any closed-loop control law, except one that has a decision-making capability as to relative performance, could result in a mirror figure that is worse than the original figure if the actuators are placed in a poor location. The ability of the modal control law to "order," or to establish a hierarchy of, likely mirror deformations through the eigenvectors and to provide a measure of relative likelihood through the ratio of eigenvalues means that the control-system designer will not place actuators in a bad location when using this control law.

Design Examples

To be specific, consider the case for four actuators and error example 1. Trial actuator locations are grid points 2, 30, 42, and 45; and the controlled modes are to be modes 1 to 4 inclusive. The H^N matrix is therefore given by

$$H^N = \begin{bmatrix} -1.092 \times 10^{-2} & 9.997 \times 10^{-3} & -1.307 \times 10^{-3} & 3.009 \times 10^{-2} \\ 5.199 \times 10^{-3} & 7.287 \times 10^{-3} & 3.454 \times 10^{-2} & -1.616 \times 10^{-2} \\ -2.278 \times 10^{-2} & -4.529 \times 10^{-2} & -3.302 \times 10^{-2} & -3.347 \times 10^{-2} \\ -1.453 \times 10^{-2} & -5.481 \times 10^{-2} & -1.235 \times 10^{-2} & -1.229 \times 10^{-2} \end{bmatrix} \quad (67)$$

The following information is then obtained from the computer program for this case:

- (1) The normalized determinant of H^N is 0.23, which is considered satisfactory.
- (2) The force vector a is $\text{col}[-2.108, 5.916, -3.256, 3.781]$ newtons ($\text{col}[-0.471, 1.33, -0.732, 0.850]$ lb), given in the same order as the actuator grid locations.

The remaining important results are tabulated below in both their relative values (J_1), as determined by the program in appendix A, and their absolute values (J'') as given by equation (41).

	<u>Relative values</u>	<u>Absolute values (rms wavelength, λ, 0.6328 μm)</u>
Total original error	1136.6	0.64
Original error in first four modes	618.0	0.474
Original error in remaining 54 modes	518.0	0.433
Error generated by the control system in the 54 uncontrolled modes	346.0	0.354
Final error by the modal control law	131.1	0.218
Final error by the optimal control law	130.4	0.217

The results correspond to the best possible location for four actuators for the deterministic error criterion and error example 1.

For the case just given, all factors worked together to produce an acceptable design; however, it is instructive to consider briefly a case that does not produce good results. For example, it was stated earlier that the first (lowest) N modes were usually controlled. Now consider a case in which this is not true. In error example 1, table I, it can be seen that the four modes which contain most of the error are modes 1, 2, 7, and 10. Suppose that the above actuator locations (2, 30, 42, and 45) are used and the control system is designed to drive these four modes to zero instead of the first four. The H^N matrix would now be different. For reference, the first column would now be

$$\text{col} \left\{ -1.092 \times 10^{-2} \quad 0.519 \times 10^{-2} \quad -0.007 \times 10^{-2} \quad 5.209 \times 10^{-2} \right\}$$

This, in itself, presents no problems; however, in equation (62) the ratio of the eigenvalue of the first mode which would be excited Λ_{11} to the eigenvalue of the highest controlled mode Λ_4 was

$$\frac{\Lambda_{11}}{\Lambda_4} = 0.106 < 1$$

which results in an attenuation of the control-system-generated error. For the case in which the four modes containing the most error are controlled, the ratio

$$\frac{\Lambda_3}{\Lambda_{10}} = \frac{3.06 \times 10^{-2}}{5.67 \times 10^{-4}} = 54 \quad (68)$$

results in an amplification of the control-system-generated error. One might therefore expect that the final error for controlling modes 1, 2, 7, and 10 could be worse than the error for controlling modes 1, 2, 3, and 4. The actual calculated final error for controlling modes 1, 2, 7, and 10 was found to be

$$J_1 = 1.83 \times 10^5$$

which is worse than the original error. It might be argued that a different actuator placement would improve this answer. Although this is probably true to some extent, a new set of actuator locations can only change the H^N matrix but not the ratio in equation (68), which is the underlying cause of the problem.

CONCLUDING REMARKS

A design procedure for selecting actuator locations on thin mirrors which are to be controlled by a modal control law has been worked out for use with typical numerical data. Instructions are given for constructing mathematical models of the system. Two ways of treating disturbances are discussed. These two techniques, deterministic and uncorrelated, are examined from the standpoint of sensitivity to various mirror errors, determining the number of actuators required, and means of finding the best locations. For the deterministic case it was found that the "best" actuator locations (those locations which will minimize the error) are very sensitive to the error distribution; these locations can presently be found only by exhaustive searches of all possible actuator locations, and the number of actuators required for a specific mirror and specific error can only be estimated after much computer time is used. For these reasons it is not recommended that errors be treated deterministically because the exact nature of the final figure-error distribution on the mirror surface will change with telescope attitude.

When the errors are treated as if they are uncorrelated, the locations are much less sensitive to variations in error distribution, an estimate of the number of actuators required to produce a desired reduction in figure error can easily be made, and locations which will yield results near these estimates can be found in a reasonable manner. At present, this technique is much preferred even though it requires more actuators than the deterministic method for a specific assumed error.

For example, the deterministic case for five actuators and 58 possible locations requires 4.6×10^6 trials. When the errors are treated as uncorrelated variables, however, it is possible to select a subset of the 58 grid points which will yield results close to the theoretical limit. This subset is chosen by selecting potential locations near the common node lines of the next few higher modes and making an exhaustive search of these

locations. Also, for the uncorrelated treatment it is possible to estimate the number of actuators a given mirror and mount configuration will require by using an estimate of only the variance of the expected errors.

Langley Research Center,
National Aeronautics and Space Administration,
Hampton, Va., November 11, 1972.

APPENDIX A

COMPUTER PROGRAM DESCRIPTION, LISTING, AND PRINTOUT

This appendix contains a listing of the program to calculate figure error of the mirror on the basis of a type 1 modal controller which controls N modes. The program contains a great deal of comment statements to aid the user, but a few additional comments are in order.

First, one must obtain a set of eigenvalues and the eigenvectors for the particular mirror to be analyzed. This is a major undertaking and should be done with a standard structural analysis program. The size of the eigenvector matrix is a critical item. Since actuators can be placed only at grid points of the structural analysis model, a sufficient number of these grid points must be used to allow reasonable flexibility in actuator placement. Too many grid points will result in a matrix that is too large to handle and requires excessive storage. The 58 grid points and the 58×58 U matrix used in this analysis have proved to be reasonable. This results in a storage requirement of 110 000g, which may be too large for some systems.

The next requirement is to obtain an error vector. This may be obtained from experimental data by estimating or determining the mirror error at each grid point and multiplying by $[U]^{-1}$, or it may be artificially generated, as were examples 2 and 3. In any case the program assumes that the error vector is already in modal coordinates. An option of multiplying this error vector by a constant (to change units) is provided also.

The next option selects the output. The short option is recommended for all runs except debugging and examining final runs. An example of the complete output is given after the program listing. The short option is the last page of output.

The final option allows the designer to change a few of the actuators and control modes without completely rewriting the data cards. By setting NEW = 1, a single actuator location (or several locations) can be shifted by one number. For example, if a set of seven actuators is being run and it is desired to vary the location of one or two actuators to several selected points on the mirror, it can be done by using this option. Assume that the original data cards contain modes 1, 2, 3, 4, 5, 6, and 7 as controlled modes and actuator locations of 6, 16, 20, 24, 38, 55, and 50, and it is desired to change an actuator location from grid point 50 to grid point 49. In this case the MOCHNGE would be zero and LOCHNGE would be 1, and the next card would contain the number 49 in proper format. The controlled modes would then be the same, but the actuator locations would be 6, 16, 20, 24, 38, 55, and 49. Note that it is necessary to place the actuator(s) to be moved at the end of the list in the original data card.

APPENDIX A - Continued

The remainder of the program sorts matrices, calculates the various quantities needed to evaluate the performance, and formats the output. One point near the end of the program might cause confusion if data on a different mirror are used, that is, the conversion of the force vectors to pounds. The value of 1.25×10^{-9} assumed that the original errors on the mirror surface were in fringes ($\lambda = 0.6328 \mu\text{m}$). If not, the error can be scaled in the first part of the program. Another potential trouble source is in the use of the eigenvalues. SAMIS eigenvalues are inversely proportional to frequency squared, and other programs (NASTRAN) output eigenvalues in frequency directly. This can be corrected at line 000467 by changing `OMEGASQ(J) = 10000./LAMBDA(I)` to `OMEGASQ(J) = 1C000. * (frequency squared)`.

```

PROGRAM ALTUATE (INPUT, OUTPUT, TAPE10)
REAL LAMBCA(58)
INTEGER UMCDC(58), ULCCAT(58)
DIMENSION U(58,58), MUDC(58), LUCA(58), UMEGAS(58), UINVDE(58),
I HN(58,58), MR(58,58), CN(58), QR(58), HOLD(58,58)
DIMENSION DUMMY(58,2), IPIVOT(58), INDEX(58,2)
DIMENSION PKCD(58,58), PROD2(58), CRSS(58)
DIMENSION HCLOUDP(58,58)
DIMENSION ANIVIDE(58)
DIMENSION ARRAY(58,58), VECTOR(58)
DIMENSION ALPHA(58), ALPSTOR(58)
DIMENSION PHI(30), LABEL(8)
DIMENSION UINVFLX(58)
M = 0
NSE = 58
C
C      READ IN THE U (EIGENVECTOR) MATRIX.  THE EIGENVECTORS ARE COLUMNS
C      OF THE MATRIX.
C
DO 5 J=1,58
READ (10) (U(I,J),I=1,58)
5 CONTINUE
C
C      READ IN THE CORRESPONDING EIGENVALUES.
C
READ 203, LAMBCA
PRINT 204, LAMBCA
C
C      READ IN A DESCRIPTIVE HEADING FOR THE ERROR VECTOR.
C
READ 209, LABEL
PRINT 260, LABEL
C
C      READ IN ERROR VECTOR AND THE SCALER MULTIPLIER.
C
READ 203, UINVDE
PRINT 205, UINVDE
READ 261, FACTOR
C
C      SCALE THE DEFLECTION VECTOR.
C
DO 403 I=1, 58

```

APPENDIX A - Continued

```
000100      UINVOE(I) = UINVOE(I) + FACTOR
000102      403 CONTINUE
000104      PRINT 262, FACTOR, UINVOE
C          READ IN IPRINT. IF IPRINT = 0 PRINTOUT, WILL BE ABBREVIATED TO ONE PAGE
C          PER RUN. OTHERWISE PRINTOUT WILL INCLUDE SEVERAL INTERMEDIATE MATRICES.
C
000113      READ 206, IPRINT
C          NUMRUN IS THE NUMBER OF RUNS TO BE MADE. EACH ONE INVOLVES A
C          DISTINCT SET OF MODES CONTROLLED AND ACTUATOR LOCATIONS.
C
000121      READ 206, NUMRUNS
C          BEGINNING OF DO-LOOP WHICH PROCESSES EACH RUN.
C
000127      DG 350 IRUNS=1,NUMRUNS
C          READ IN NEW. IF NEW = 1, A NEW SET OF MODES & ACT. LOCATIONS IS READ IN.
C
000131      READ 206, NEW
000136      IF (NEW .EQ.1) GO TO 415
C          IF NEW .NE. 1, READ IN THE FOLLOWING TWO VALUES WHICH INDICATE THE NUMBER
C          OF MODES AND ACT. LOCATIONS TO BE CHANGED.
C
000140      READ 206, MOCHNGE, LCCHNGE
000150      IF (MOCHNGE.EQ. 0) GO TO 405
000151      MOCHNGE = MODE + 1 - MOCHNGE
C          REPLACE THE LAST MOCHNGE MODE NUMBERS WITH THE FOLLOWING--
C
000153      READ 206, (MODC(I),I=MOCHNGE, MODE)
000166      405 IF (LCCHNGE .EQ. 0 ) GO TO 420
000167      LCCHNGE = NACT + 1 - LCCHNGE
C          REPLACE THE LAST LCCHNGE ACT. LOCATIONS WITH THE FOLLOWING--
C
000171      READ 206, (ULOCAT(I),I=LCCHNGE,NACT )
000204      GO TO 420
C          READ IN AN ENTIRE NEW SET OF MODES AND ACT. LOCATIONS.
```

APPENDIX A - Continued

```
000205      415 READ 200, MODE, (OMCCC(I), I=1,MODE )
000222      READ 200, (ULOCAT(I), I=1, MODE)
000235      NACT = MODE
000237      420 DO 422 I=1,MODE
000241      MDC(I) = OMCCC(I)
000243      LOCAT(I) = ULOCAT(I)
000244      422 CONTINUE
000246      IF (MCDE .EQ. 1) GO TO 9
C
C      THE FOLLOWING LOOPS SORT THE MODES AND ACTUATOR LOCATIONS IN ASCENDING
C      ORDER.
C
000250      LIMIT = MODE - 1
000251      DO 8 I=1, LIMIT
000252      IBEGIN = I + 1
000254      DO 6 JJ=IBEGIN, MODE
000256      IF (MDC(I) .LT. MDC(JJ)) GO TO 6
000258      IHOLD = MDC(I)
000263      MDC(I) = MDC(JJ)
000265      MDC(JJ) = IHOLD
000266      6 CONTINUE
000271      DO 7 JJ=IBEGIN, NACT
000273      IF (LLCAT(I) .LT. LOCAT(JJ)) GO TO 7
000276      IHOLD = LOCAT(I)
000300      LCCAT(I) = LOCAT(JJ)
000302      LOCAT(JJ) = IHOLD
000303      7 CONTINUE
000304      8 CONTINUE
000310      9 IF (IFPRINT .EQ. 0) GO TO 15
000311      PRINT 207, MODE, (MCCE(J), J=1, MODE)
000326      PRINT 208, (LOCAT(I), I=1, NACT)
000341      15 MMINSN= 58 - NACT
C
C      CONSTRUCT THE MN AND MR PARTITIONS OF THE EIGENVECTOR MATRIX.
C
000343      II = 1
000344      NMN = 1
000345      AMR = 1
000346      DO 40 I=1,58
000350      IF (I .EQ. MDC(II)) 20,30
000354      20 II= II + 1
000356      IF (II .GT. MODE) MDC(II)=0
000361      DO 25 J=1,NACT
```

APPENDIX A - Continued

```

500363      MOLE = LOCAT(J)
000365      HN(NHN,J) = U(MOLD,I)
000373      25 CONTINUE
C0C375      NHN = AHN + 1
000376      GO TO 40
000377      30 DO 35 J=1, NACT
            MOLE = LOCAT(J)
            HR(AFR,J) = U(MULD,I)
000401      35 CONTINUE
000413      NHM = AHR + 1
000414      40 CONTINUE
            IF (IPRINT .EQ. 0 ) GO TO 50
000417      PRINT 210
000423      DO 45 I=1, NACT
            PRINT 211, (HN(I,J), J=1, NACT)
000425      45 CONTINUE
C          NOW, PARTITION Q BY THE MODES CONTROLLED.
C
000444      50 II = 1
            NR = 1
            DO 60 I=1,58
            IF (I .EQ. MGOC(II)) 52,54
            52 CN(II) = UINVDE(II)
            OMEGASQ(II) = 10000./LAMBOA(II)
            II = II + 1
            GO TO 60
            54 QR(NR) = UINVDE(II)
            J = MODE + NR
            OMEGASQ(J) = 10000./LAMBOA(II)
            NR = NR+ 1
            60 CONTINUE
            IF (IPRINT .EQ. 0 ) GO TO 61
            PRINT 213, (CN(I), I=1,NACT)

C          STORE MATRIX HN IN MOLD AND THEN INVERT IT.
C
000511      61 DO 65 J=1,MODE
            DO 65 I=1,NACT
            MOLD(I,J) = HN(I,J)
            65 CONTINUE
            CALL PATINV (HN, NACT, DUMMY, M, DETERM, IPIVOT, INDEX, NSB,
            1 ISCALE )

```

APPENDIX A - Continued

```
6 000540      IF (ISCALE .EQ. 0) GO TO 66
000541      PRINT 231
000545      GO TO 350
C
C      PRINTS OUT MN INVERSE.
C
000546      66 IF (IPRINT .EQ. 0) GO TO 675
000547      PRINT 218
000553      DO 67 I=1,NACT
000555      PRINT 211, (MN(I,J),J = 1, MODE)
000571      67 CONTINUE
C
C      NORMALIZE THE DETERMINANT OF MN.
C
000574      675 DIV = 1.
000576      DO 70 I=1,MODE
000577      ADIVIDE(I) = 0.
000600      DO 68 J=1,NACT
000602      ADIVIDE(I) = ADIVIDE(I) + HCLC(I,J)**2
000610      68 CONTINUE
000612      ADIVIDE(I) = SQRT(ADIVIDE(I))
000617      DIV = DIV * ADIVIDE(I)
000621      70 CONTINUE
000623      DNORMAL = DETERM / DIV
C
C      CHECK THE INVERSION ROUTINE BY RE-MULTIPLYING
C
000625      DO 72 J=1,MODE
000627      DO 72 I=1,NACT
000630      PROD(I,J) = 0.0
000633      DO 72 K=1,MODE
000635      PROD(I,J) = PROD(I,J) + MCLO(I,K) * MN(K,J)
000647      72 CONTINUE
000656      IF (IPRINT .EQ. 0) GO TO 735
000657      PRINT 219
000663      DO 73 I=1, NACT
000665      PRINT 211, (PROD(I,J),J=1, MODE)
000701      73 CONTINUE
C
C      CALCULATE THE ALPHA VECTOR UNDER THE MODAL CONTROL LAW.
C
000704      735 DO 740 I=1,NACT
000706      ALPHA(I) = 0.0
```

APPENDIX A — Continued

```
000707      DO    74 J=1,MODE
000711        ALPHA(IJ) = ALPHAI(I) + RAI,I,J* * OMEGASQ(J) * QK(J)
000721        74 CONTINUE
000723        740 ALPSTOK(I) = ALPHA(I)
000730        ATAM = 0.
000731        DO 140 I=1,NACT
000732          ATAM = ATAM + ALPHA(I)**2
000735        140 CONTINUE
000737          ATAM = SQRT(ATAM)

C
C      CALCULATE THE ALPHA VECTOR UNDER THE OPTIMAL CONTROL LAW.
C      COMPLETE  L (LAM*H)TR * (LAH*H) )-1 * (LAH*H)TR * Q
C

000741      DC    150  I=1, MMINUSN
000742      DO    150  J=1, NACT
000743        MGLD = I + MODE
000745        HOLC(MGLD,J) = KRI(I,J)
000752        150 CONTINUE
000757      DO 156 I=1,58
000760        DO 155 J=1, NACT
000761        HOLC(I,J) = HOLC(I,J)/ OMEGASQ(I)
000767        155 CONTINUE
000771        156 CONTINUE
000773        IF (IPRINT .EQ. 0 ) GO TO 157
000774        PRINT 257
000777        PRINT 202, (HOLD(I,J), J=1, NACT )

C
C      INVEST THE MATRIX, AND NORMALIZE ITS DETERMINANT IN THE CALCULATION
C      OF Z-PHA.
C

001014      157 DIV = 1.
001016      DO 169  I= 1, NACT
001017        ADIVIDE(I) = 0.0
001020      DO 167  J= 1, NACT
001022        ARRAY(I,J) = 0.0
001025      DO 165  K= 1,58
001027        ARRAY(I,J) = ARRAY(I,J) + MGLD(K,I)*MGLD(K,J)
001041      165 CONTINUE
001043        ADIVIDE(I) = ADIVIDE(I) + ARRAY(I,J)**2
001046      167 CONTINUE
001051        ADIVCE(I) = SQRT(ADIVIDE(I))
001055        DIV = QIV * ADIVIDE(I)
001057      169 CONTINUE
```

APPENDIX A - Continued

```
48
C
0J1061      CALL MATINV (ARRAY, NACT, CUMRY, H, DETERM, IPIVUT, INDEX, NSB,
1  ISCALE )
DETERM = DETERM / DIV
IF (IPRINT .LE. 0) GO TO 175
PRINT 247, DETERM, ISCALE, DETERMN
C
C PRINT OUT THE INVERSE OF ( (LAM+H)T * (LAM+H) )
C
0J1107      PRINT 258
0J1113      DO 171 I=1,NACT
0J1115      PRINT 202, (ARRAY(I,J),J=1,NACT)
0J1131      171 CONTINUE
C
C
0J1134      175 DO 180 J= 1,MODE
0J1136          VECTOR(J) = CN(J)
0J1140      180 CONTINUE
0J1142          MOLD = I + MODE
0J1143          DO 185 J= MOLD, 58
0J1144          VECTOR(J) = CR(J-MODE)
0J1147      185 CONTINUE
0J1151      DO 193 I=1,NACT
0J1153          ALPHA(I) = 0.0
0J1154          DO 193 J=1,58
0J1250          PROJ(I,J) = 0.0
0J1161          DO 190 K= 1,NACT
0J1163          PREC(I,J) = PREC(I,I) + ARRAY(I,K) * HOLD(J,K)
0J1176      190 CONTINUE
0J1200          ALPH(I) = ALPHA(I) + PROJ(I,J) * VECTOR(J)
0J1206      193 CONTINUE
0J1212          ALPHSUM = 0.0
0J1213          DO 194 I=1,NACT
0J1214          ALPHSUM = ALPHSUM + ALPHA(I)**2
0J1217      194 CONTINUE
0J1221          ALPHSLM = SQRT(ALPHSUM)
C
C NOW CALCULATE E TRANSPOSE E
C
0J1223      DO 195 I=1,58
0J1224          VECTOR(I) = 0.0
0J1225          DO 195 J=1,NACT
```

APPENDIX A - Continued

```
00127 VECTOR(I) = VECTOR(I) + HOLD(I,J) * ALPHA(J)
00128 195 CONTINUE
00129 DO 196 I=1, MODE
00130 VECTOR(I) = VECTOR(I) - CN(I)
00131 196 CONTINUE
00132 DO 197 I=1,MMINUSN
00133 J = MODE + I
00134 VECTOR(J) = VECTOR(J) - QR(I)
00135 197 CONTINUE
00136 SUM = 0.0
00137 DO 198 I=1,58
00138 SUM = SUM + VECTOR(I)*I*2
00139 198 CONTINUE
00140 EYE = SQRT(SUM)
C
C   CALCULATE PFOO, THE MATRIX PRODUCT--
C   LAMBDA(I) * H(I) * H(N) INVERSE * LAMBDA(N) INVERSE.  THE MULTIPLICATION
C   IS SIMPLIFIED BECAUSE THE LAMBDA MATRICES ARE DIAGONAL.
C
00141 DO 80 J= 1, MODE
00142 DC 80 I= 1, MMINUSN
00143 PROD(I,J) = C.O.
00144 DO 75 K=1, MODE
00145 PROD(I,J) = PFOO(I,J) + NR(I,K)* HR(K,J)
00146 75 CONTINUE
00147 PROD(I,J) = PFOO(I,J) * CMEGASQ(J) / UMEGASQ(MODE + J)
00148 80 CONTINUE
C
C-----CALCULATE AND PRINT INTERMEDIATE DATA FOR PSI MATRIX.
C
00149 IF (IPRINT .EQ. 0 ) GO TO 83
00150 PR11,I 294
00151 DO 82 J=1, MODE
00152 PRINT 299, J, (PROD(I,J), I=1, MMINUSN )
00153 82 CONTINUE
00154 83 DO 84 J=1,MODE
00155 PH1(I,J) = 0.
00156 DO 84 I= 1, MMINUSN
00157 PH1(I,J) = PH1(I,J) + PROD(I,J)*I*2
00158 84 CONTINUE
00159 IF (IPRINT .EQ. 0 ) GO TO 94
00160 PRINT 296, (PH1(I),I=1, MODE )
C
```

APPENDIX A - Continued

```

C      MULTPLY PROD BY THE ERROR VECTOR IN THE CONTROLLED MODES.
C
001411 94 DO 55 I= 1,MMINLSH
001413 PRC02(I) = 0.0
001414 DC 55 K= 1,MODE
001416 PRC02(I) = PROD2(I) + PROUT(I,K) * QN(I,K)
001423 95 CONTINUE
001432 IF (IPRINT .EQ. 0 ) GO TO 98
001433 PR141 230, (PR002(I),I=1,MMINUSH)

C      CALCULATE THE ERROR OF CONTROL.
C
001445 98 EC 99 I=1, MMINUSH
001447 CRSS(I) = QR(I,I) - PROD2(I)
001452 99 CONTINUE

C      CALCULATE THE ORIGINAL ERROR IN THE CONTROLLED MODES, THE UNCON-
C      TROLLED MODES, THE ERROR GENERATED BY THE CONTROL SYSTEM, AND
C      THE ERROR OF CONTROL.

001454 ECM = C*
001455 DC 100 I=1,MODE
001456 ECM = ECM + QM(I,I)**2
001461 100 CONTINUE
001463 SQRTECM = SQRT(ECM)
001465 EUM = 0.
001466 DO 105 I=1, MMINUSH
001467 SLM = EUM + QR(I,I)**2
001472 105 CONTINUE
001474 SQRTELM = SQRT(EUM)
001476 ED = ECM + EUM
001500 SQRTEOD = SQRT(ED)
001502 CRC = 0.0
001503 DC 110 I=1, MMINUSH
001506 CRC = CRC + PR002(I)**2
001507 110 CONTINUE
001511 SQRTCRC = SQRT(CRC)
001513 CRS = 0.0
001514 DO 115 I = 1,MMINUSH
001515 CRS = CRS + CRSS(I,I)**2
001520 115 CONTINUE
001522 SQRTRS = SQRT(CRS)
C

```

APPENDIX A - Continued

C EXPAND THE ERROR OF CONTROL VECTOR TO 56 ELEMENTS WITH ZEROS
C CORRESPONDING TO THE CONTROLLED MODES. THEN MULTIPLY BY THE U MATRIX,
C TO CALCULATE THE FINAL DEFLECTION VECTOR.

C

001524 DO 120 I=1, MN2NUSC
001525 HUL0(I,J) = CRSS(I,J)
001532 120 CONTINUE
001532 II = 1
001533 N = 1
001534 DO 133 I=1,58
001536 IF (INCC(I,I)) .EQ. 11 GO TO 123, 128
001542 123 CRSS(I,I) = 0.0
001544 II = II + 1
001545 GO TO 133
001546 128 CRSS(I,I) = HUL0(N,I)
001551 N = N + 1
001552 133 CONTINUE
001554 DO 136 I=1,58
001556 PRLU2(I,I) = C.0
001557 DO 136 J=1,58
001561 PHLU2(I,J) = PRLU2(I,I) + U(I,J) * CRSS(J,I)
001570 136 CONTINUE
001574 IF (I.EQ. 0) GO TO 137
001575 PRINT 255, (PHLU2(I,I),I=1,58)

C

C CONVERT FORCE VALUES TO POUNDS FOR PRINT OUT.

C

001606 137 ATAM = ATAM + 1.25E-09
001610 ALPHSLM = ALPHSLM + 1.25E-09
001611 DO 138 I=1, NACT
001613 ALPSTUR(I,I) = ALPSTUR(I,I) + 1.25E-09
001615 ALPHAI(I,I) = ALPHAI(I,I) + 1.25E-09
001617 138 CONTINUE
001621 PRINT 207, MODE, (INJECT(I), I=1, MODE)
001636 PRINT 206, (LOCATE(I), I=2, NACT)
001651 PRINT 232, DNUMLAL
001657 PRINT 246, (ALPSTUR(I,I), I=1,NACT)
001672 IF (NACT .LE. 8) PRINT 270
001701 PRINT 254, ATAM
001707 PRINT 207, (ALPHAI(I,I), I=1, NACT)
001722 IF (NACT .LE. 8) PRINT 270
001731 PRINT 253, ALPHSUM
001737 PRINT 251, LTE

APPENDIX A - Continued

```

5 001745      PRINT 279, CO,SURTOU, ECH, SURTECH, EUM, SURTEUM, GRL, SURTCRG,
               1 CRS, SURTCRS
C01725      350 CONTINUE
LC20L0      STOP
C02L02      202 FORMAT (1E15.5) 1
C02002      203 FORMAT (1E13.5) 1
C02002      204 FORMAT (1=1, * THE EIGENVALUES CORRESPONDING TO THE EIGENVECTOR
               1MATHIA U.P/FF, (1E15.5)) 1
C02002      205 FORMAT (1H , // (1E15.5)) 1
C02002      206 FORMAT (20I6)
C02002      207 FORMAT (1H1, *NUMBER OF CONTROLLED MODES = *, 13,/// * THEY ARE
               1 MODES *, 1215, (1/19, 1215) 1
C02002      208 FORMAT (1H , /* ACTUATOR LOCATIONS*, 1215, (1/19, 1215) 1
C02002      209 FORMAT (1B10)
C02002      210 FORMAT (1H , // * MN PARTITION OF THE EIGENVECTUR MATRIX *) 1
C02002      211 FORMAT (1H , // (1E15.4)) 1
C02002      213 FORMAT (1H , // * THE LN PARTITION OF THE Q VECTOR IS *, // *
               1 (1E15.4)) 1
C02032      218 FORMAT (1H , // * MN INVERSE LISTED BY KUNS.*// 1
C02002      219 FORMAT (1H , // * MATRIX TO CHECK MN INVERSION - SHOULD BE IDENTITY
               1 MATRIX. LISTED BY KUNS.* / 1
C02002      225 FORMAT (1H , // 37X, *MEAN SQUARE RMS LRRRKA, / 37X,
               1 *ERRDRP, // 6X, *ORIGINAL DISTURBANCE*, 4X, 2E15.4, // 6X,
               2 *ORIGINAL ERROR IN*, 1X, 2E10.4, / 6X, *THE CONTROLLED MODES* //
               3 6X, *ORIGINAL ERROR IN THE*, 3X, 2E10.4, / 6X, *UNCONTROLLED
               40 MODES* // 4X, *ERROR GENERATED IN THE *, 2E20.4, / 6X,
               5 *UNCONTROLLED MODES BY*, / 6X, *CONTROL SYSTEM*, // 6X, *ERRCR D
               6F CONTROL*, 6X, 2E16.4) 1
C02002      230 FORMAT (1H , // 60K PSI MATRIX * ERROR VECTOR (ERRCR VECTOR IS
               1 IN THE MODAL DOMAIN.) /* * THIS COLUMN VECTUR GIVES THE LRR
               2UR GENERATED IN EACH MODE.* // (1E15.4)) 1
C02002      231 FORMAT (1H1, // * THE DETERMINANT APPEARS EXCESSIVELY LARGE OR
               1SMALL. THE RUN WAS STOPPED.* / 1
C02002      232 FORMAT (1H , // E12.4, * IS THE VALUE OF THE NORMALIZED DETERMIN
               1ANT OF MN. IF THIS VALUE IS SMALL * / 15X, * COMPARED TO 1, THE
               2MATRIX IS ILL-CONDITIONED.* / 1
C02002      246 FORMAT (1H , / * FORCE VECTOR UNDER THE MODAL CONTROL LAW (POUN
               105).// (E12.4, 7E15.4)) 1
C02002      247 FORMAT (1H , // (12.4, 1H * 10**1,12,10UH#10)) IS THE VALUE
               1OF THE DETERMINANT OF THE MATRIX ( (LA=M)IT * (LA=M) ) USED IN
               2FINDING ALPHA.,// E13.5, * IS THE NORMALIZED DETERMINANT. IF TH
               3S VALUE IS SMALL COMPARED TO 1, THE MATRIX IS ILL-CONDITIONED.*)
C02002      250 FORMAT (1H , // * THE FORCE VECTOR UNDER THE OPTIMAL CONTROL LAW

```

APPENDIX A - Continued

```
1 (POUNDS).*, // (E12.4, 7E15.4) )
002002 251 FORMAT (1H, // * THE FINAL ERROR UNDER THE OPTIMAL CONTROL LAW
           1 IS *, E15.4 )
002002 253 FORMAT (1H, / * THE RSS VALUE OF THE FORCE VECTOR UNDER THE OP
           ITIMAL CONTROL LAW IS*, E15.4, * POUNDS.* )
002002 254 FORMAT (1H, / * THE RSS VALUE OF THE FORCE VECTOR UNDER THE MU
           IDEAL CONTROL LAW IS*, E15.4, * POUNDS.* )
002002 255 FORMAT (1H, // * THIS COLUMN VECTOR GIVES THE DEFLECTION OF TH
           IE MIRROR AT EACH GRID POINT. *, / * UNITS ARE THE SAME AS THE ORI
           PGINAL W VECTOR.*, // (8E15.4) )
002002 257 FORMAT (1H, // 31H LAMBDA * H LISTED BY ROWS. ,)
002002 258 FORMAT (1H, // 60H THE INVERSE OF ( (LAM*H)T * (LAM*H) ). LISTE
           1D BY ROWS. // )
002002 260 FORMAT (1H1, 8A10 )
002002 261 FORMAT (F10.4)
002002 262 FORMAT (1H, // * ERROR VECTOR, EACH TERM MULTIPLIED BY *,
           1 F10.4, // (8E15.4) )
002002 270 FORMAT (1H )
002002 294 FORMAT (1H, // // 49H THE MATRIX PRODUCT -- LAMBDA(R) * H(R) *
           LN(R) INVERSE * LAMBDA(R) INVERSE -- LISTED BY COLUMNS. / * THIS
           2 MATRIX IS CALLED THE PSI MATRIX. * )
002002 296 FORMAT (1H, // 60H THE DIAGONAL ELEMENTS OF THE PSI TRANSPUSE
           1* PSI MATRIX. . / * THESE ARE THE PHI SQUARED TERMS.* //
           2 (8E15.4) )
002002 299 FORMAT (1H, // * COLUMN NO. *, 14, // (8E15.4) )
002002          ENC
```

54 THE EIGENVALUES CORRESPONDING TO THE EIGENVECTOR MATRIX U.

3.50970E-02	3.5C880E-02	3.05860E-02	2.94660E-03	2.50740E-03	2.50450E-03	2.49790E-03
8.98400E-04	8.97990E-04	5.66980E-04	4.89340E-04	4.89050E-04	3.44690E-04	3.44330E-04
2.36100E-04	1.79640E-04	1.79510E-04	1.79100E-04	1.70370E-04	1.36050E-04	1.05800E-04
1.05520E-04	9.19350E-05	9.18190E-05	7.49770E-05	7.08320E-05	7.00340E-05	5.66260E-05
5.29110E-05	5.28E30E-05	5.10C90E-05	5.09740E-05	4.90350E-05	3.87970E-05	3.87810E-05
3.58890E-05	3.35360E-05	3.34770E-05	3.21660E-05	2.94680E-05	2.797760E-05	2.79340E-05
2.74803E-05	2.47400E-05	2.23090E-05	2.22760E-05	2.04840E-05	2.04740E-05	2.01290E-05
2.01170E-05	1.95690E-05	1.86400E-05	1.59650E-05	1.59520E-05	1.57770E-05	1.57630E-05
1.31130E-05	1.30820E-05					

THE ERROR VECTOR IS UINV * ERROR EXAMPLE NO. 1

-1.7184E+01	-1.2100E+01	7.4458E+00	-1.1009E+01	-3.6741E+00	2.7612E+00	-1.5698E+01	-1.4058E+00
3.9529E+00	-1.2362E+01	9.2392E-01	-9.0744E-01	-2.1174E-01	1.0400E+00	5.3853E+00	1.6003E-01
6.1081E-01	-1.3558E+00	-2.0440E+00	-1.1568E+00	9.7822E-02	-2.7951E+00	-2.7975E-01	5.3307E-02
-1.2237E+00	-3.6520E-01	-5.0349E-01	-3.7334E+00	3.8240E-01	9.6029E-01	6.2557E-02	5.9744E-01
2.5570E-01	-3.4355E-02	-7.6660E-01	-2.5507E+00	7.9209E-01	6.0366E-01	-8.8768E-02	4.3418E-02
3.7177E-01	5.6847E-01	-7.4978E-01	5.1395E-01	6.0208E-01	4.1106E-02	-3.2221E-01	-1.3675E-01
-8.5519E-02	2.4347E-01	4.5098E-01	6.1734E-02	1.6936E-01	2.1140E-01	-1.9399E-01	2.4991E-01
-2.0575E-01	5.1006E-02						

ERROR VECTOR, EACH TERM MULTIPLIED BY 1.0000

-1.7184E+01	-1.2100E+01	7.4458E+00	-1.1009E+01	-3.6741E+00	2.7612E+00	-1.5698E+01	-1.4058E+00
3.9529E+00	-1.2362E+01	9.2392E-01	-9.0744E-01	-2.1174E-01	1.0400E+00	5.3853E+00	1.6003E-01
6.1081E-01	-1.3558E+00	-2.0440E+00	-1.1568E+00	9.7822E-02	-2.7951E+00	-2.7975E-01	5.3307E-02
-1.2237E+00	-3.6520E-01	-5.0349E-01	-3.7334E+00	3.8240E-01	9.6029E-01	6.2557E-02	5.9744E-01
2.5570E-01	-3.4355E-02	-7.6660E-01	-2.5507E+00	7.9209E-01	6.0366E-01	-8.8768E-02	4.3418E-02
3.7177E-01	5.6847E-01	-7.4978E-01	5.1395E-01	6.0208E-01	4.1106E-02	-3.2221E-01	-1.3675E-01
-8.5519E-02	2.4347E-01	4.5098E-01	6.1734E-02	1.6936E-01	2.1140E-01	-1.9399E-01	2.4991E-01
-2.0575E-01	5.1006E-02						

APPENDIX A - Continued

NUMBER OF CONTROLLED MODES = 5

THEY ARE MODES	1	2	3	4	5
ACTUATOR LOCATIONS	2	30	31	44	45

MN PARTITION OF THE EIGENVECTOR MATRIX

-1.0324E-02	9.9971E-03	1.3983E-03	7.6825E-04	3.0095E-02
5.1990E-03	7.2879E-03	3.0486E-02	-1.1727E-02	-1.6167E-02
-2.2785E-02	-4.5298E-02	-4.2840E-02	-2.2867E-02	-3.3475E-02
-1.4533E-02	-5.4817E-02	-3.4064E-02	-1.4801E-02	-1.2290E-02
-5.5135E-02	1.8150E-02	2.2451E-02	2.7355E-02	1.7254E-02

MN PARTITION OF THE Q VECTOR IS

-1.7184E+01	-1.2100E+01	7.4458E+00	-1.1009E+01	-3.0741E+00
-------------	-------------	------------	-------------	-------------

MN INVERSE LISTED BY FCWS.

-1.1002E+01	-5.7141E+00	-1.5412E+01	6.0853E+00	-1.1731E+01
1.0608E+01	-6.3121E+00	2.5464E+01	-3.9150E+01	-2.9000E+00
-3.1447E+00	2.4583E+01	-1.9392E+01	2.0553E+01	5.5376E+00
-4.3863E+01	-2.7237E+01	-2.4137E+01	1.2582E+01	1.2737E+01
2.6971E+01	-4.2413E+01	-1.2536E+01	1.3938E+01	-3.8769E+00

56 MATRIX TO CHECK MA INVERSION - SHOULD BE IDENTITY MATRIX. LISTED BY ROWS.

1.0000E+00	-4.7740E-15	-5.3291E-15	>.3291E-15	-2.6645E-15
-3.5527E-15	1.0000E+00	4.4409E-15	-3.5527E-15	-8.8818E-16
3.5527E-15	1.5377E-14	1.0000E+00	-1.0658E-14	-2.6645E-15
0.	3.6915E-15	2.1316E-14	1.0000E+00	-6.6613E-16
5.3291E-15	-1.2018E-14	-8.8818E-15	1.2434E-14	1.0000E+00

LAMBDA * H LISTED BY ROWS.

5.92001E-12	E.45662E-11	2.02445E-11	5.65436E-12	4.36641E-11
-------------	-------------	-------------	-------------	-------------

2.1982E-73 * 10**(-0*100) IS THE VALUE OF THE DETERMINANT OF THE MATRIX I (LAM*HIT * (LAM*H)) USED IN FINDING ALPHA.
1.81460E-05 IS THE NORMALIZED DETERMINANT. IF THIS VALUE IS SMALL COMPARED TO 1, THE MATRIX IS ILL-CONDITIONED.

THE INVERSE OF I (LAM*HIT * (LAM*H)) . LISTED BY ROWS.

2.22455E+15	-5.26994E+14	-4.22980E+14	-1.81642E+15	1.01795E+15
-5.26994E+14	3.87520E+15	-2.10272E+15	-1.22750E+15	-1.33708E+15
-4.22980E+14	-2.10272E+15	1.41347E+15	1.29669E+15	4.47075E+14
-1.81642E+15	-1.22750E+15	1.29669E+15	2.58135E+15	-6.85070E+14
1.01795E+15	-1.33708E+15	4.47075E+14	-6.85070E+14	8.01606E+14

THE MATRIX PRODUCT -- LAMBDA(R) * H(R) * H(N) INVERSE * LAMBDA(N) INVERSE -- LISTED BY COLUMNS.
THIS MATRIX IS CALLED THE PSI MATRIX.

COLUMN NO. 1

APPENDIX A - Continued

-6.9926E-02	-1.8712E-02	-2.8060E-02	3.3064E-02	-3.5966E-02	-1.1681E-02	2.6704E-02	-1.0880E-02
1.0242E-02	1.1800E-03	1.6174E-03	-4.9203E-03	-6.7810E-03	-1.3398E-02	-5.2258E-03	-1.2386E-03
-3.4167E-03	-3.4800E-04	-7.2812E-03	-6.3705E-03	-9.4871E-03	-2.7494E-03	-3.3195E-03	1.2648E-03
3.5813E-03	4.1392E-03	3.3449E-03	3.0714E-04	-7.5638E-04	-1.9905E-04	1.2205E-03	-1.3893E-03
2.2993E-03	4.6207E-03	1.3537E-03	1.6704E-03	-2.3943E-03	1.0575E-04	-2.2775E-03	3.6553E-03
-9.7242E-04	7.1592E-05	2.6849E-05	1.9872E-04	-2.28d7E-03	-8.2513E-04	-2.3649E-03	9.1699E-04
8.4294E-04	9.9540E-04	8.5389E-04	1.3525E-03	4.7843E-04			
COLUMN NO. 2							
-6.4093E-02	-1.4076E-01	1.6509E-02	4.9403E-02	-2.8849E-02	-1.7861E-03	4.0145E-03	-1.2093E-02
-8.3515E-03	-5.8100E-03	6.6166E-03	-1.3067E-03	-6.0329E-03	-9.8692E-03	-6.5430E-03	2.9423E-03
-2.2016E-04	3.7681E-03	-5.3932E-03	-4.7038E-03	-1.3153E-03	-1.8702E-03	-4.6569E-03	-1.0951E-03
-1.4526E-03	1.5910E-03	2.7064E-03	-1.0571E-03	-1.3214E-03	1.0466E-04	-2.5247E-04	7.4949E-04
4.1553E-06	-2.2332E-03	-1.8217E-03	-2.3106E-05	-3.7824E-04	-4.2359E-04	-1.4516E-03	1.3170E-03
-4.5038E-04	-4.5967E-04	1.6059E-03	-3.0404E-05	-6.8636E-04	-7.0412E-04	-1.1745E-03	2.0333E-03
1.7232E-04	-1.5547E-04	3.9006E-04	-4.4464E-04	-1.3616E-05			
COLUMN NO. 3							
9.5341E-03	-1.6432E-01	-1.1585E-02	1.9781E-02	-6.9402E-02	-1.6185E-02	-1.6243E-02	-2.9674E-02
3.8298E-03	1.2666E-02	5.7135E-04	8.0743E-04	-4.3301E-03	-1.0643E-02	9.1368E-03	-6.0402E-03
-1.6442E-03	8.1700E-04	-2.3389E-03	-4.0466E-03	-1.6870E-03	4.4213E-04	-1.2591E-03	-1.7008E-03
4.2249E-03	-1.9741E-03	3.4574E-03	8.4637E-04	1.2977E-03	1.0629E-03	-0.8240E-04	-3.9154E-04
1.5416E-03	4.5929E-03	1.0722E-03	-9.6061E-04	3.7124E-03	7.2481E-04	-5.8027E-04	2.5045E-03
9.3193E-04	1.0643E-03	-2.4427E-03	4.5725E-04	6.2493E-04	-4.2155E-04	1.0091E-04	-9.3585E-04
-9.7241E-05	2.1738E-04	-8.5882E-04	1.7504E-03	2.7006E-04			
COLUMN NO. 4							
-1.6776E-01	1.7128E+00	1.7735E-01	-2.7455E-01	6.0177E-01	7.3349E-02	2.2553E-01	2.9817E-01
-4.0249E-02	-1.9457E-01	-5.16C3E-02	-3.0342E-02	-4.4345E-02	9.6663E-02	-1.0280E-01	8.0014E-02
4.2644E-02	-3.1075E-02	-2.2993E-02	1.9326E-02	1.5259E-02	-4.3657E-03	-1.1782E-02	2.7942E-02
-6.1520E-02	1.1913E-02	-1.4954E-02	-9.2634E-03	-1.2381E-02	-6.7831E-03	1.4985E-02	4.9455E-03
-1.7477E-02	-3.5102E-02	-1.1504E-02	1.1042E-02	-9.0737E-02	-9.3192E-03	-1.9354E-03	-2.4149E-02
-1.1370E-02	-1.7824E-02	3.0644E-07	-7.9081E-03	-1.3497E-02	-4.9938E-03	-1.4550E-02	1.6446E-02
-1.3354E-03	-9.0560E-03	1.9153E-02	-1.9471E-02	-6.8907E-03			
COLUMN NO. 5							
1.1112E-01	1.9047E-01	-9.7258E-02	-6.0842E-02	-1.3189E-02	8.8094E-02	1.2982E-01	6.9740E-02
-1.9080E-01	-2.0101E-02	-7.6812E-02	1.7205E-02	-6.5282E-02	-4.2258E-04	-8.3280E-03	1.6290E-02
4.2524E-03	-4.6043E-02	3.1884E-02	-6.3002E-04	-1.4438E-02	4.8079E-03	-5.9319E-03	-1.1486E-02
-1.4011E-02	-3.7498E-02	-1.8610E-02	-3.6419E-03	3.3466E-03	-2.5785E-03	-2.9674E-03	-3.2021E-03
-8.1581E-03	-3.1808E-03	-8.5076E-03	-3.2367E-03	-1.3229E-02	1.1136E-02	5.6924E-04	-1.3500E-02
1.7941E-02	-3.6309E-04	6.3595E-03	-7.1911E-03	6.5014E-03	-5.9240E-04	6.6869E-04	-2.0893E-04
-8.6667E-03	-5.3043E-03	-2.2289E-03	-4.0112E-03	-1.0251E-03			

58

THE DIAGONAL ELEMENTS OF THE PSI TRANSPOSE * PSI MATRIX.
THESE ARE THE PMI SQUARED TERMS.

9.3296E-03 2.4120E-02 3.6231E-02 3.6638E+00 1.4164E-01

PSI MATRIX * ERROR VECTOR (ERROR VECTOR IS IN THE MODAL DOMAIN.)
THIS COLUMN VECTOR GIVES THE ERROR GENERATED IN EACH MODE.

3.4865E+00	-1.8792E+01	-1.6036E+00	2.1540E+00	-6.125E+00	-1.9293E+00	-3.1753E+00	-3.6246E+00
1.0973E+00	2.3601E+00	7.2952E-01	3.7719E-01	4.7542E-01	-8.3688E-01	1.4002E+00	-1.0121E+00
-4.3640E-01	4.7279E-01	3.0889E-01	-7.4174E-02	-1.4057E-01	8.3817E-03	2.5551E-01	-2.8656E-01
7.1504E-01	-9.7937E-02	1.6853E-01	1.2918E-01	1.6317E-01	9.4215E-02	-1.7655E-01	-3.0788E-02
1.8899E-01	3.2590E-01	1.6284E-01	-1.4525E-01	4.0813E-01	7.0387E-02	7.0909E-02	2.5535E-01
8.8688E-02	2.0593E-01	-4.0278E-01	1.1460E-01	1.7699E-01	7.6567E-02	2.0817E-01	-2.2762E-01
2.9250E-02	6.4817E-02	-1.8442E-01	2.2427E-01	7.3617E-02			

THIS COLUMN VECTOR GIVES THE DEFLECTION OF THE MIRROR AT EACH GRID POINT.
UNITS ARE THE SAME AS THE ORIGINAL W VECTOR.

-2.2337E-01	-8.6315E-01	-2.2854E-01	-2.6746E-02	-7.3074E-01	-2.4536E-01	-8.1407E-01	-1.0865E-01
4.1102E-01	-5.8820E-01	7.7151E-02	7.7709E-01	4.5373E-01	-2.6323E-01	1.1898E-01	8.0724E-01
-4.2389E-02	-1.3922E-01	2.3703E-01	2.7464E-02	1.0516E+00	4.2002E-01	-1.1042E-01	4.5738E-01
3.9117E-01	-4.0547E-01	6.3e16E-02	2.3595E-01	1.7538E-01	8.1325E-02	8.3272E-01	-1.4576E-01
8.7793E-02	-2.7399E-02	6.7060E-01	-5.4019E-01	3.4375E-01	-1.8325E-01	1.3576E-01	-3.5522E-01
-5.7575E-01	-4.5873E-01	-2.3912E-01	-4.9820E-01	2.4546E-01	1.9739E-01	-3.4312E-01	-8.7047E-01
-1.1446E+00	-8.4857E-01	-2.5712E-01	-6.0909E-02	3.5950E-01	3.2948E-01	5.4920E-01	-3.8262E-02
-1.4136E-01	3.4C05E-01						

APPENDIX A - Concluded

NUMBER OF CONTROLLED MODES = 5

THEY ARE MODES 1 2 3 4 5
ACTUATOR LOCATIONS 2 30 31 44 45

1.5384E-01 IS THE VALUE OF THE NORMALIZED DETERMINANT OF MN. IF THIS VALUE IS SMALL COMPARED TO 1, THE MATRIX IS ILL-CONDITIONED.

FORCE VECTOR UNDER THE MODAL CONTROL LAW (POUNDS).

-2.4256E-02 1.6213E+00 -1.2070E+01 -5.0983E-01 -7.8129E-01

THE RSS VALUE OF THE FORCE VECTOR UNDER THE MODAL CONTROL LAW IS 2.4534E+00 POUNDS.

THE FORCE VECTOR UNDER THE OPTIMAL CONTROL LAW (POUNDS).

-6.5169E-02 1.6345E+00 -1.1433E+01 -4.3576E-01 -7.6830E-01

THE RSS VALUE OF THE FORCE VECTOR UNDER THE OPTIMAL CONTROL LAW IS 2.3360E+00 POUNDS.

THE FINAL ERROR UNDER THE OPTIMAL CONTROL LAW IS 1.1336E+01

	MEAN SQUARE ERROR	RMS ERROR
ORIGINAL DISTURBANCE	1.1360E+03	3.3713E+01
ORIGINAL ERROR IN THE CONTROLLED MODES	6.3184E+02	2.5136E+01
ORIGINAL ERROR IN THE UNCONTROLLED MODES	5.0473E+02	2.2466E+01
ERROR GENERATED IN THE UNCONTROLLED MODES BY CONTROL SYSTEM	4.4596E+02	2.1118E+01
ERROR OF CONTROL	1.3071E+02	1.1433E+01

APPENDIX B

EIGENVECTORS OF THE MIRROR

This appendix contains a listing of the U matrix (matrix of eigenvectors) for the 76-cm-diameter (30-inch) thin mirror. This matrix was obtained from the SAMIS program in reference 4. A more graphic display of the first 10 eigenvectors is contained in appendix C. The eigenvalues associated with each eigenvector are given in appendix D. $\Lambda(1)$ is associated with column (1), and so forth. The diagonal mass matrix m is also given in appendix D. The U matrix is orthogonal with respect to the mass matrix (refs. 4 and 5):

$$U^T m U = I$$

APPENDIX B - Continuec

COLUMN NO.	I OF J MATRIX	COLUMN NO.	I OF J MATRIX
-2.45F-02	-1.09E-02	3.65E-03	-4.98E-02
2.27E-03	-7.31E-02	-4.1E-02	-7.75E-02
-2.15E-03	-9.32E-02	-6.4E-02	-1.17E-02
-4.43E-03	-9.82E-03	-7.91E-02	-6.84E-03
1.62E-02	1.03E-02	1.06E-03	-1.56E-02
-2.17E-02	1.03E-03	-1.31E-02	-9.76E-02
-5.16E-02	7.6M-04	-5.01E-02	-7.13E-02
9.59E-03	-9.1E-03	4.27E-02	8.93E-02
5.55E-02	1.23E-02		

COLUMN NO.	2 OF U MATRIX		CDL JUMP NO.	8 OF U MATRIX	
-2.9E-02	5.70E-03	3.94E-02	-4.34E-02	-1.80E-02	7.21E-03
6.6E-02	5.67E-02	-1.01E-02	-1.35E-02	5.53E-03	7.59E-02
9.25E-02	-9.57E-02	-4.42E-02	-2.68E-02	-1.15E-02	1.76E-04
4.76E-02	7.93E-02	1.12E-01	-4.76E-02	-3.24E-02	-2.03E-02
-9.45E-03	1.29E-01	3.98E-02	9.14E-02	-3.04E-02	-1.73E-02
-2.08E-02	1.16E-02	-6.08E-02	-2.01E-02	-9.01E-03	3.65E-03
1.19E-02	1.15E-02	-1.62E-02	-2.40E-02	-3.14E-02	-7.71E-02
6.81E-03	3.39E-02	-6.74E-03	7.10E-02	-1.44E-02	-4.44E-02
-1.35E-02	22.9E-02				

COLUMN NO.	S	U	V	MATRIX	COLUMN NO.	S	U	V	MATRIX	
-9.67E-02	-5.53E-02	-9.65E-02	-6.97E-02	-6.52E-02	-6.37E-02	-6.51E-02	8.95E-02	2.30E-05	-8.43E-02	
-6.65E-02	-6.67E-02	-6.67E-02	-6.74E-02	-7.04E-02	-6.73E-02	-6.66E-02	-6.61E-02	-1.15E-02	-6.55E-02	
-6.05E-02	-3.13E-02	-3.06E-02	-9.56E-02	-1.16E-02	-1.22E-02	-1.01E-02	1.16E-02	-5.08E-02	-1.15E-02	
-9.95E-03	-3.55E-03	-1.31E-02	-5.55E-02	-3.06E-02	-2.25E-02	-1.91E-02	-6.11E-02	-5.05E-02	-2.61E-02	
2.17E-02	1.62E-02	2.72E-02	1.64E-02	3.53E-02	7.26E-02	7.97E-02	6.11E-02	6.61E-02	7.40E-02	
4.76E-02	3.17E-02	7.73E-02	1.59E-02	2.68E-02	3.17E-02	6.751E-02	1.37E-02	2.65E-02	2.10E-02	
5.16E-02	2.74E-02	1.71E-02	1.02E-02	5.65E-02	1.02E-02	1.74E-02	6.61E-02	6.83E-03	7.11E-02	
2.76E-02	3.14E-02	-5.26E-03	-7.92E-03	-1.45E-02	-2.92E-02	-1.08E-02	-8.31E-03	-4.74E-02	-3.31E-02	
-7.47E-03	-6.91E-01						-8.19E-02	-2.67E-03	5.44E-03	8.56E-02

APPENDIX B - Continued

COLUMN NO.	12 OF U MATRIX	COLUMN NO.	13 OF U MATRIX										
-6.526E-02	-3.196E-02	-6.437E-02	-2.516E-02	-6.538E-03	-2.538E-02	-6.008E-02	3.853E-03	6.021E-02	-6.117E-03	3.10E-02	-3.665E-05	-1.047E-02	
-5.665E-02	-3.126E-02	-7.52E-03	-1.89E-02	-2.92E-02	-1.07E-02	7.47E-03	8.1E-03	1.04E-02	3.49E-02	1.07E-02	-1.035E-06	-1.045E-02	
-1.572E-03	2.74E-22	3.19E-02	3.64E-02	2.64E-02	-1.11E-03	7.50E-02	-1.30E-02	-3.97E-02	2.14E-02	1.519E-02	-2.92E-02	8.11E-07	2.91E-02
1.535E-02	3.27E-02	2.81E-02	1.04E-02	2.16E-02	7.04E-02	-1.21E-02	-1.515E-02	-1.515E-02	-2.10E-02	3.94E-02	-2.617E-02	8.67E-03	-3.31E-02
-5.135E-02	-1.747E-02	2.12E-02	2.19E-02	1.94E-02	-1.31E-02	-1.945E-02	6.17E-03	6.19E-02	3.52E-02	6.53E-03	2.42E-02	6.52E-03	-5.02E-02
-2.335E-03	3.04E-03	-3.01E-02	-7.45E-02	-1.97E-02	3.00E-03	-2.73E-02	1.43E-02	-2.30E-02	-5.39E-03	-2.67E-05	5.02E-02	2.30E-02	-1.01E-02
-6.88E-02	1.01E-02	2.04E-02	2.18E-02	-6.54E-02	-2.75E-02	2.97E-02	5.84E-02	5.83E-02	2.49E-02	-6.51E-02	-5.56E-05	6.56E-02	-2.31E-02
1.77E-02	-5.08E-02	9.56E-02	7.96E-02	-6.50E-02	-5.50E-02	-6.70E-02	-5.50E-02	-7.01E-02	1.12E-01	1.25E-02	-8.82E-02	6.53E-05	8.82E-02
7.73E-02	9.48E-02								-1.12E-01				

COLUMN NO.	13 OF U MATRIX	COLUMN NO.	14 OF U MATRIX										
-2.038E-02	3.82E-03	3.09E-02	7.539E-02	-3.83E-02	9.04E-04	3.94E-02	-1.12E-02	-1.23E-02	-5.29E-02	2.01E-02	6.14E-02	2.039E-02	
-1.195E-02	6.31E-02	-3.01E-02	-6.50E-02	6.27E-02	5.01E-02	3.65E-02	-2.12E-02	6.39E-02	6.73E-02	6.73E-02	6.88E-03	6.71E-03	-2.61E-02
-6.61E-02	1.04E-01	-5.59E-03	-5.12E-02	-2.30E-02	4.72E-02	2.27E-02	6.63E-03	1.27E-01	3.91E-03	-3.51E-02	-2.72E-02	-2.91E-02	-2.49E-02
3.65E-02	5.82E-03	-2.33E-01	7.70E-03	-2.70E-02	2.24E-04	3.09E-02	-2.51E-02	-7.98E-03	1.24E-01	3.02E-03	-2.77E-02	3.06E-03	1.19E-03
6.63E-02	-2.01E-01	-1.71E-03	3.27E-02	-6.23E-02	5.15E-02	-2.10E-02	1.10E-03	5.01E-03	-2.71E-02	7.01E-03	-3.23E-02	5.93E-03	
1.221E-02	6.31E-02	9.30E-02	6.53E-02	-5.08E-02	-6.44E-02	-1.16E-02	-1.80E-02	6.59E-02	-2.23E-02	-3.66E-02	5.93E-03	6.65E-02	7.03E-02
-1.372E-02	5.79E-02	5.11E-02	4.64E-03	8.04E-05	-3.51E-03	-5.10E-02	-1.03E-02	-2.94E-02	-2.05E-02	-2.94E-03	-7.65E-02	2.97E-02	
-2.242E-02	3.33E-02	7.27E-03	-6.37E-02	-6.99E-02	-1.42E-03	6.91E-02	-6.25E-02	-1.15E-02	-2.25E-02	7.18E-03	1.24E-01	7.19E-03	
6.42E-02	-6.01E-03						-5.25E-02	-1.15E-02					

COLUMN NO.	15 OF U MATRIX	COLUMN NO.	16 OF U MATRIX										
-3.627E-03	5.68E-02	-3.198E-03	-5.831E-02	7.746E-02	7.646E-02	3.64E-02	-1.04E-02	-3.04E-02	-2.17E-02	-5.74E-02	4.337E-06	5.74E-02	
-5.501E-02	-9.04E-02	-1.02E-02	3.01E-02	1.04E-02	2.59E-02	-1.71E-02	-2.12E-02	3.04E-02	-5.74E-02	-6.80E-02	6.62E-02	6.60E-02	5.74E-02
-6.674E-02	5.81E-02	-3.171E-03	-2.819E-02	-2.130E-02	2.727E-02	-1.54E-02	-2.06E-02	2.65E-02	1.04E-02	1.57E-02	7.11E-02	6.70E-02	2.11E-02
-2.995E-02	-5.11E-03	6.67E-02	7.659E-02	-2.104E-02	-5.455E-02	-1.077E-02	-1.04E-02	-1.04E-02	-1.04E-02	-2.09E-02	5.71E-02	6.89E-02	-5.13E-02
2.606E-02	-1.171E-02	-5.63E-02	-2.130E-02	7.651E-02	2.681E-02	2.771E-02	1.20E-02	5.91E-02	6.69E-02	5.24E-02	1.18E-02	-2.13E-02	-5.13E-02
-5.627E-02	-5.74E-02	2.514E-02	5.389E-02	2.956E-02	-1.32E-02	-5.24E-02	-5.24E-02	-6.62E-02	-6.62E-02	2.13E-02	3.44E-02	-2.13E-02	-5.13E-02
-6.595E-02	-2.234E-02	1.517E-02	-6.099E-02	6.01E-02	4.81E-02	-1.51E-02	-1.51E-02	-1.51E-02	-1.51E-02	5.71E-02	-5.19E-02	2.13E-02	-5.13E-02
-2.871E-02	3.29E-02	1.92E-02	2.627E-02	-3.248E-02	-1.026E-01	-3.608E-02	-5.631E-02	3.08E-02	3.11E-02	2.114E-02	-2.087E-02	3.139E-04	-3.021E-02

COLUMN NO.	15 OF J MATRIX	COLUMN NO.	16 OF J MATRIX											
3.601E-02	3.724E-02	3.031E-02	-3.645E-02	-7.70E-03	-2.644E-02	-9.70E-02	-6.008E-02	-3.04E-02	-2.17E-02	-5.74E-02	4.337E-06	5.74E-02		
3.604E-02	-6.92E-02	-1.011E-02	3.037E-02	1.045E-02	2.595E-02	-1.715E-02	-2.12E-02	3.04E-02	-5.74E-02	-6.80E-02	6.62E-02	6.60E-02	5.74E-02	
1.677E-02	6.177E-02	-9.71E-02	-6.34E-02	1.018E-02	1.018E-02	7.761E-02	-1.53E-02	-2.06E-02	2.65E-02	1.04E-02	1.57E-02	7.11E-02	6.70E-02	2.11E-02
-6.661E-02	-5.64E-02	9.71E-02	-6.34E-02	-6.666E-02	-1.03E-02	5.64E-02	-1.53E-02	-2.06E-02	-2.06E-02	-2.06E-02	-2.06E-02	-2.06E-02	-2.06E-02	
2.771E-02	2.515E-02	9.71E-02	-6.34E-02	-6.666E-02	-1.03E-02	5.64E-02	-1.53E-02	-2.06E-02	-2.06E-02	-2.06E-02	-2.06E-02	-2.06E-02	-2.06E-02	
-1.642E-02	-5.64E-02	9.71E-02	-6.34E-02	-6.666E-02	-1.03E-02	5.64E-02	-1.53E-02	-2.06E-02	-2.06E-02	-2.06E-02	-2.06E-02	-2.06E-02	-2.06E-02	
2.695E-02	2.515E-02	9.71E-02	-6.34E-02	-6.666E-02	-1.03E-02	5.64E-02	-1.53E-02	-2.06E-02	-2.06E-02	-2.06E-02	-2.06E-02	-2.06E-02	-2.06E-02	
2.698E-02	2.515E-02	9.71E-02	-6.34E-02	-6.666E-02	-1.03E-02	5.64E-02	-1.53E-02	-2.06E-02	-2.06E-02	-2.06E-02	-2.06E-02	-2.06E-02	-2.06E-02	
2.701E-02	2.515E-02	9.71E-02	-6.34E-02	-6.666E-02	-1.03E-02	5.64E-02	-1.53E-02	-2.06E-02	-2.06E-02	-2.06E-02	-2.06E-02	-2.06E-02	-2.06E-02	
2.704E-02	2.515E-02	9.71E-02	-6.34E-02	-6.666E-02	-1.03E-02	5.64E-02	-1.53E-02	-2.06E-02	-2.06E-02	-2.06E-02	-2.06E-02	-2.06E-02	-2.06E-02	
2.707E-02	2.515E-02	9.71E-02	-6.34E-02	-6.666E-02	-1.03E-02	5.64E-02	-1.53E-02	-2.06E-02	-2.06E-02	-2.06E-02	-2.06E-02	-2.06E-02	-2.06E-02	
2.710E-02	2.515E-02	9.71E-02	-6.34E-02	-6.666E-02	-1.03E-02	5.64E-02	-1.53E-02	-2.06E-02	-2.06E-02	-2.06E-02	-2.06E-02	-2.06E-02	-2.06E-02	
2.713E-02	2.515E-02	9.71E-02	-6.34E-02	-6.666E-02	-1.03E-02	5.64E-02	-1.53E-02	-2.06E-02	-2.06E-02	-2.06E-02	-2.06E-02	-2.06E-02	-2.06E-02	
2.716E-02	2.515E-02	9.71E-02	-6.34E-02	-6.666E-02	-1.03E-02	5.64E-02	-1.53E-02	-2.06E-02	-2.06E-02	-2.06E-02	-2.06E-02	-2.06E-02	-2.06E-02	
2.719E-02	2.515E-02	9.71E-02	-6.34E-02	-6.666E-02	-1.03E-02	5.64E-02	-1.53E-02	-2.06E-02	-2.06E-02	-2.06E-02	-2.06E-02	-2.06E-02	-2.06E-02	
2.722E-02	2.515E-02	9.71E-02	-6.34E-02	-6.666E-02	-1.03E-02	5.64E-02	-1.53E-02	-2.06E-02	-2.06E-02	-2.06E-02	-2.06E-02	-2.06E-02	-2.06E-02	
2.725E-02	2.515E-02	9.71E-02	-6.34E-02	-6.666E-02	-1.03E-02	5.64E-02	-1.53E-02	-2.06E-02	-2.06E-02	-2.06E-02	-2.06E-02	-2.06E-02	-2.06E-02	
2.728E-02	2.515E-02	9.71E-02	-6.34E-02	-6.666E-02	-1.03E-02	5.64E-02	-1.53E-02	-2.06E-02	-2.06E-02	-2.06E-02	-2.06E-02	-2.06E-02	-2.06E-02	
2.731E-02	2.515E-02	9.71E-02	-6.34E-02	-6.666E-02	-1.03E-02	5.64E-02	-1.53E-02	-2.06E-02	-2.06E-02	-2.06E-02	-2.06E-02	-2.06E-02	-2.06E-02	
2.734E-02	2.515E-02	9.71E-02	-6.34E-02	-6.666E-02	-1.03E-02	5.64E-02	-1.53E-02	-2.06E-02	-2.06E-02	-2.06E-02	-2.06E-02	-2.06E-02	-2.06E-02	
2.737E-02	2.515E-02	9.71E-02	-6.34E-02	-6.666E-02	-1.03E-02	5.64E-02	-1.53E-02	-2.06E-02	-2.06E-02	-2.06E-02	-2.06E-02	-2.06E-02	-2.06E-02	
2.740E-02	2.515E-02	9.71E-02	-6.34E-02	-6.666E-02	-1.03E-02	5.64E-02	-1.53E-02	-2.06E-02	-2.06E-02	-2.06E-02	-2.06E-02	-2.06E-02	-2.06E-02	
2.743E-02	2.515E-02	9.71E-02	-6.34E-02	-6.666E-02	-1.03E-02	5.64E-02	-1.53E-02	-2.06E-02	-2.06E-02	-2.06E-02	-2.06E-02	-2.06E-02	-2.06E-02	
2.746E-02	2.515E-02	9.71E-02	-6.34E-02	-6.666E-02	-1.03E-02	5.64E-02	-1.53E-02	-2.06E-02	-2.06E-02	-2.06E-02	-2.06E-02	-2.06E-02	-2.06E-02	
2.749E-02	2.515E-02	9.71E-02	-6.34E-02	-6.666E-02	-1.03E-02	5.64E-02	-1.53E-02	-2.06E-02	-2.06E-02	-2.06E-02	-2.06E-02	-2.06E-02	-2.06E-02	
2.752E-02	2.515E-02	9.71E-02	-6.34E-02	-6.666E-02	-1.03E-02	5.64E-02	-1.53E-02	-2.06E-02	-2.06E-02	-2.06E-02	-2.06E-02	-2.06E-02	-2.06E-02	
2.755E-02	2.515E-02	9.71E-02	-6.34E-02	-6.666E-02	-1.03E-02	5.64E-02	-1.53E-02	-2.06E-02	-2.06E-02	-2.06E-02	-2.06E-02	-2.06E-02	-2.06E-02	
2.758E-02	2.515E-02	9.71E-02	-6.34E-02	-6.666E-02	-1.03E-02	5.64E-02	-1.53E-02	-2.06E-02	-2.06E-02	-2.06E-02	-2.06E-02	-2.06E-02	-2.06E-02	
2.761E-02	2.515E-02	9.71E-02	-6.34E-02	-6.666E-02	-1.03E-02	5.64E-02	-1.53E-02	-2.06E-02	-2.06E-02	-2.06E-02	-2.06E-02	-2.06E-02	-2.06E-02	
2.764E-02	2.515E-02	9.71E-02	-6.34E-02	-6.666E-02	-1.03E-02	5.64E-02	-1.53E-0							

APPENDIX B – Continued

CAL 4900 940 - 40 OF 49 STATES

-2.970-02	-3.000-01	-3.070-01	3.100-01	3.130-01	3.170-01	-3.200-01	3.230-01	3.260-01	3.290-01	3.320-01	3.350-01	3.380-01	3.410-01	3.440-01	3.470-01	3.500-01	3.530-01	3.560-01	3.590-01	3.620-01	3.650-01	3.680-01	3.710-01	3.740-01	3.770-01	3.800-01	3.830-01	3.860-01	3.890-01	3.920-01	3.950-01	3.980-01	4.010-01	4.040-01	4.070-01	4.100-01	4.130-01	4.160-01	4.190-01	4.220-01	4.250-01	4.280-01	4.310-01	4.340-01	4.370-01	4.400-01	4.430-01	4.460-01	4.490-01	4.520-01	4.550-01	4.580-01	4.610-01	4.640-01	4.670-01	4.700-01	4.730-01	4.760-01	4.790-01	4.820-01	4.850-01	4.880-01	4.910-01	4.940-01	4.970-01	5.000-01	5.030-01	5.060-01	5.090-01	5.120-01	5.150-01	5.180-01	5.210-01	5.240-01	5.270-01	5.300-01	5.330-01	5.360-01	5.390-01	5.420-01	5.450-01	5.480-01	5.510-01	5.540-01	5.570-01	5.600-01	5.630-01	5.660-01	5.690-01	5.720-01	5.750-01	5.780-01	5.810-01	5.840-01	5.870-01	5.900-01	5.930-01	5.960-01	5.990-01	6.020-01	6.050-01	6.080-01	6.110-01	6.140-01	6.170-01	6.200-01	6.230-01	6.260-01	6.290-01	6.320-01	6.350-01	6.380-01	6.410-01	6.440-01	6.470-01	6.500-01	6.530-01	6.560-01	6.590-01	6.620-01	6.650-01	6.680-01	6.710-01	6.740-01	6.770-01	6.800-01	6.830-01	6.860-01	6.890-01	6.920-01	6.950-01	6.980-01	7.010-01	7.040-01	7.070-01	7.100-01	7.130-01	7.160-01	7.190-01	7.220-01	7.250-01	7.280-01	7.310-01	7.340-01	7.370-01	7.400-01	7.430-01	7.460-01	7.490-01	7.520-01	7.550-01	7.580-01	7.610-01	7.640-01	7.670-01	7.700-01	7.730-01	7.760-01	7.790-01	7.820-01	7.850-01	7.880-01	7.910-01	7.940-01	7.970-01	8.000-01	8.030-01	8.060-01	8.090-01	8.120-01	8.150-01	8.180-01	8.210-01	8.240-01	8.270-01	8.300-01	8.330-01	8.360-01	8.390-01	8.420-01	8.450-01	8.480-01	8.510-01	8.540-01	8.570-01	8.600-01	8.630-01	8.660-01	8.690-01	8.720-01	8.750-01	8.780-01	8.810-01	8.840-01	8.870-01	8.900-01	8.930-01	8.960-01	8.990-01	9.020-01	9.050-01	9.080-01	9.110-01	9.140-01	9.170-01	9.200-01	9.230-01	9.260-01	9.290-01	9.320-01	9.350-01	9.380-01	9.410-01	9.440-01	9.470-01	9.500-01	9.530-01	9.560-01	9.590-01	9.620-01	9.650-01	9.680-01	9.710-01	9.740-01	9.770-01	9.800-01	9.830-01	9.860-01	9.890-01	9.920-01	9.950-01	9.980-01	10.010-01	10.040-01	10.070-01	10.100-01	10.130-01	10.160-01	10.190-01	10.220-01	10.250-01	10.280-01	10.310-01	10.340-01	10.370-01	10.400-01	10.430-01	10.460-01	10.490-01	10.520-01	10.550-01	10.580-01	10.610-01	10.640-01	10.670-01	10.700-01	10.730-01	10.760-01	10.790-01	10.820-01	10.850-01	10.880-01	10.910-01	10.940-01	10.970-01	11.000-01	11.030-01	11.060-01	11.090-01	11.120-01	11.150-01	11.180-01	11.210-01	11.240-01	11.270-01	11.300-01	11.330-01	11.360-01	11.390-01	11.420-01	11.450-01	11.480-01	11.510-01	11.540-01	11.570-01	11.600-01	11.630-01	11.660-01	11.690-01	11.720-01	11.750-01	11.780-01	11.810-01	11.840-01	11.870-01	11.900-01	11.930-01	11.960-01	11.990-01	12.020-01	12.050-01	12.080-01	12.110-01	12.140-01	12.170-01	12.200-01	12.230-01	12.260-01	12.290-01	12.320-01	12.350-01	12.380-01	12.410-01	12.440-01	12.470-01	12.500-01	12.530-01	12.560-01	12.590-01	12.620-01	12.650-01	12.680-01	12.710-01	12.740-01	12.770-01	12.800-01	12.830-01	12.860-01	12.890-01	12.920-01	12.950-01	12.980-01	13.010-01	13.040-01	13.070-01	13.100-01	13.130-01	13.160-01	13.190-01	13.220-01	13.250-01	13.280-01	13.310-01	13.340-01	13.370-01	13.400-01	13.430-01	13.460-01	13.490-01	13.520-01	13.550-01	13.580-01	13.610-01	13.640-01	13.670-01	13.700-01	13.730-01	13.760-01	13.790-01	13.820-01	13.850-01	13.880-01	13.910-01	13.940-01	13.970-01	14.000-01	14.030-01	14.060-01	14.090-01	14.120-01	14.150-01	14.180-01	14.210-01	14.240-01	14.270-01	14.300-01	14.330-01	14.360-01	14.390-01	14.420-01	14.450-01	14.480-01	14.510-01	14.540-01	14.570-01	14.600-01	14.630-01	14.660-01	14.690-01	14.720-01	14.750-01	14.780-01	14.810-01	14.840-01	14.870-01	14.900-01	14.930-01	14.960-01	14.990-01	15.020-01	15.050-01	15.080-01	15.110-01	15.140-01	15.170-01	15.200-01	15.230-01	15.260-01	15.290-01	15.320-01	15.350-01	15.380-01	15.410-01	15.440-01	15.470-01	15.500-01	15.530-01	15.560-01	15.590-01	15.620-01	15.650-01	15.680-01	15.710-01	15.740-01	15.770-01	15.800-01	15.830-01	15.860-01	15.890-01	15.920-01	15.950-01	15.980-01	16.010-01	16.040-01	16.070-01	16.100-01	16.130-01	16.160-01	16.190-01	16.220-01	16.250-01	16.280-01	16.310-01	16.340-01	16.370-01	16.400-01	16.430-01	16.460-01	16.490-01	16.520-01	16.550-01	16.580-01	16.610-01	16.640-01	16.670-01	16.700-01	16.730-01	16.760-01	16.790-01	16.820-01	16.850-01	16.880-01	16.910-01	16.940-01	16.970-01	17.000-01	17.030-01	17.060-01	17.090-01	17.120-01	17.150-01	17.180-01	17.210-01	17.240-01	17.270-01	17.300-01	17.330-01	17.360-01	17.390-01	17.420-01	17.450-01	17.480-01	17.510-01	17.540-01	17.570-01	17.600-01	17.630-01	17.660-01	17.690-01	17.720-01	17.750-01	17.780-01	17.810-01	17.840-01	17.870-01	17.900-01	17.930-01	17.960-01	17.990-01	18.020-01	18.050-01	18.080-01	18.110-01	18.140-01	18.170-01	18.200-01	18.230-01	18.260-01	18.290-01	18.320-01	18.350-01	18.380-01	18.410-01	18.440-01	18.470-01	18.500-01	18.530-01	18.560-01	18.590-01	18.620-01	18.650-01	18.680-01	18.710-01	18.740-01	18.770-01	18.800-01	18.830-01	18.860-01	18.890-01	18.920-01	18.950-01	18.980-01	19.010-01	19.040-01	19.070-01	19.100-01	19.130-01	19.160-01	19.190-01	19.220-01	19.250-01	19.280-01	19.310-01	19.340-01	19.370-01	19.400-01	19.430-01	19.460-01	19.490-01	19.520-01	19.550-01	19.580-01	19.610-01	19.640-01	19.670-01	19.700-01	19.730-01	19.760-01	19.790-01	19.820-01	19.850-01	19.880-01	19.910-01	19.940-01	19.970-01	20.000-01	20.030-01	20.060-01	20.090-01	20.120-01	20.150-01	20.180-01	20.210-01	20.240-01	20.270-01	20.300-01	20.330-01	20.360-01	20.390-01	20.420-01	20.450-01	20.480-01	20.510-01	20.540-01	20.570-01	20.600-01	20.630-01	20.660-01	20.690-01	20.720-01	20.750-01	20.780-01	20.810-01	20.840-01	20.870-01	20.900-01	20.930-01	20.960-01	20.990-01	21.020-01	21.050-01	21.080-01	21.110-01	21.140-01	21.170-01	21.200-01	21.230-01	21.260-01	21.290-01	21.320-01	21.350-01	21.380-01	21.410-01	21.440-01	21.470-01	21.500-01	21.530-01	21.560-01	21.590-01	21.620-01	21.650-01	21.680-01	21.710-01	21.740-01	21.770-01	21.800-01	21.830-01	21.860-01	21.890-01	21.920-01	21.950-01	21.980-01	22.010-01	22.040-01	22.070-01	22.100-01	22.130-01	22.160-01	22.190-01	22.220-01	22.250-01	22.280-01	22.310-01	22.340-01	22.370-01	22.400-01	22.430-01	22.460-01	22.490-01	22.520-01	22.550-01	22.580-01	22.610-01	22.640-01	22.670-01	22.700-01	22.730-01	22.760-01	22.790-01	22.820-01	22.850-01	22.880-01	22.910-01	22.940-01	22.970-01	23.000-01	23.030-01	23.060-01	23.090-01	23.120-01	23.150-01	23.180-01	23.210-01	23.240-01	23.270-01	23.300-01	23.330-01	23.360-01	23.390-01	23.420-01	23.450-01	23.480-01	23.510-01	23.540-01	23.570-01	23.600-01	23.630-01	23.660-01	23.690-01	23.720-01	23.750-01	23.780-01	23.810-01	23.840-01	23.870-01	23.900-01	23.930-01	23.960-01	24.000-01	24.030-01	24.060-01	24.090-01	24.120-01	24.150-01	24.180-01	24.210-01	24.240-01	24.270-01	24.300-01	24.330-01	24.360-01	24.390-01	24.420-01	24.450-01	24.480-01	24.510-01	24.540-01	24.570-01	24.600-01	24.630-01	24.660-01	24.690-01	24.720-01	24.750-01	24.780-01	24.810-01	24.840-01	24.870-01	24.900-01	24.930-01	24.960-01	25.000-01	25.030-01	25.060-01	25.090-01	25.120-01	25.150-01	25.180-01	25.210-01	25.240-01	25.270-01	25.300-01	25.330-01	25.360-01	25.390-01	25.420-01	25.450-01	25.480-01	25.510-01	25.540-01	25.570-01	25.600-01	25.630-01	25.660-01	25.690-01	25.720-01	25.750-01	25.780-01	25.810-01	25.840-01	25.870-01	25.900-01	25.930-01	25.960-01	26.000-01	26.030-01	26.060-01	26.090-01	26.120-01	26.150-01	26.180-01	26.210-01	26.240-01	26.270-01	26.300-01	26.330-01	26.360-01	26.390-01	26.420-01	26.450-01	26.480-01	26.510-01	26.540-01	26.570-01	26.600-01	26.630-01	26.660-01	26.690-01	26.720-01	26.750-01	26.780-01	26.810-01	26.840-01	26.870-01	26.900-01	26.930-01	26.960-01	27.000-01	27.030-01	27.060-01	27.090-01	27.120-01	27.150-01	27.180-01	27.210-01	27.240-01	27.270-01	27.300-01	27.330-01	27.360-01	27.390-01	27.420-01	27.450-01	27.480-01	27.510-01	27.540-01	27.570-01	27.600-01	27.630-01	27.660-01	27.690-01	27.720-01	27.750-01	27.780-01	27.810-01	27.840-01	27.870-01	27.900-01	27.930-01	27.960-01	28.000-01	28.030-01	28.060-01	28.090-01	28.120-01	28.150-01	28.180-01	28.210-01

APPENDIX B – Concluded

APPENDIX C

EIGENVECTOR DIAGRAMS

This appendix contains schematic representations of the first 10 modes of the thin mirror (figs. C1 to C10). For each of these modes the mirror deflection along the Z-axis at each grid point is written beside that grid point. The contour lines indicate the nodes of each mode. Note that mode 3 is a bowl-shaped mode and therefore has no node line. The numbers at the grid points are taken directly from appendix B, columns 1 to 10 inclusive, and are displayed in this manner to provide more insight into actual shapes than can be obtained from looking at columns of numbers. Each number has been multiplied by 100 for scaling purposes.

APPENDIX C – Continued

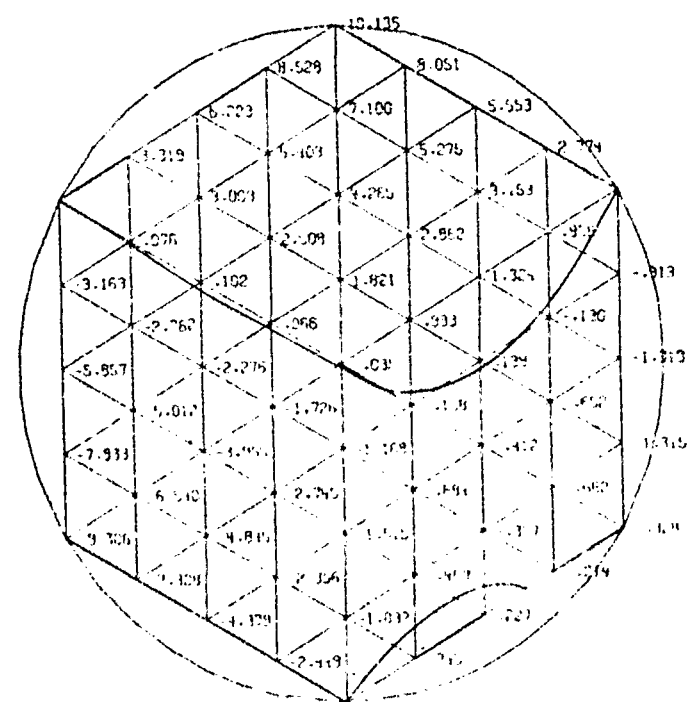


Figure Cl.- Mode 1 of the thin mirror.

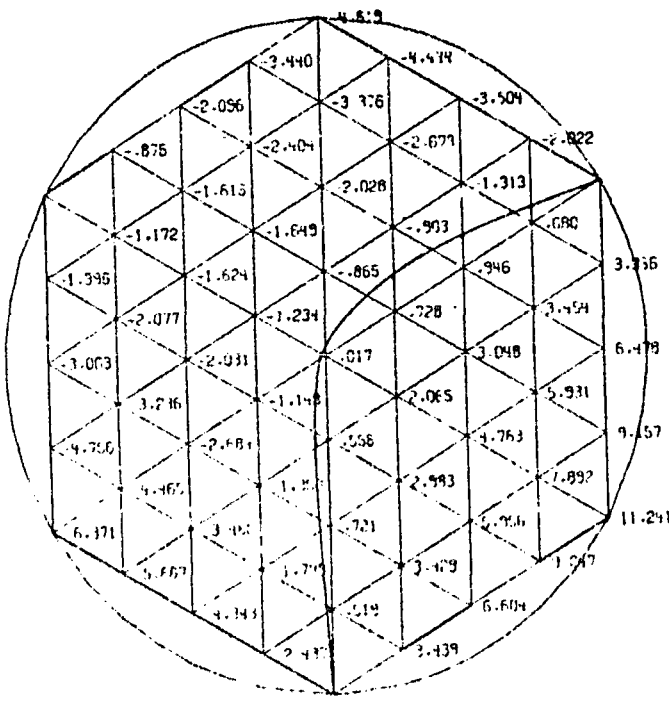


Figure C2.- Mode 2 of the thin mirror.

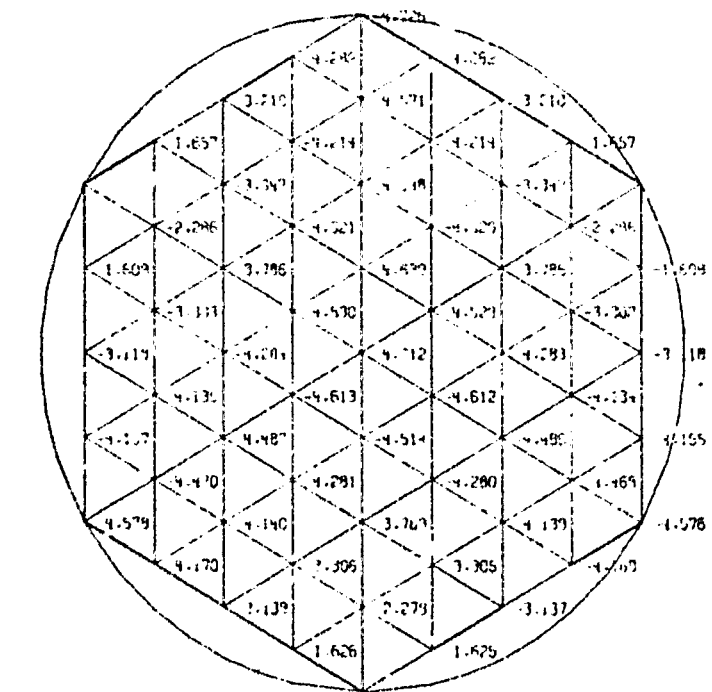


Figure C3.- Mode 3 of the thin mirror.

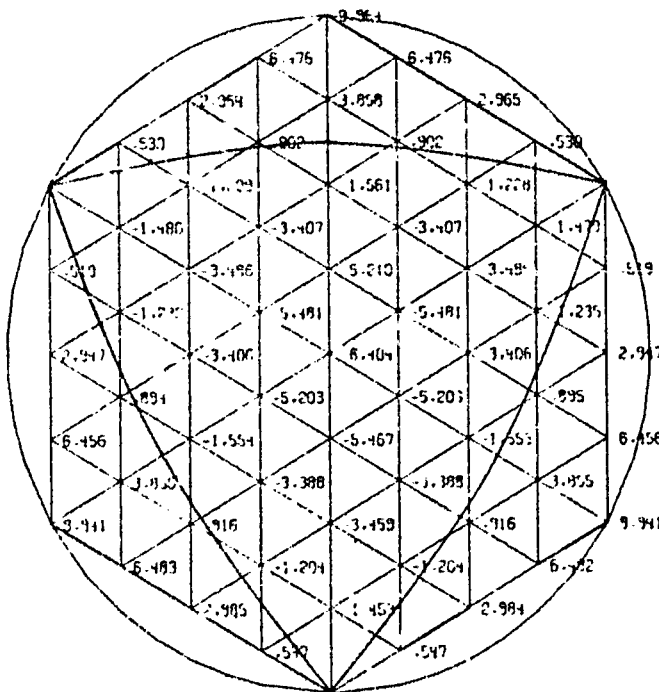


Figure C4.- Mode 4 of the thin mirror.

APPENDIX C - Continued

APPENDIX C - Continued

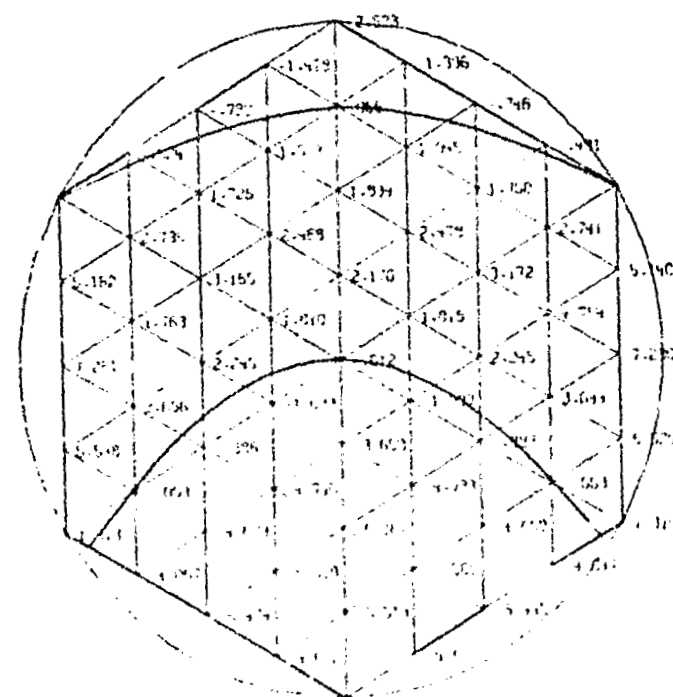


Figure C₅.- Rule 5 of the thin mirror.

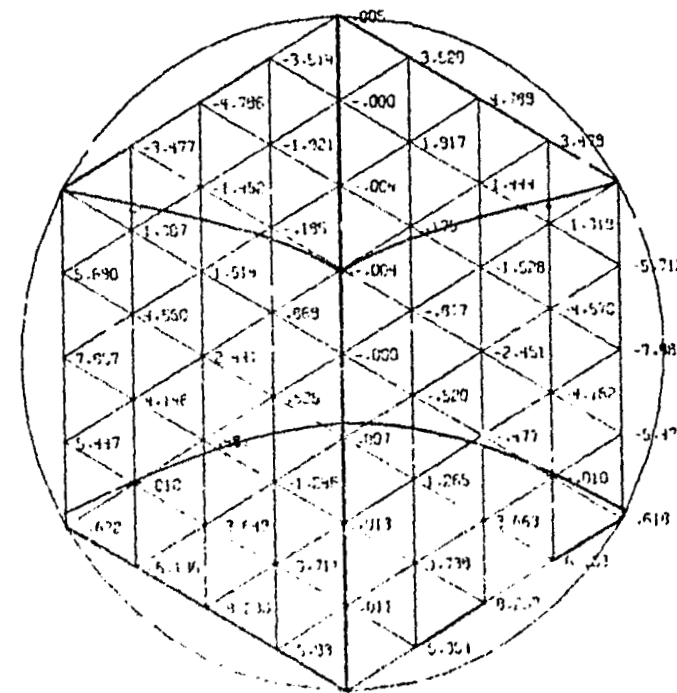


Figure C6.- Mode 6 of the thin mirror.

APPENDIX C - Continued

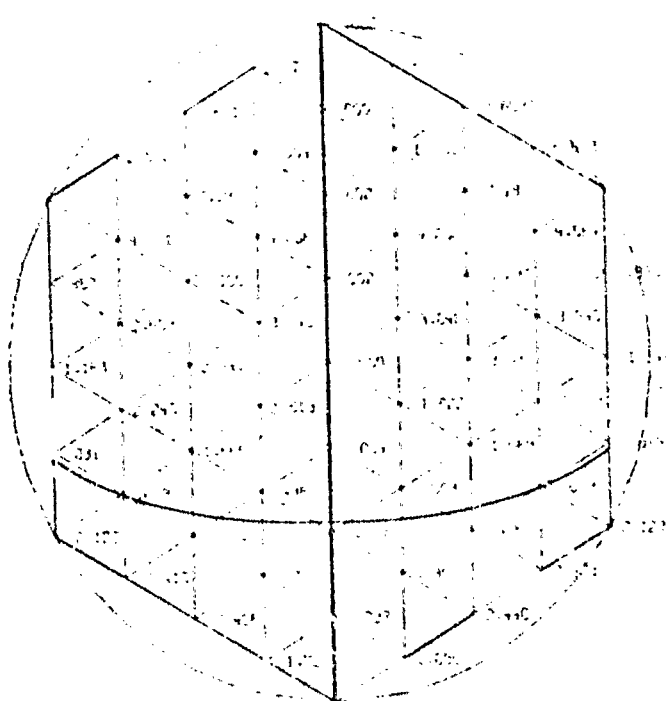


Figure 27.- Mode 7 of the thin mirror.

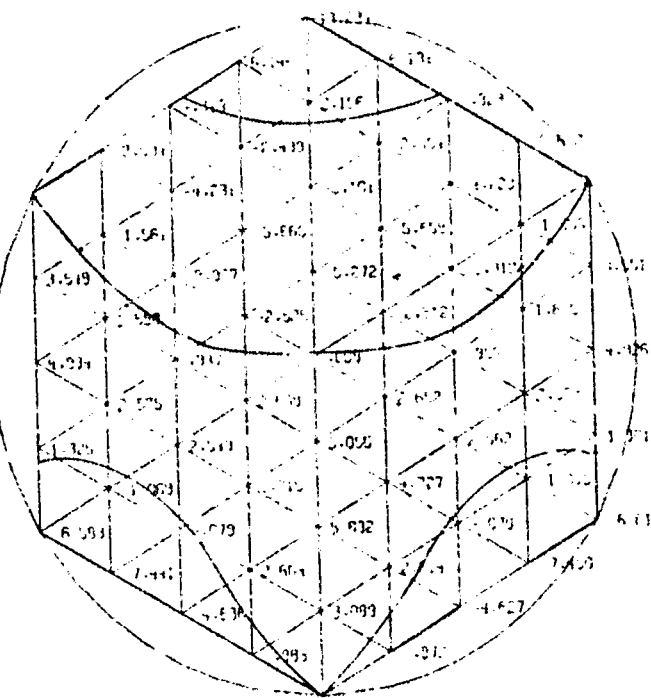


Figure C8.- Hole 8 of the thin mirror.

APPENDIX C – Concluded

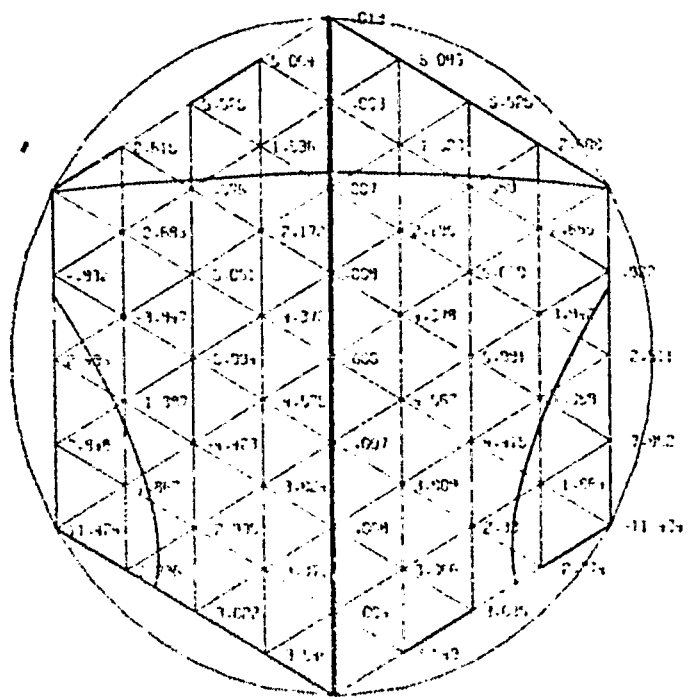


Figure C9.- Mode 9 of the thin mirror.

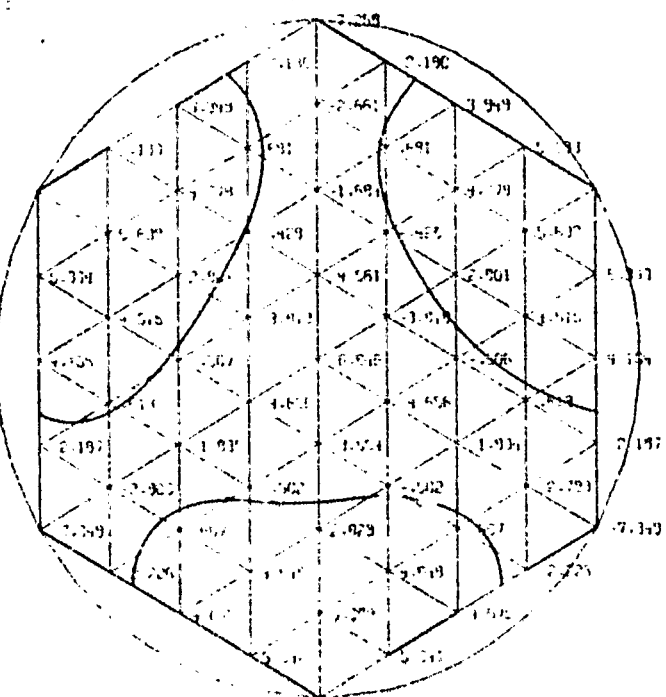


Figure C10.- Mode 10 of the thin mirror.

APPENDIX D

EIGENVALUES AND MASS MATRIX FOR THE MIRROR

This appendix contains a listing of the eigenvalues and the diagonal mass matrix m . The SAMIS program eigenvalues are inversely proportional to frequency squared and may be converted to frequency (in hertz) by the following relationship:

$$f_i = \frac{1}{2\pi} \sqrt{\frac{0.97 \times 10^{-4}}{\lambda_i}} \quad (i = 1, \dots, M)$$

The elements of the mass matrix have the units of lb-sec²/in.

The eigenvalues of the U matrix are

LAMBDA(1)	=	5.01E-02	LAMBDA(30)	=	5.29E-05
LAMBDA(2)	=	3.51E-02	LAMBDA(31)	=	5.10E-05
LAMBDA(3)	=	3.08E-02	LAMBDA(32)	=	5.10E-05
LAMBDA(4)	=	2.95E-03	LAMBDA(33)	=	4.50E-05
LAMBDA(5)	=	2.51E-03	LAMBDA(34)	=	3.88E-05
LAMBDA(6)	=	2.50E-03	LAMBDA(35)	=	3.88E-05
LAMBDA(7)	=	2.50E-03	LAMBDA(36)	=	3.59E-05
LAMBDA(8)	=	3.90E-04	LAMBDA(37)	=	3.35E-05
LAMBDA(9)	=	3.90E-04	LAMBDA(38)	=	3.35E-05
LAMBDA(10)	=	2.67E-04	LAMBDA(39)	=	3.22E-05
LAMBDA(11)	=	2.89E-04	LAMBDA(40)	=	2.95E-05
LAMBDA(12)	=	2.84E-04	LAMBDA(41)	=	2.80E-05
LAMBDA(13)	=	3.43E-04	LAMBDA(42)	=	2.76E-05
LAMBDA(14)	=	3.44E-04	LAMBDA(43)	=	2.75E-05
LAMBDA(15)	=	2.36E-04	LAMBDA(44)	=	2.47E-05
LAMBDA(16)	=	2.80E-04	LAMBDA(45)	=	2.23E-05
LAMBDA(17)	=	1.80E-04	LAMBDA(46)	=	2.23E-05
LAMBDA(18)	=	1.79E-04	LAMBDA(47)	=	2.05E-05
LAMBDA(19)	=	1.70E-04	LAMBDA(48)	=	2.05E-05
LAMBDA(20)	=	1.30E-04	LAMBDA(49)	=	2.01E-05
LAMBDA(21)	=	1.00E-04	LAMBDA(50)	=	2.01E-05
LAMBDA(22)	=	1.06E-04	LAMBDA(51)	=	1.96E-05
LAMBDA(23)	=	3.19E-05	LAMBDA(52)	=	1.86E-05
LAMBDA(24)	=	4.10E-05	LAMBDA(53)	=	1.60E-05
LAMBDA(25)	=	7.50E-05	LAMBDA(54)	=	1.60E-05
LAMBDA(26)	=	7.00E-05	LAMBDA(55)	=	1.58E-05
LAMBDA(27)	=	7.00E-05	LAMBDA(56)	=	1.58E-05
LAMBDA(28)	=	3.00E-05	LAMBDA(57)	=	1.31E-05
LAMBDA(29)	=	3.24E-05	LAMBDA(58)	=	1.31E-05

APPENDIX D - Concluded

The elements of the diagonal mass matrix are

MASS(1, 1) =	1.19E-03	MASS(30,30) =	1.25E-03
MASS(2, 2) =	1.25E-03	MASS(31,31) =	1.25E-03
MASS(3, 3) =	1.19E-03	MASS(32,32) =	1.25E-03
MASS(4, 4) =	1.43E-03	MASS(33,33) =	1.19E-03
MASS(5, 5) =	1.25E-03	MASS(34,34) =	1.43E-03
MASS(6, 6) =	1.25E-03	MASS(35,35) =	1.25E-03
MASS(7, 7) =	1.25E-03	MASS(36,36) =	1.25E-03
MASS(8, 8) =	1.43E-03	MASS(37,37) =	1.25E-03
MASS(9, 9) =	1.19E-03	MASS(38,38) =	1.43E-03
MASS(10,10) =	1.25E-03	MASS(39,39) =	1.25E-03
MASS(11,11) =	1.25E-03	MASS(40,40) =	1.25E-03
MASS(12,12) =	1.25E-03	MASS(41,41) =	1.25E-03
MASS(13,13) =	1.25E-03	MASS(42,42) =	1.25E-03
MASS(14,14) =	1.25E-03	MASS(43,43) =	1.19E-03
MASS(15,15) =	1.19E-03	MASS(44,44) =	1.25E-03
MASS(16,16) =	5.50E-04	MASS(45,45) =	1.25E-03
MASS(17,17) =	1.25E-03	MASS(46,46) =	1.25E-03
MASS(18,18) =	1.25E-03	MASS(47,47) =	1.25E-03
MASS(19,19) =	1.25E-03	MASS(48,48) =	1.25E-03
MASS(20,20) =	1.25E-03	MASS(49,49) =	1.25E-03
MASS(21,21) =	1.25E-03	MASS(50,50) =	1.25E-03
MASS(22,22) =	1.25E-03	MASS(51,51) =	1.19E-03
MASS(23,23) =	1.25E-03	MASS(52,52) =	1.19E-03
MASS(24,24) =	5.50E-04	MASS(53,53) =	1.43E-03
MASS(25,25) =	1.19E-03	MASS(54,54) =	1.19E-03
MASS(26,26) =	1.25E-03	MASS(55,55) =	5.50E-04
MASS(27,27) =	1.25E-03	MASS(56,56) =	1.19E-03
MASS(28,28) =	1.25E-03	MASS(57,57) =	1.43E-03
MASS(29,29) =	1.25E-03	MASS(58,58) =	1.19E-03

APPENDIX E

BEST ACTUATOR LOCATIONS - DETERMINISTIC CASE

This appendix contains an enumeration of actuator locations which were found to produce minimum error when the errors were considered to be completely known (deterministic) and nonvarying (figs. E1 to E12). Each figure contains 10 diagrams which show the best 10 actuator locations for one of the three error examples and a specific number of actuators. Grid numbers for the actuator locations can be found by comparison with the numbered pattern in the lower right-hand portion of each figure. The values of the final error for the modal control law and the optimal control law are given beside each figure in the form:

$$\frac{A}{B}$$

where A is the error under the modal control law and B is the error under the optimal control law. These final errors are those given by the square root of equation (53), which requires that these values be multiplied by 0.49 to obtain rms error in microinches or by 0.019 to obtain rms error in wavelengths.

A particular point of interest occurred in figure E10 (two actuators, error example 3). In this figure the H^N matrix was decidedly ill conditioned for most of the examples. The normalized determinant was as low as 6×10^{-5} and the best value was 3.5×10^{-2} . If this case arose in practice, it would be best to look at three actuators or more. In figure E11 (three actuators) the normalized determinant was of the order of 0.3, which is very good.

APPENDIX E - Continued

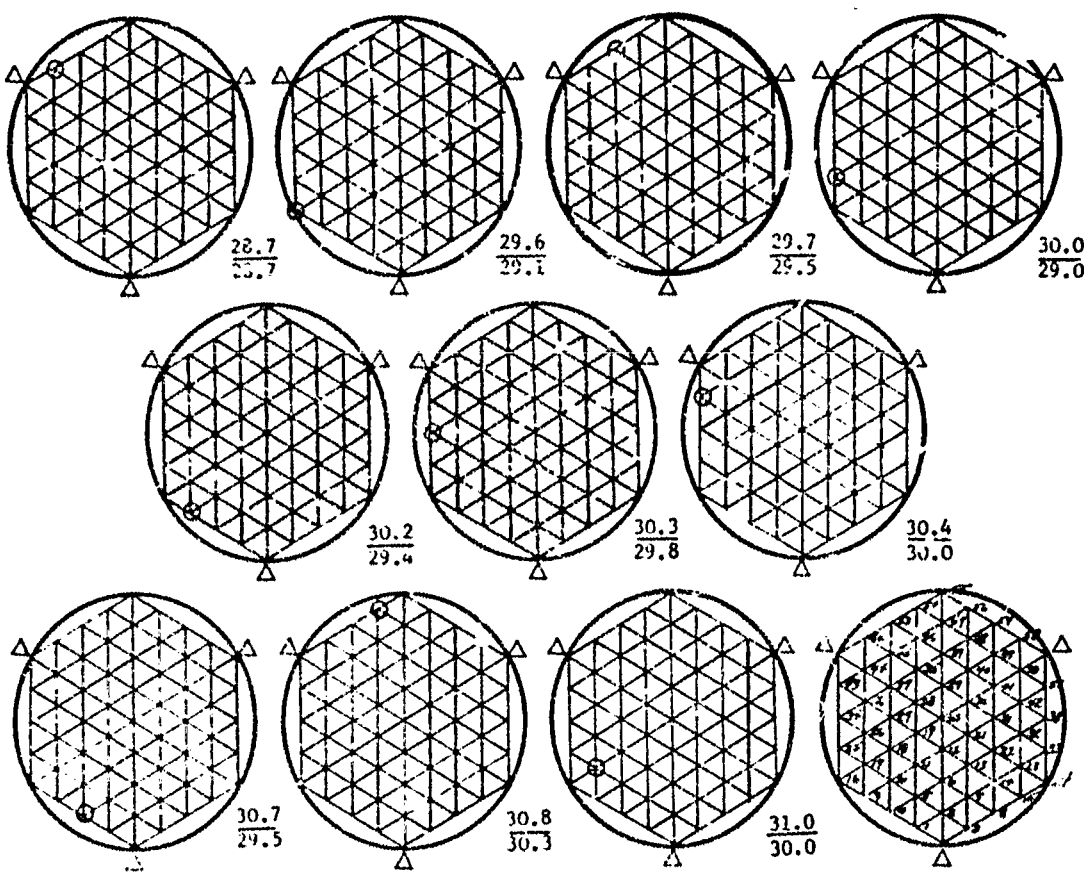


Figure 11.- Actuator locations which minimize the rms error or the mirror for one actuator and error example 1.

APPENDIX E – Continued

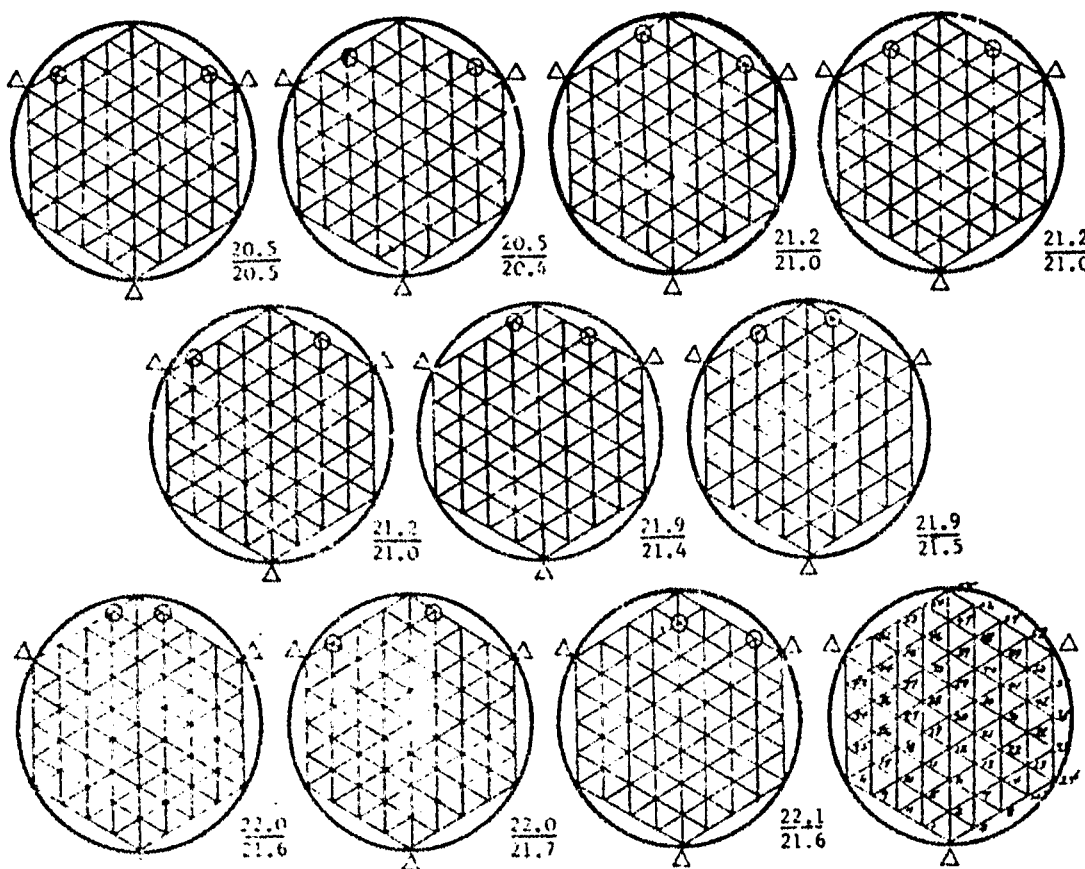


Figure E.1. - 12 actuators which minimize the rms error of the mirror for two actuators and error example 1.

APPENDIX E - Continued

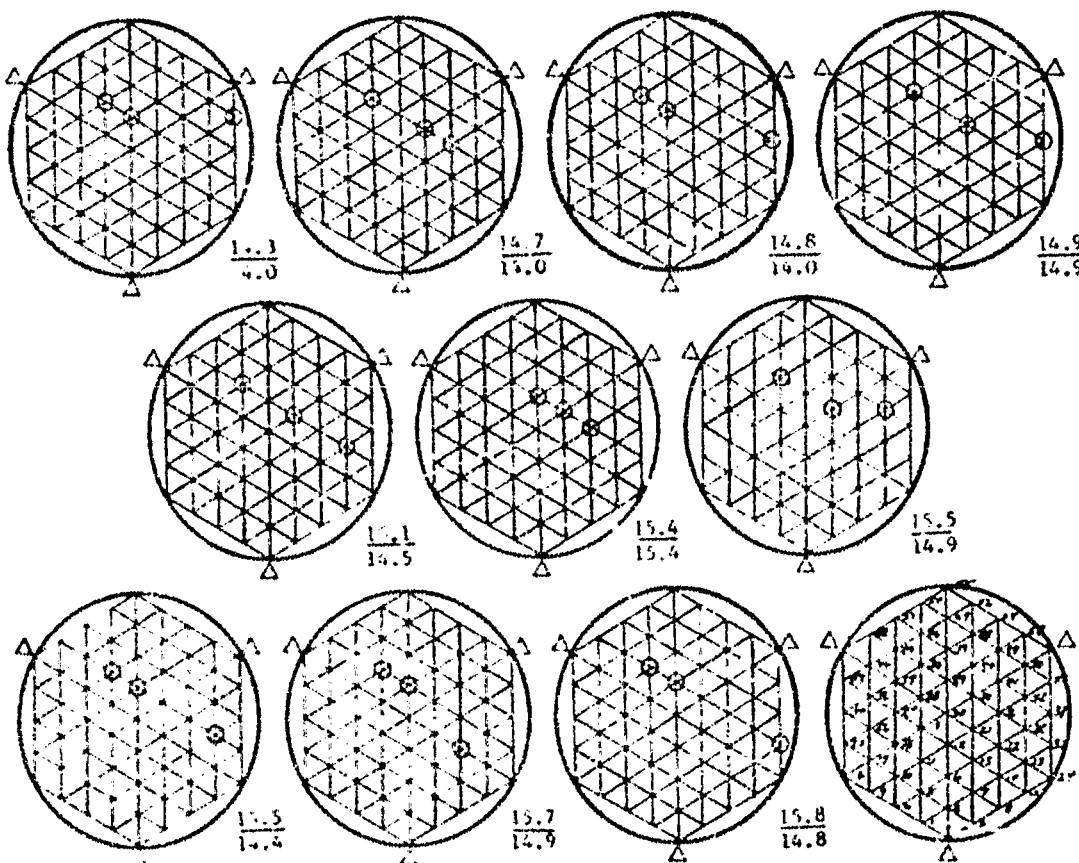


Figure 14.4: Actuator locations which minimize the rms error of the mirror for three actuators and error example 1.

APPENDIX E - Continued

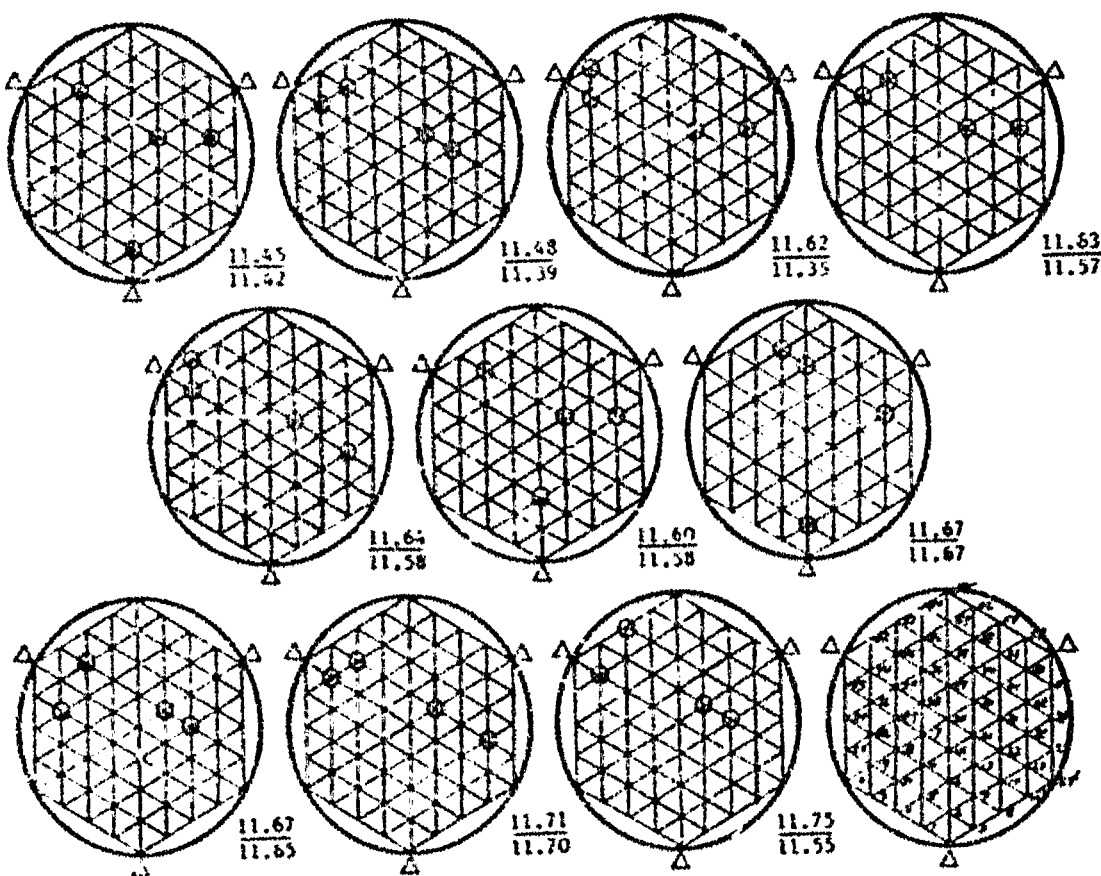


Figure E.4: Actuator locations which minimize the rms error of the mirror for four actuators and error example 1.

APPENDIX E - Continued

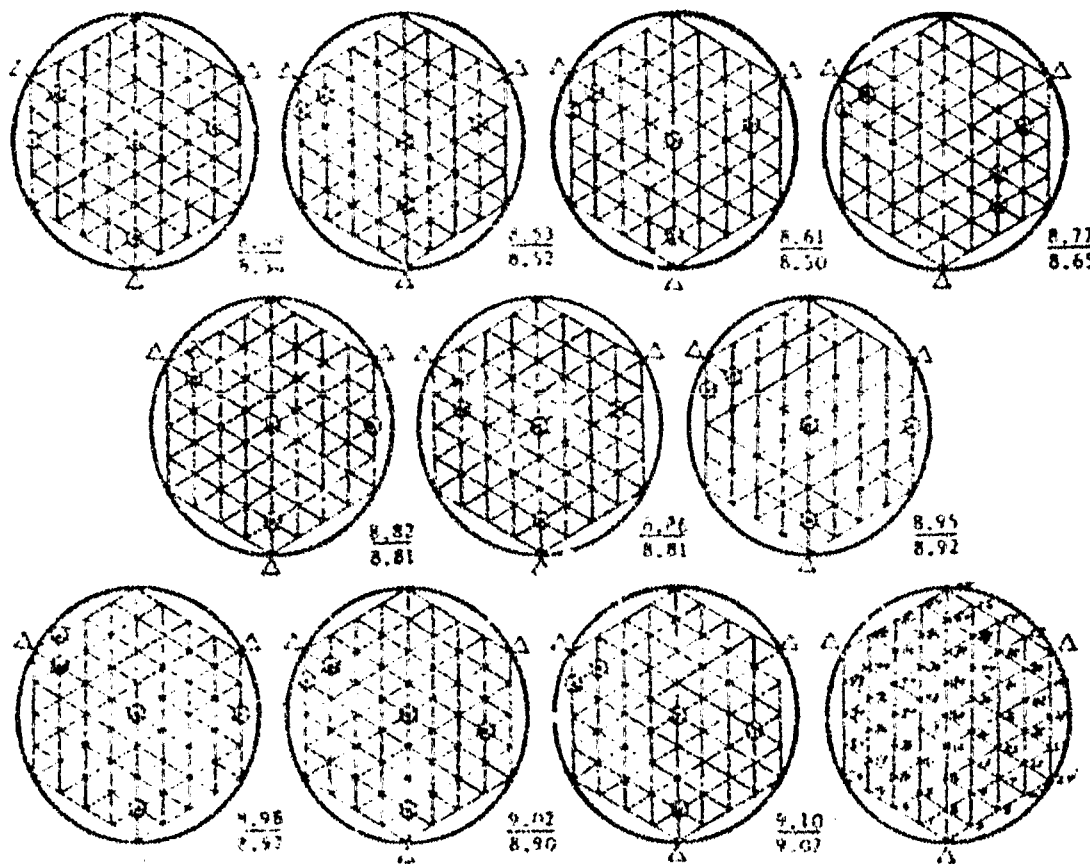


Figure 11. Antenna locations which yield the relative error of the antenna's position in sample 1.

APPENDIX E - Continued

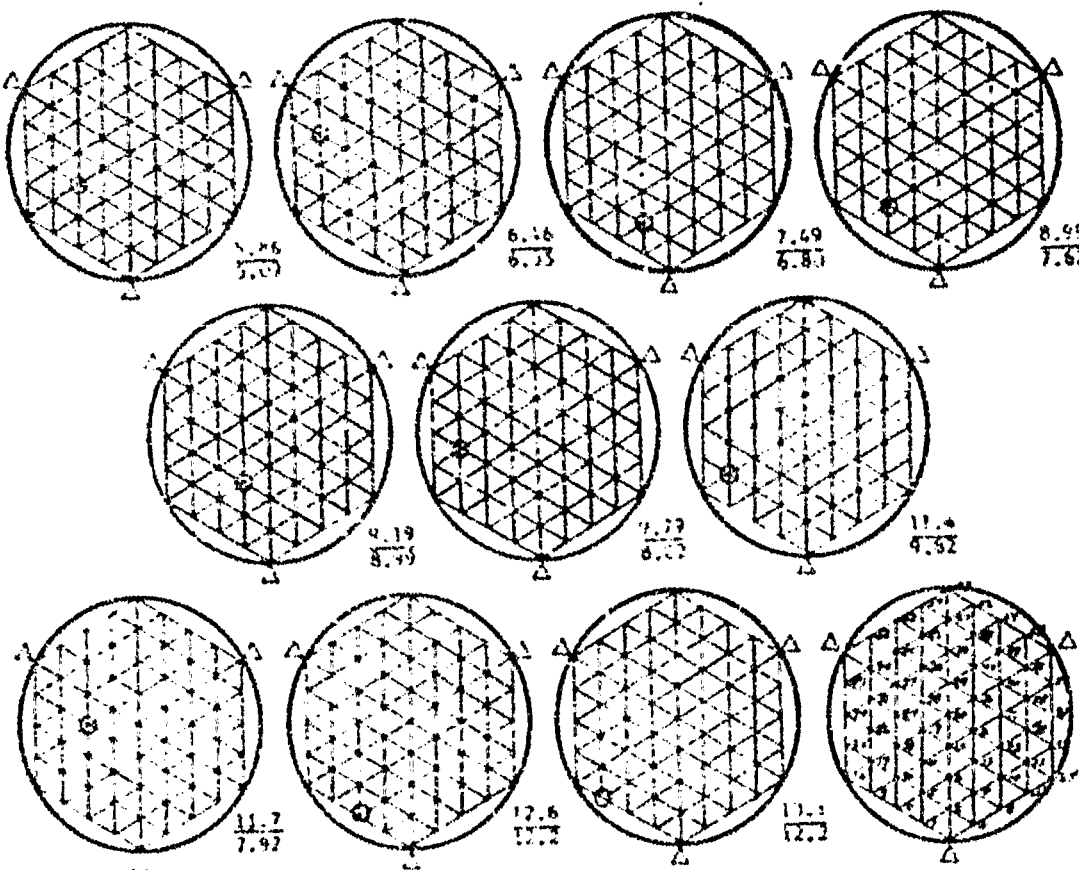


Figure 14. Results of the error per cell after an error example.

APPENDIX E - Continued

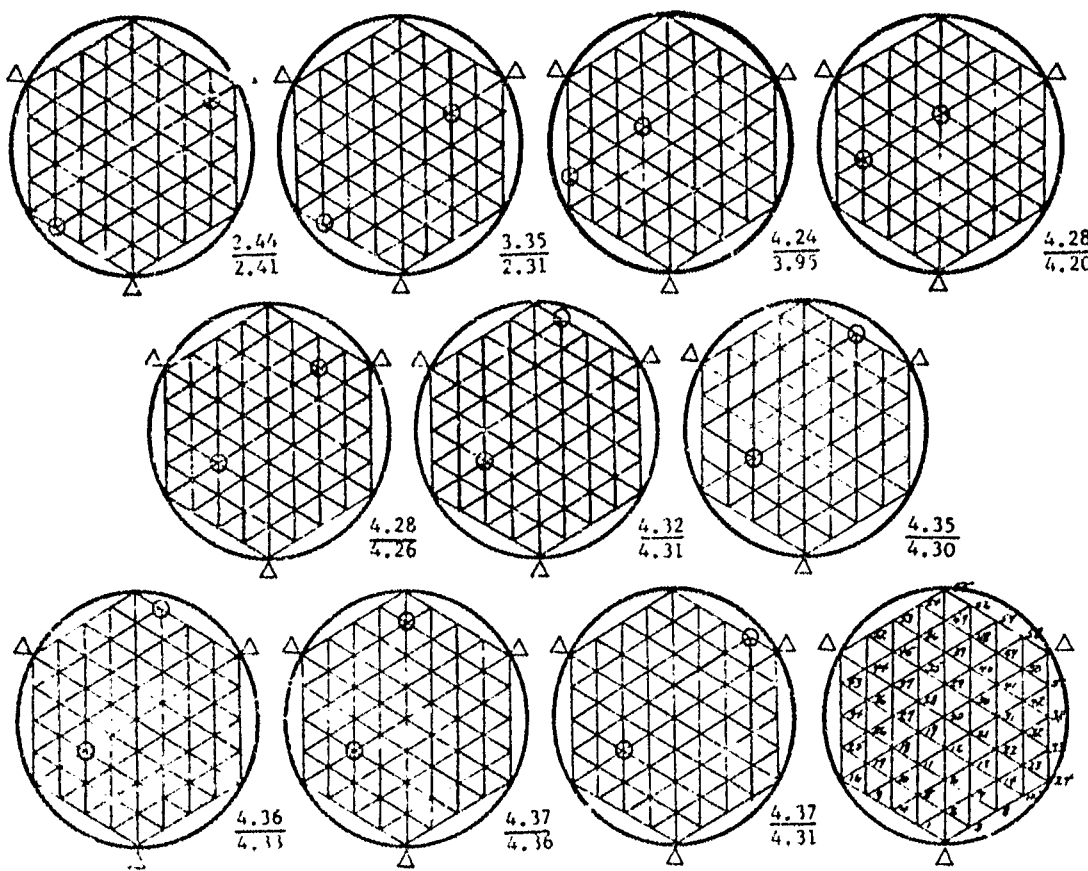
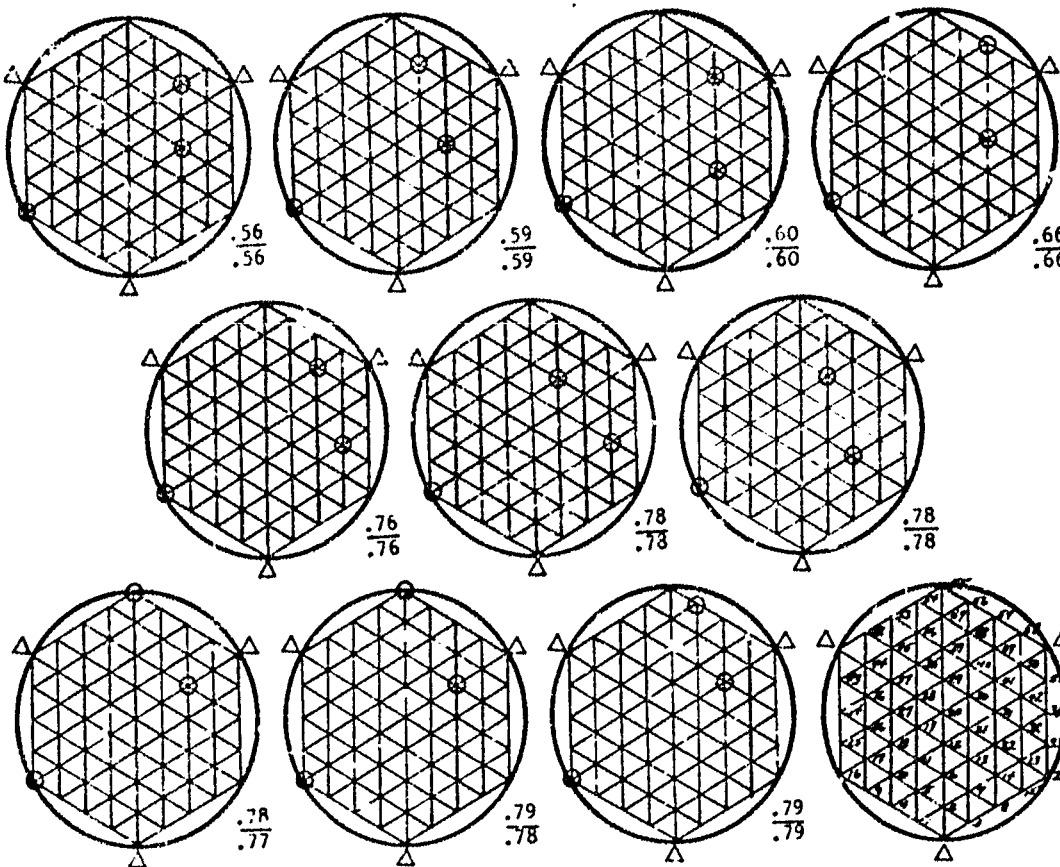


Figure 13.- Actuator locations which minimize the rms error of the mirror for two actuators and error example 2.

APPENDIX E - Continued



APPENDIX E – Continued

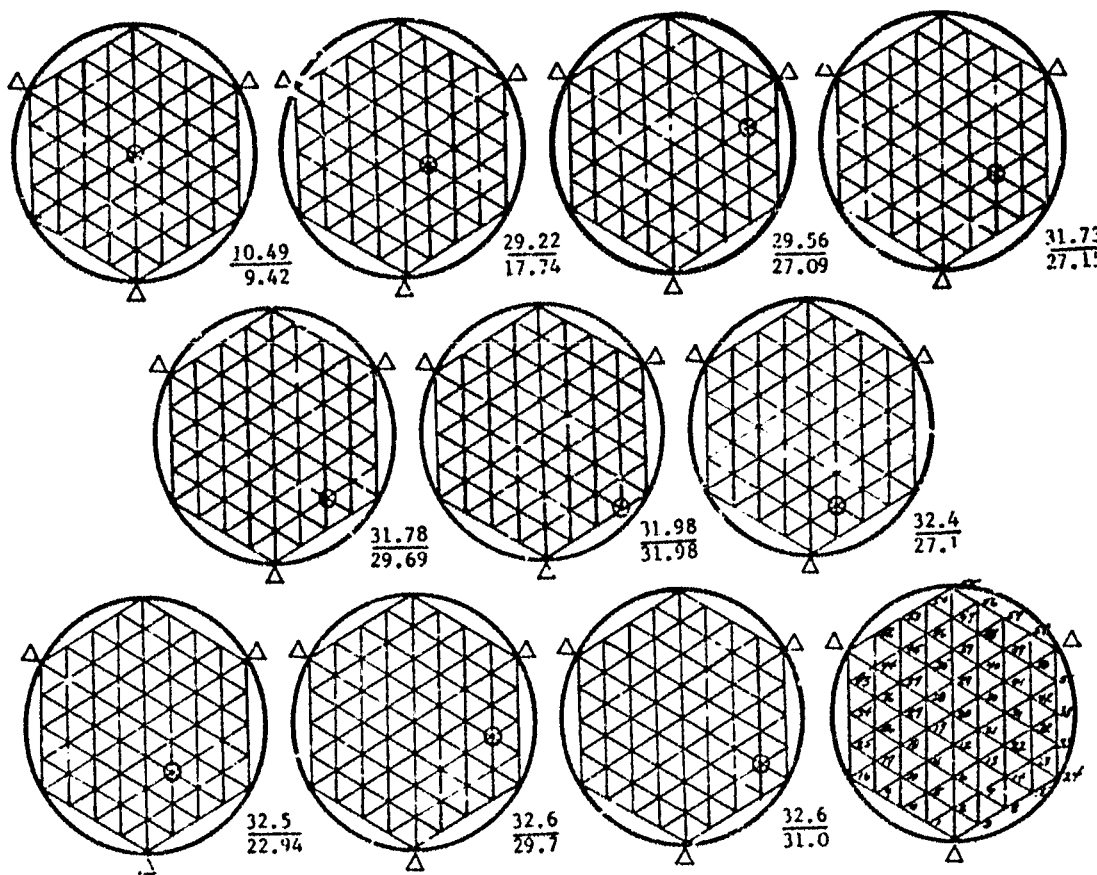


Figure 19.- Actuator locations which minimize the rms error of the mirror for one actuator and error example 3.

APPENDIX E – Continued

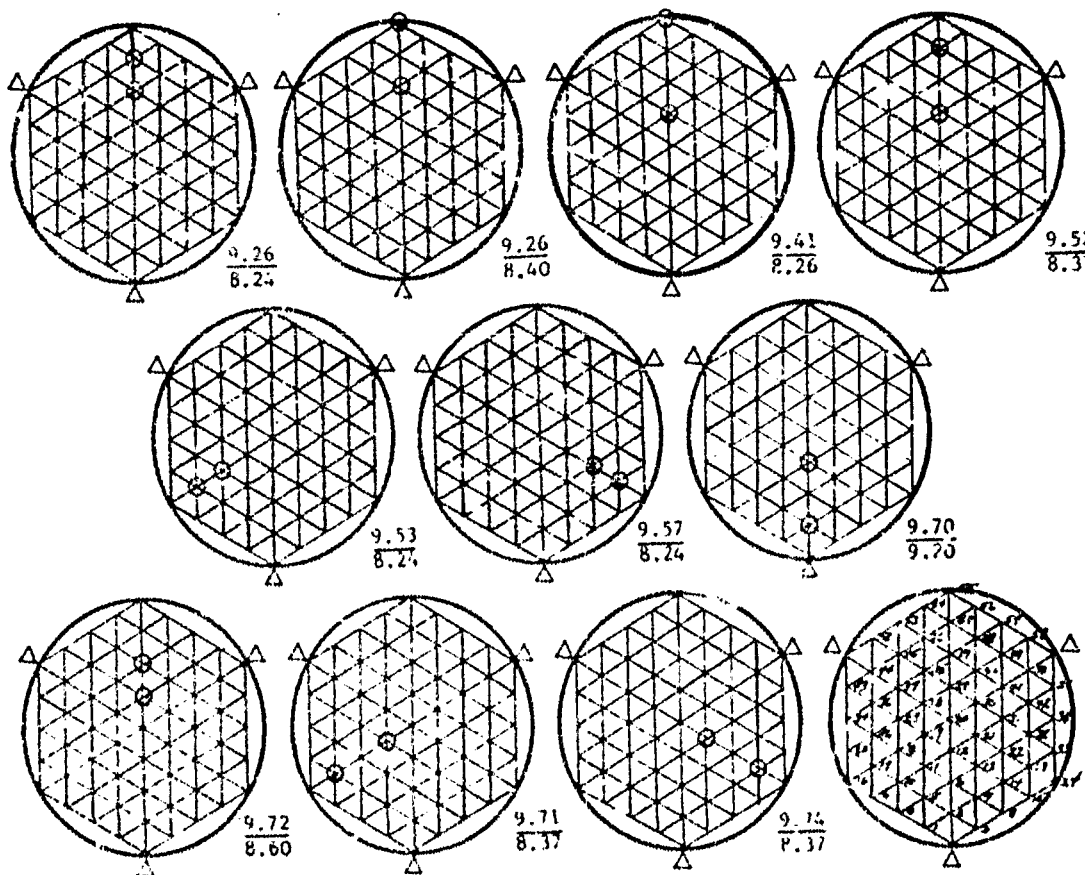


Figure F10.- Actuator locations which minimize the rms error of the mirror for two actuators and error example 3.

APPENDIX E – Continued

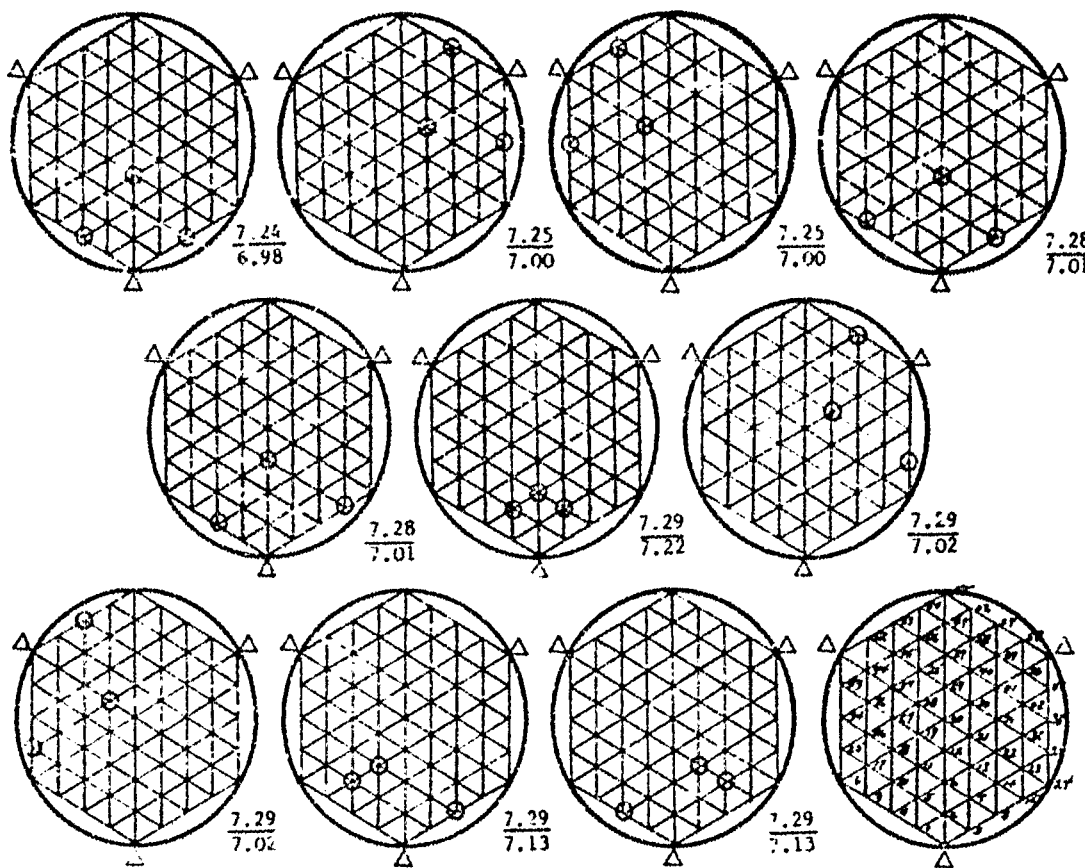


Figure Ell.: Actuator locations which minimize the rms error of the mirror for three actuators and error example 3.

APPENDIX E – Concluded

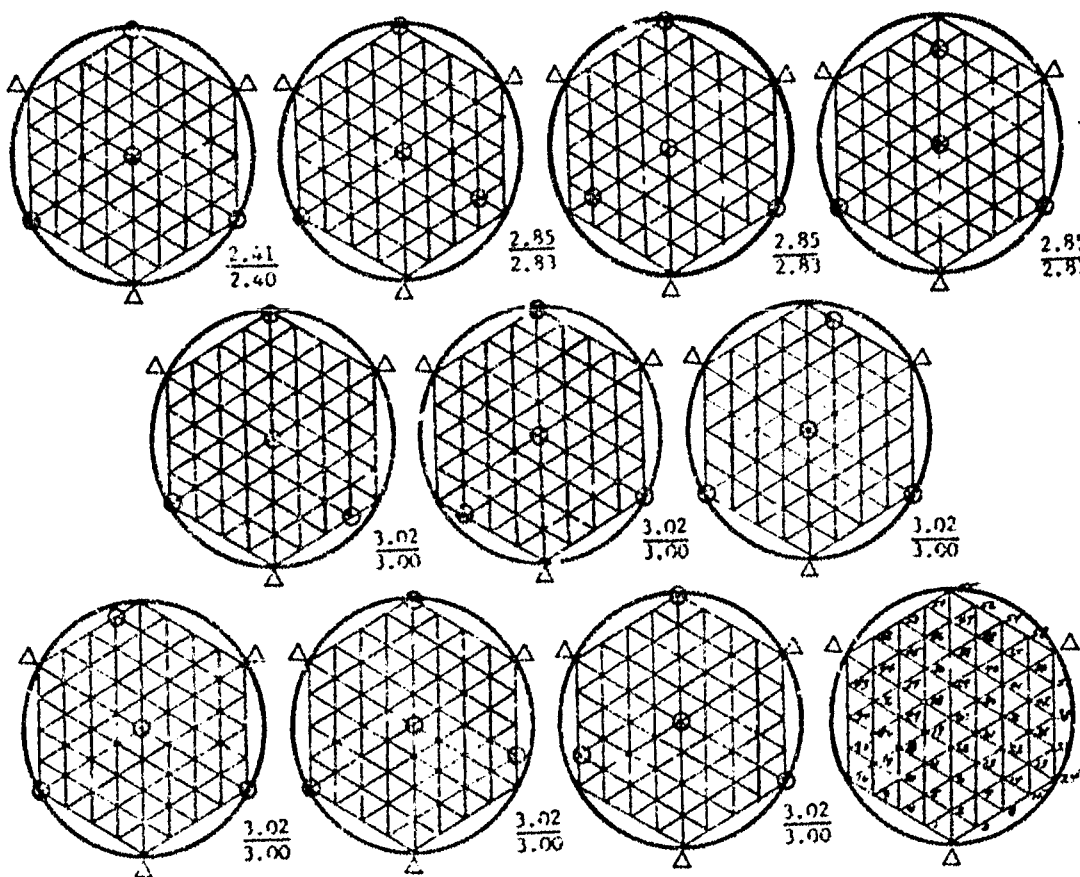


Figure E12.- Actuator locations which minimize the rms error of the mirror for four actuators and error example 4.

APPENDIX F

BEST ACTUATOR LOCATIONS - UNCORRELATED ERRORS

This appendix contains an enumeration of actuator locations which were found to generate minimum error under the modal control law (figs. F1 to F5). These were obtained by using the errors of example 1. The answers are given beside each diagram in the figures in the following form:

A
B
C

where

- A the error predicted by equation (61) assuming all values of ϕ_{IN}^2 are 0
- B the error obtained from equations (53) and (29)
- C the error under the optimal control law

The performance index is that obtained from the square root of equation (53) and must be multiplied by 0.49 to obtain rms error in microinches or by 0.019 to obtain rms error in wavelengths.

Selecting other error examples would, of course, result in the selection of different actuator locations; however, it can be seen from the values of ϕ_{IN}^2 in table II that the effect of a different actuator location could not make the final answer much better because the values of ϕ_{IN}^2 are already very small. For this reason the searches for actuator locations were restricted to the one example. The searches for one to four actuators inclusive considered all possible combinations, whereas those for seven actuators considered only a small subset of all possible combinations. This subset was chosen from those locations near the nodes of the next three higher order modes. This reduced the number of runs required to a reasonable value and resulted in a selection of actuator locations which were reasonably close to the theoretical limit.

APPENDIX F - Continued

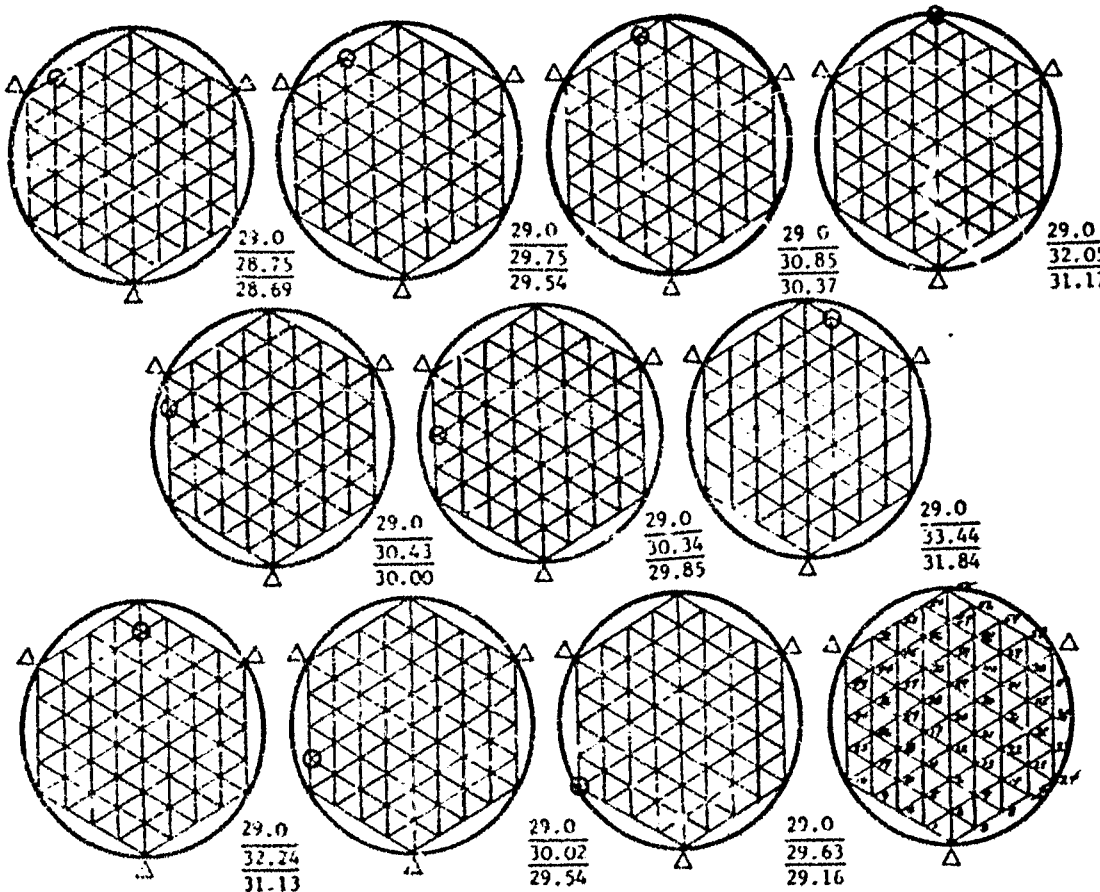


Figure F1.- Actuator locations which minimize the error generated by the control system in driving the first mode to zero using one actuator. Error distribution is taken from error example 1.

APPENDIX F - Continued

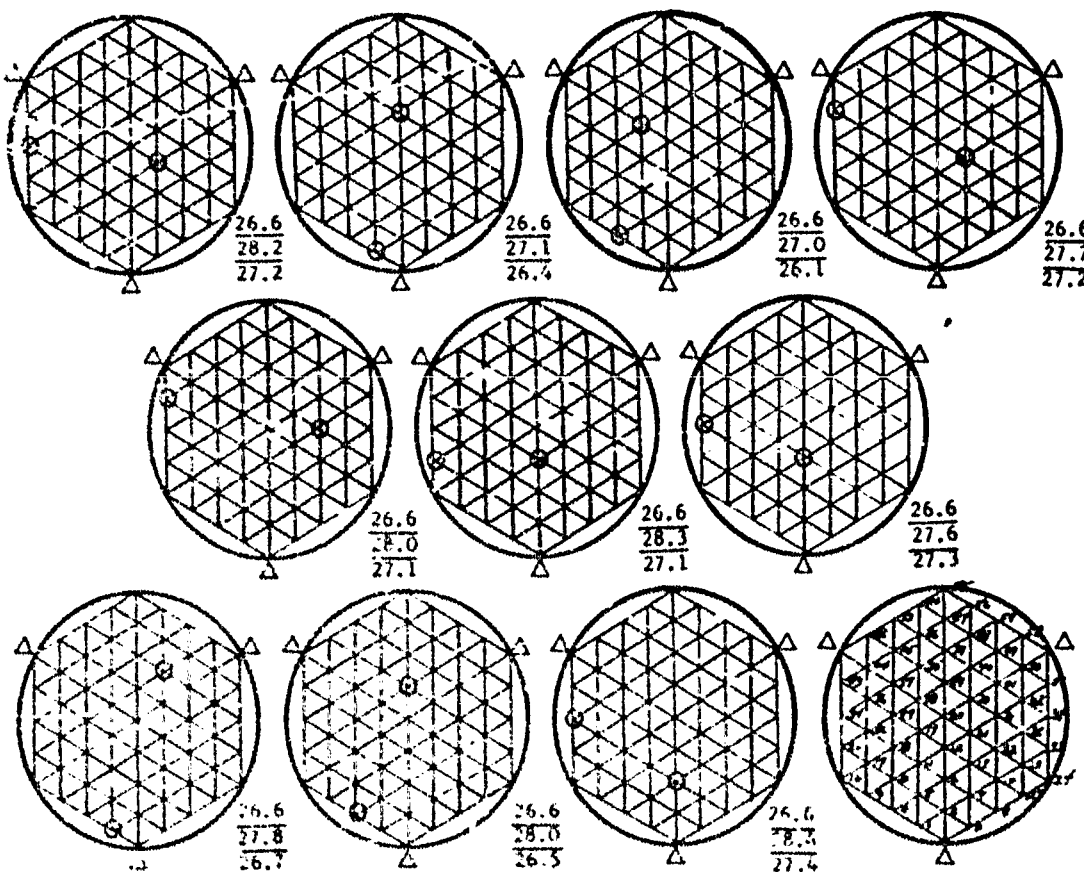


Figure 5. Actuator locations which minimize the error generated by the control system in driving the first two modes to zero using two actuators. Error distribution is taken from err_r example 1.

APPENDIX F - Continued

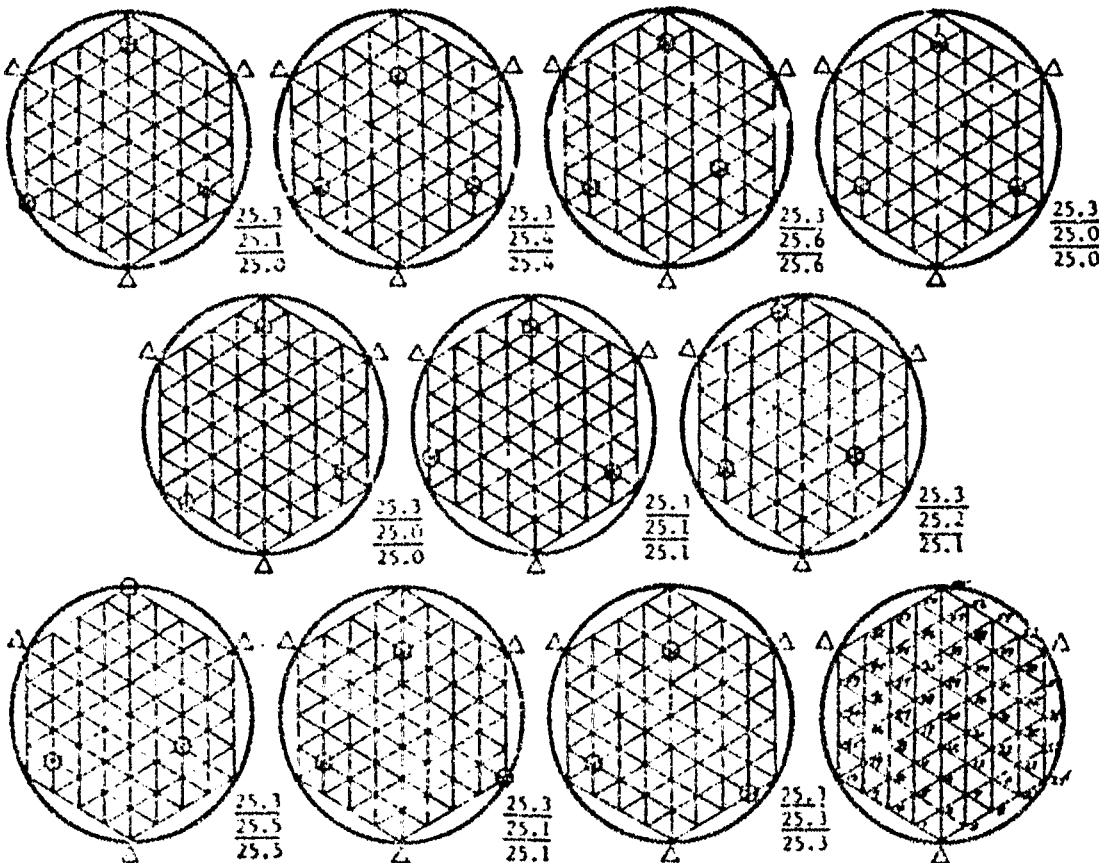


Figure 1'.- Actuator locations which minimize error generated by the control system in driving the first three notes to zero using three actuators. Error distribution is taken from error example 1.

APPENDIX F - Continued

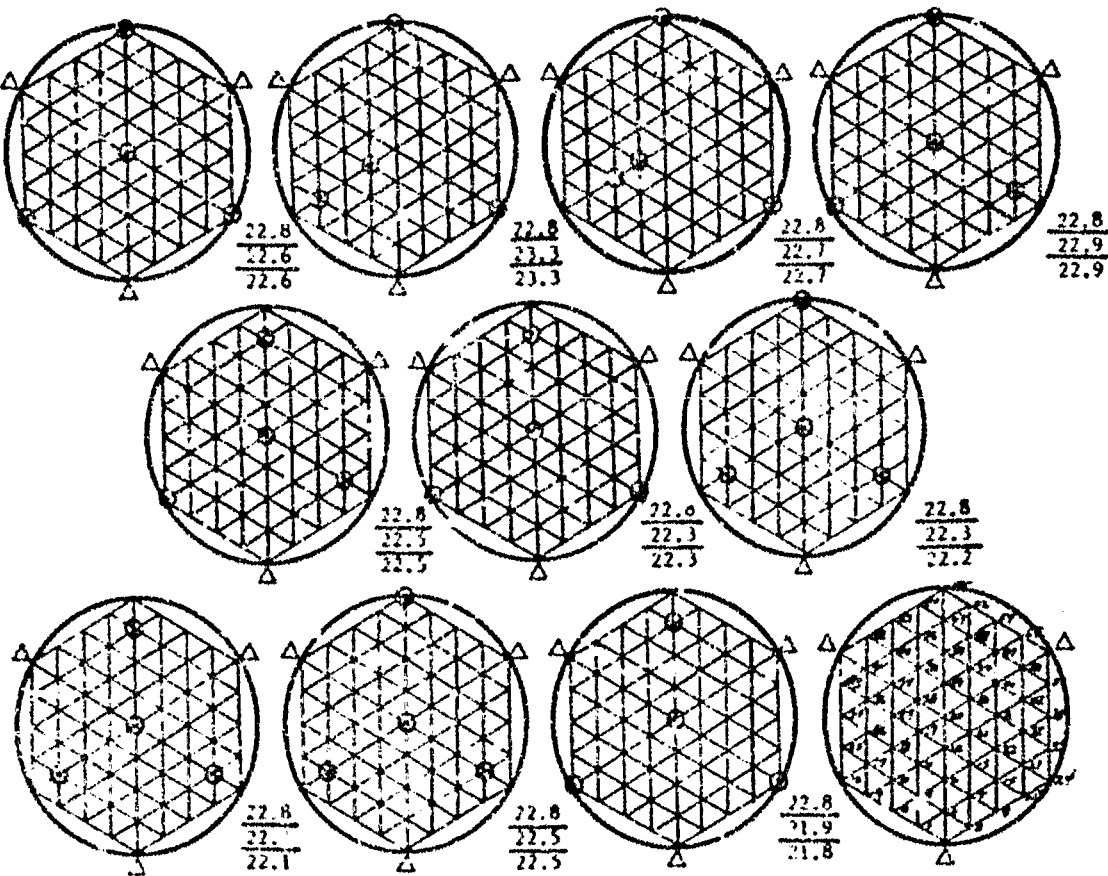


Figure F-1: Actuator locations which minimize the error generated by the control system in driving the first four modes to zero using four actuators. Error distribution is taken from error example 1.

APPENDIX F - Concluded

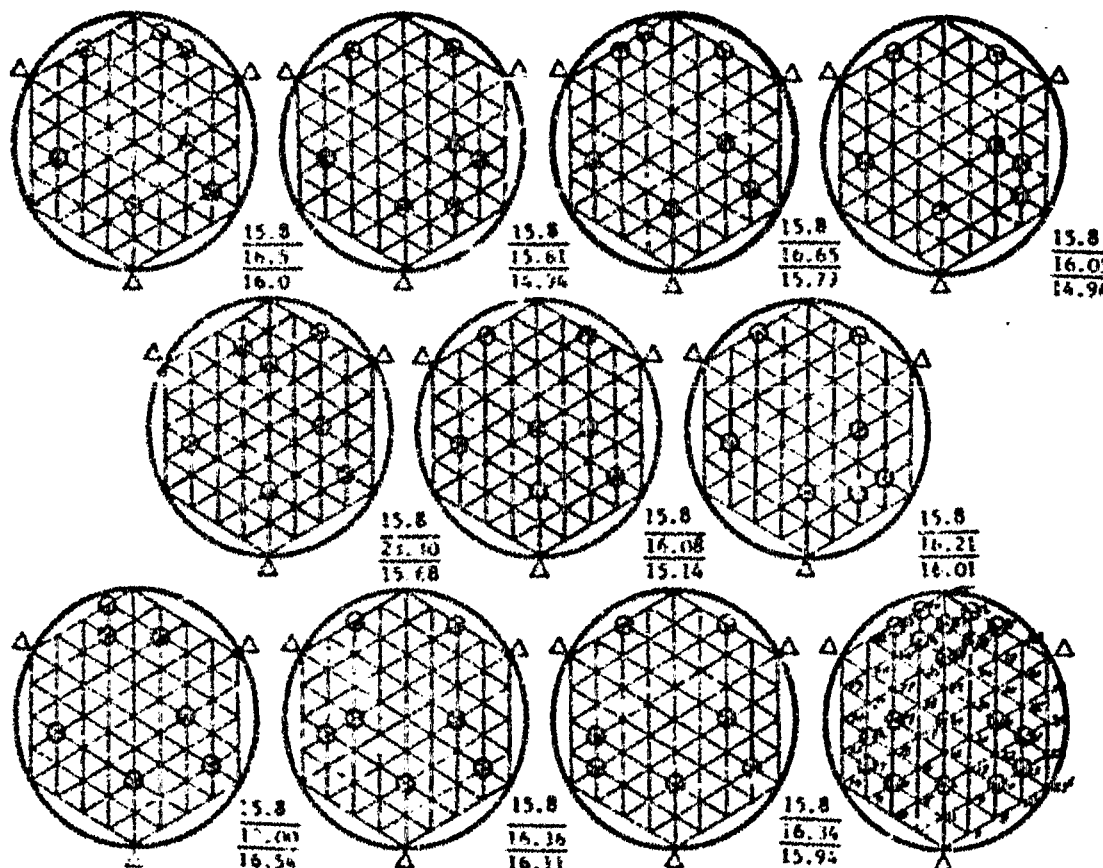


Figure F.1. Actuator locations which resulted in the minimum generated error for error example 1. The following 16 grid points were used in the search procedure: 6, 10, 14, 17, 20, 25, 26, 27, 31, 32, 33, 46, 47, 48, 53, 54, 56, and 57.

REFERENCES

1. Joint Space Panels: The Space Program in the Post-Apollo Period - a Report of the President's Science Advisory Committee. U.S. Govt. Printing Office, Feb. 1967.
2. Robertson, Hugh J.: Development of an Active Optics Concept Using a Thin Deformable Mirror. NASA CR-1593, 1970.
3. Creedon, J. F.; and Lindgren, A. G.: Control of the Optical Surface of a Thin, Deformable Primary Mirror With Application to an Orbiting Astronomical Observatory. *Automatica*, vol. 6, no. 5, Sept. 1970, pp. 643-660.
4. McIosh, Robert J.; and Christiansen, Henry N.: Structural Analysis and Matrix Interpretive System (SAMIS) Program: Technical Report. Tech. Memo. No. 33-311 (Contract NAS 7-100), Jet Propulsion Lab., California Inst. Technol., Nov. 1, 1966. (Available as NASA CR-83268.)
5. MacNeal, Richard H., ed.: The NASTRAN Theoretical Manual NASA SP-221, 1970.
6. Chi, Changhwi; Creedon, Jeremiah F.; Volpe, Jerald T.; and Robertson, Hugh J.: Vibrational Modes of the Circular Mirror With Three Support Points (Abstract). *J. Opt. Soc. Amer.*, vol. 61, no. 8, Aug. 1971, p. 1130.
7. Creedon, Jeremiah F.; and Robertson, Hugh J.: Evaluation of Multipoint Interaction in the Design of a Thin Diffraction-Limited Active Mirror. *IEEE Trans. Aerosp. & Electron. Syst.*, Mar. 1969, pp. 287-293.
8. Born, Max; and Wolf, Emil: *Principles of Optics*. Second rev. ed., Macmillan Co., c.1964.
9. Conte, S. D.: *Elementary Numerical Analysis*. McGraw-Hill Book Co., Inc., c.1965.

TABLE I.- MODAL COEFFICIENTS FOR EXAMPLE FIGURE ERRORS

Mode number	Modal e ₁₁ , w coefficients for =		
	Error example 1	Error example 2	Error example 3
1	-17.18	-29.47	.23
2	-12.10	-15.40	-.13
3	.44	-22.56	30.93
4	-11.00	1.91	13.79
5	.67	.57	.02
6	.78	.20	-----
7	-11.70	-1.71	-----
8	.10	.72	-----
9	3.93	1.37	-----
10	-12.36	.26	.49
11	.92	.05	-.01
12	-.91	.05	-----
13	-.81	.32	-----
14	1.04	.22	-----
15	6.28	.07	1.17
16	.18	.26	-----
17	.81	.01	-----
18	1.39	.06	-----
19	2.04	.20	-.06
20	3.16	.46	-----
21	.69	.05	-----
22	-2.79	.04	-----
23	-.28	.03	-----
24	.05	.13	-.126
25	-1.22	-----	-----
26	-.16	.01	-----
27	-.10	.03	-----
28	35.73	.13	-.353
29	1.58	-----	.01
30	.96	.03	-----
31	.06	-----	-----
32	.59	.05	-----
33	.25	-----	-----
34	-.03	.01	-----
35	.78	.07	-----
36	2.35	-----	-.03
37	.78	-----	-----
38	.60	.03	-----
39	-.08	-----	-----
40	.05	.02	-----
41	.57	-----	-----
42	.57	-----	-----
43	-.78	-.03	-----
44	.91	-----	-----
45	.00	-.01	-----
46	.04	-----	-----
47	.13	-.03	-----
48	.14	-.01	-----
49	-.16	-----	-----
50	.26	-----	-----
51	.49	.04	-.08
52	.08	-----	-----
53	.17	-----	-----
54	.19	-----	-----
55	.28	-----	-----
56	-.20	-----	-----
57	.03	-.01	-----
$\sum_{i=1}^N e_{11}^2$		1136.6	1135.7
			1135.1

TABLE II.- VALUES OF ϕ_{1N}^2 FOR N = 1, 2, 3, 4, AND 7

[Determined for error example 1; actuator grid locations corresponding to these values are tabulated below the values of ϕ_{1N}^2]

Mode	ϕ_{11}^2	ϕ_{12}^2	ϕ_{13}^2	ϕ_{14}^2	ϕ_{17}^2
1	0.29	2.011	1.46×10^{-3}	1.35×10^{-3}	2.1×10^{-2}
2		3.336	7.58×10^{-4}	1.35×10^{-3}	8.6×10^{-3}
3			1.41×10^{-2}	9.8×10^{-4}	9.7×10^{-4}
4				4.4×10^{-3}	2.60
5					0.541
6					7.94
7					1.51
Actuator grid locations	52	34, 21	16, 23, 47	16, 20, 24, 55	6, 23, 26, 31, 53, 56, 57

END

DATE

FILED

MAR

10